Development of SIVsmmPBj- and HIV-2-derived lentiviral vector systems to correct *gp91^{phox}* gene defects in monocytes

Dissertation
zur Erlangung des Doktorgrades
der Naturwissenschaften

vorgelegt beim Fachbereich Biochemie, Chemie und Pharmazie der
Johann Wolfgang Goethe-Universität
in Frankfurt am Main

von
Björn-Philipp Kloke
aus Berlin

Frankfurt am Main 2009
(D30)

Vom Fachbereich Biochemie, Chemie und Pharmazie der
Johann Wolfgang Goethe-Universität als Dissertation angenommen.

Dekan:	Prof. Dr. Dieter Steinhilber
Gutachter:	Prof. Dr. Volker Dötsch Prof. Dr. Klaus Cichutek
Datum der Disputation:	17.08.2009

1 SUMMARY 1

2 INTRODUCTION 3

2.1 Lentiviral vectors – Origin, Structure and Applications 3

2.1.1 Lentiviruses 3

2.1.2 Lentiviral vectors 6

2.1.3 Risk associated to lentiviral vector transduction 9

2.1.4 Gene Therapy 10

2.2 Monocytes 12

2.3 Chronic granulomatous disease 14

2.4 Objective 17

3 MATERIAL AND METHODS 19

3.1 Material 19

3.1.1 Chemicals and consumables 19

3.1.2 Enzymes and antibiotics 19

3.1.3 Kits 19

3.1.4 Plasmids 20

3.1.5 Oligonucleotides 22

3.1.6 Bacterial strains and culture media 24

3.1.7 Cell lines and culture media 24

3.1.8 Mouse strains 25

3.2 Methods of molecular biology 26

3.2.1 Cultivation of bacteria 26

3.2.2 Cloning processes 26

3.2.3 Generation and transformation of competent bacteria 28

3.2.4 Plasmid preparation 28

3.2.5 Agarose gel electrophoresis 29

3.2.6 Gel extraction of DNA fragments 29

3.2.7 Nucleic acid sequencing 30

3.2.8 Polymerase chain reaction (PCR) 30

3.2.9 Fusion-PCR 31

3.2.10 QuikChange™ site-directed mutagenesis kit 32

3.2.11 *Staphylococcus aureus* killing assay 32

3.3 Cell culture and virological methods 33

3.3.1 Cultivation of cell lines 33

3.3.2 Freezing and thawing of cultured cells 33

3.3.3 Isolation of human peripheral blood mononuclear cells (PBMC) 33

3.3.4 Isolation of primary human monocytes 34

3.3.5 Isolation of murine monocytes from BM 34
3.3.6 Production and concentration of vector particles 35
3.3.7 Transfection of cells in six well plates 36
3.3.8 Titration of vector particles 36
3.3.9 Transduction of primary monocytes 37
3.3.10 Fluorescence activated cell sorting (FACS) 37
3.3.11 Determination of *in vivo* biodistribution of murine monocytes 38
3.3.12 Intracellular flavocytochrome b_{558} staining of murine monocytes 39
3.3.13 Analysis of murine monocyte half-life in bloodstream 39
3.3.14 Phagocytosis assay 40
3.3.15 Phagoburst assay 41
3.4 Methods of protein biochemistry 41
3.4.1 Preparation of cell- and vector lysates and Bradford assay 41
3.4.2 SDS-polyacrylamide-gelelectrophoresis 42
3.4.3 Western blot analysis 42

4 RESULTS 44
4.1 HIV-2-derived lentivectors are able to transduce primary human monocytes 44
4.1.1 Comparison of HIV-1-, SIVsmmPBj- and HIV-2-derived lentiviral vector transduction of primary human monocytes 44
4.1.2 Monocyte transduction with Vpx-supplemented SIVsmmPBj-4xKOeGFP vectors 46
4.2 Construction of novel HIV-2- and PBj-derived lentiviral vector systems 49
4.2.1 Construction of a PBj-derived transfer vector – the conventional way 49
4.2.2 Constructing lentiviral transfer vectors – the new way 53
4.2.3 Enhancing the transfer vectors generated by Fusion-PCR 57
4.3 Analyzing human monocytes as potential target for *gp91^{phox}* gene correction 63
4.3.1 Flavocytochrome b_{558} is ubiquitously expressed by human monocytes 64
4.3.2 Phagocytosis and phagoburst ability of human monocytes 64
4.3.3 *Staphylococcus aureus* killing by human monocytes 65
4.3.4 HIV-2 based lentiviral transfer vector for *gp91^{phox}* gene-transfer 66
4.4 *Gp91^{phox}* gene correction of murine monocytes 68
4.4.1 Cell-composition of murine bone marrow 68
4.4.2 Isolation and purification of functional murine monocytes from bone marrow 69
4.4.3 Phagocytosis ability of murine monocytes 71
4.4.4 Phagoburst ability of murine monocytes 72
4.4.5 *Staphylococcus aureus* killing by murine monocytes 72
4.4.6 Biodistribution of murine monocytes 73
4.4.7 Determination of the half-life of murine monocytes *in vivo* 74
4.4.8 Gene correction of *gp91^{phox}*-deficient murine monocytes 76

5 DISCUSSION 81

5.1 Vpx of the HIV-2/SIVsmm/SIVmac lentivirus lineage facilitates monocyte transduction 81

5.2 Generation of PBj- and HIV-2-derived lentiviral vectors 82

5.2.1 Gradual enhancement of a PBj-derived transfer vector 83

5.2.2 Generation of lentiviral transfer vectors by Fusion-PCR 85

5.2.3 Monocyte transduction of novel generated PBj- and HIV-2-derived lentivectors 86

5.3 Clinical applications for PBj- and HIV-2-derived lentivectors 87

5.3.1 A novel concept of xCGD treatment 88

5.3.2 Setting up the system 89

5.3.3 Functional analysis of murine monocytes for *gp91^{phox}* gene therapy 90

5.4 Outlook 93

6 SUMMARY (GERMAN) 94

7 REFERENCES 100

8 ABBREVIATIONS 110

9 APPENDIX 113

9.1 Plasmid map of pVpxPBjsyn 113

9.2 Plasmid map of pMD.G2 113

9.3 Plasmid map of pCMVΔR8.9 114

9.4 Plasmid map of pPBj-pack 114

9.5 Plasmid map of pHIV-2d4 115

9.6 Plasmid map of pPBj-SR-SEW-cSIN 115

9.7 Plasmid map of pPBj-MCS 116

9.8 Plasmid map of pPBj-SR-g'-SEW 116

9.9 Plasmid map of pHIV-2-MCS 117

9.10 Plasmid map of pHIV-2-SR-g'-SEW 117

9.11 Plasmid map of pHIV-2-SgW 118

9.12 Plasmid map of pHIV-1-SgpSw 118

9.13 Plasmid map of pHIV-1-SEW 119

10 DANKSAGUNG 120

11 CURRICULUM VITAE 122

12 PUBLIKATIONEN 124

1 Summary

SIVsmmPBj-derived lentiviral vectors are capable of efficient primary human monocyte transduction, a capacity which is linked to the viral accessory protein Vpx. To enable novel gene therapy approaches targeting monocytes, in this thesis it was aimed to generate enhanced lentiviral vectors that meet the required standards for clinical applications with respect to gene transfer efficiency and safety. The vectors were tested for their suitability in a relevant therapeutic gene transfer approach.

At first, it was investigated whether vectors derived from another Vpx-carrying lentivirus reveal the same capacity for monocyte transduction as SIVsmmPBj-derived vectors. A transduction experiment using HIV-2-derived vectors in comparison to PBj-derived vectors revealed a comparable transduction capacity, thus disproving the assumed uniqueness of the PBj vectors. The further generation and analysis of expression constructs for the *vpx* genes of HIV-2 and SIVmac demonstrated a similar functionality in monocyte transduction as the Vpx of PBj. As VpxPBj, both Vpx proteins facilitated monocyte transduction of a *vpx*-deficient PBj-derived vector system.

For the generation of enhanced SIVsmmPBj and HIV-2 vector systems, only the transfer vectors were optimized, since the packaging vectors available already meet current standards. At first, several modifications were introduced into an available preliminary PBj-derived transfer vector by conventional cloning. The modifications included insertions of cPPT/CTS and WPRE as well as the deletions of the remaining *pol* sequence, the second exons of *tat* end *rev*, and the U3-region within the 3'LTR to generate a SIN vector. Thus, beside safety enhancement, the vector titers were also increased from $9.1x10^5$ TU/ml achieved after concentration with the initial transfer vector up to $1.1x10^7$ TU/ml with the final transfer vector. The PBj vector retained its capability of monocyte transduction when supplemented with Vpx.

This conventional method of vector enhancement is time-consuming and may result in only sub-optimal vectors, since it depends on the presence of restriction sites which may not allow deletion of all needless sequences. Moreover, mutations may accumulate during the high number of cloning and amplification steps. Therefore, a new and easier method for lentiviral transfer vector generation was conceived. Three essential segments of the viral genome (5'-LTR, RRE, ΔU3-3' LTR) are amplified on the template of the lentiviral wild-type genome and fused by Fusion-PCR. Further necessary elements namely the cPPT/CTS-element, MCS, and PPT are included into the resulting vector by extension of the nucleotide primers

used for the PCRs. The amplified and fused vector-scaffold can easily be integrated into a plasmid backbone, followed by insertion of the expression cassette of choice. By applying this approach, two novel lentiviral transfer vectors, based on the non-human SIVsmmPBj and the human HIV-2, were derived. Vector titers achieved for PBj and HIV-2 vectors supplemented with Vpx reached up to $4.0x10^8$ TU/ml and $5.4x10^8$ TU/ml, respectively. The capacity for monocyte transduction was maintained. Thus, safe and efficient, state of the art HIV-2- and PBj-derived vector systems are now available for future gene therapy strategies.

Finally, the new vectors were used to set up an approach for gene correction of *gp91^{phox}*-deficient monocytes for the treatment of X-linked chronic granulomatous disease (xCGD). The administration of autologous, gene-corrected monocytes to counteract systemic and acute infections could lead to a decreased infection load, dissolve granulomas and therefore improve the survival rate of hematopoietic stem cell transplantation (HSCT) which is the current treatment of choice for this disease. First, methods for analysis of gp91^{phox} function were established. Next, they were employed to demonstrate the capacity of monocytes, obtained from healthy humans or mice, for phagocytosis, oxidative burst, and *Staphylococcus aureus* killing. The *in vivo* half-life of murine monocytes in the bloodstream and their distribution to specific tissues was determined. Lastly, HIV-1 vectors were used to transfer the *gp91^{phox}* gene into monocytes from *gp91^{phox}*-deficient mice. This resulted in the successful restoration of the oxidative burst ability in the cells.

In summary, the general suitability of the new vectors for treatment of CGD by monocyte transduction was demonstrated. The results of the mouse experiments provide the foundation for future challenge experiments to evaluate the capability of gene-corrected monocytes to kill off microbes *in vivo*.

2 Introduction

2.1 Lentiviral vectors – Origin, Structure and Applications

Lentiviral gene transfer vectors can be derived from different lentiviruses, a genus of the family *Retroviridae*. In order to appreciate the design and function of a lentiviral vector, it is important to understand their origin, the wild-type lentivirus.

2.1.1 Lentiviruses

The most prominent members of the lentivirus family are the human immunodeficiency virus-1 (HIV-1) and HIV-2, followed by the simian immunodeficiency viruses of rhesus macaques (SIVmac) and sooty mangabeys (SIVsmm).

Structure and genome

All lentiviruses share the same structure of a lipid-enveloped virus particle of approx. 100 nm in diameter. A host-derived membrane embeds the envelope complex. It interacts with the matrix (MA) proteins which encompass the cone-shaped viral core, consisting of the capsid (CA) proteins. Within the core, two positive-strand RNA copies of about 7-10 kb, covered by nucleocapsid (NC) proteins, encode the viral genome (Figure 1).

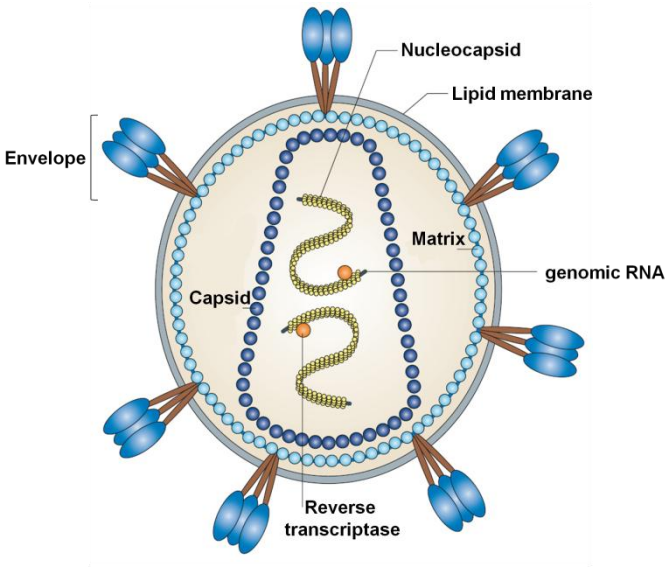

Figure 1: Structure of a lentivirus. (Modified from Karlsson Hedestam et al., 2008)

The different lentiviral genomes are flanked by two long terminal repeats (LTRs), harboring the viral enhancer and promoter elements (U3 region) as well as the polyadenylation signal (R region). They encode the structural proteins Gag and Env, the *pol*-encoded enzymes, the

regulatory proteins Tat and Rev, and depending on the virus, several of the accessory proteins: Vif, Vpr, Nef, Vpu, or Vpx. Apart from the viral genes, the genomic RNA contains a number of cis-acting elements necessary for reverse transcription (primer binding site (PBS), central polypurine tract (cPPT), polypurine tract (PPT)), integration (attachment sites), mRNA export (Rev-responsive element (RRE)), and packaging (Ψ-site) (Figure 2).

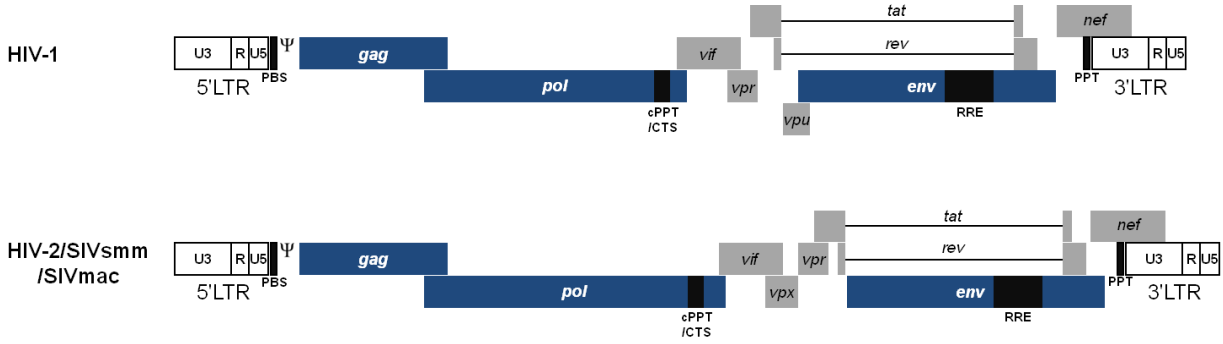

Figure 2: Schematic representation of the lentiviral genomes of HIV-1- and the HIV-2/SIVsmm/SIVmac-group.

The products of the *gag* gene are precursor proteins which are necessary for particle formation and sufficient for the development of noninfectious, viruslike particles. They perform several major functions during viral assembly like (I) forming the structural framework of the virion, (II) packaging of the viral genome and (III) acquiring the lipid bilayer with associated Env glycoproteins during particle release, a process called budding. After budding, the Gag precursor polyprotein is cleaved by the viral protease into matrix, capsid, nucleocapsid, and p6 proteins to form a mature virus particle (Figure 1). The Env protein, encoded by the *env* gene, consists of a transmembrane glycoprotein and an external envelope glycoprotein. The external envelope glycoprotein dictates the tropism of the virus.

From lentiviral binding to DNA integration

By binding to the CD4-receptor and subsequently to a co-receptor such as CCR5 or CXCR4, the viral membrane fuses with the host membrane resulting in the release of the viral core into the cytoplasm. After the virion core has entered the cytoplasm of the infected cell, reverse transcription of the viral single-stranded RNA to the proviral double-stranded DNA is initiated. This reaction is catalyzed by the reverse transcriptase (RT) in conjugation with its associated ribonuclease H (RNase H). Whereas the reverse transcriptase copies either the RNA template (minus strand synthesis) or the DNA templates (for second- or plus-strand synthesis), the RNase H degrades the RNA in generated RNA-DNA hybrids. Many cis-acting elements of the viral genome are important for the reverse transcription. The primer binding site (PBS), which participates in the placement and stabilization of the transfer tRNA-primer necessary for initiation of reverse transcription, is located downstream of the 5'LTR. The

central polypurine tract (cPPT) and the polypurine tract (PPT) are resistant to RNase degradation and can therefore be used by the reverse transcriptase to initiate plus-strand synthesis. The plus-strand synthesis terminates either at the end of the template or at the central termination sequence (CTS). Thereby, a triple helix structure named the DNA flap is formed at the position of the cPPT upstream of the CTS. The DNA flap is necessary for efficient replication and nuclear import (De Rijck and Debyser, 2006).

The generated viral DNA is transported into the nucleus (Figure 3). After the completion of reverse transcription, the viral complex is referred to as the viral preintegration complex (PIC). Several cellular (e.g. high-mobility group protein A1 and barrier-to-autointegration factor (BAF)) and viral proteins (RT, IN, MA, Vpr, and NC) as well as the DNA flap are described to be part of the preintegration complex, but the import mechanism into the nucleus remains to be clarified (Freed and Martin, 2007). Once inside the nucleus, the viral DNA is integrated randomly into the host genome, a process which is catalyzed by the integrase. The sequences at the end of the viral DNA, the attachment sites, are cleaved endonucleolytically by the integrase leaving 3'-recessed ends. Subsequently, the integrase catalyses a staggered cleavage in the cellular DNA where the 5' termini are joined with the 3' ends of the viral DNA.

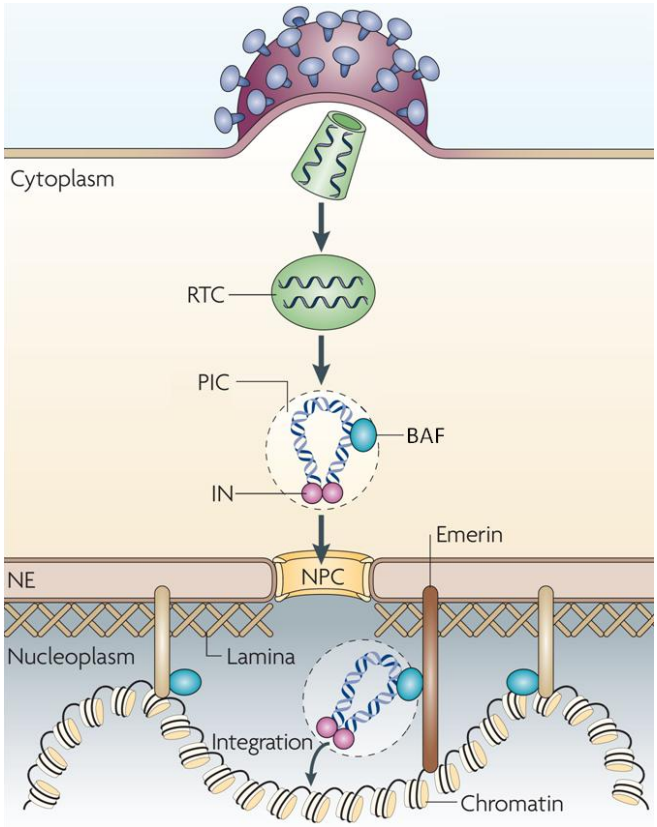

Figure 3: Lentiviral DNA integration. After the viral particle binding, the viral core is released into the cytoplasm, the viral genome reverse transcribed, transported into the nucleus and integrated in the host genome. BAF: barrier-to-autointegration factor; IN, integrase; NPC, nuclear pore complex; PIC, pre-integration complex; RTC, reverse transcription complex. (Modified from Suzuki and Craigie, 2007)

Regulatory and accessory proteins

The provirus serves as template for the synthesis of viral RNA. The nuclear protein Tat transactivates the LTR-directed transcription. It binds to the TAR (trans activation response) - stem loop, a secondary single stem-loop (HIV-1) or double stem-loop (HIV-2) RNA-structure within the U3 region of the viral LTRs (Emerman et al., 1987). After binding to the TAR loop, Tat recruits the cellular cyclin T-CDK9 complex – the so-called Tat-associated kinase complex. By this Tat mediates the hyperphosphorylation of the C-terminal domain of the RNA polymerase II resulting in a processive synthesis of viral messenger RNA (mRNA) (Garriga and Grana, 2004). In the absence of Tat binding to the TAR loop, the processivity of the RNA polymerase II is impaired.

The viral pre-mRNAs are processed by the cellular transcription machinery (capping, 3'-end cleavage, polyadenylation, and splicing). Lentiviruses produce several alternatively spliced mRNAs but the cellular export machinery is only capable of transporting fully spliced mRNAs coding for Rev, Tat, or Nef, into the cytoplasm. The partially spliced mRNAs (encoding Vif, Vpr, Vpx, Vpu, and Env) as well as the unspliced primary transcript rely on a Rev-mediated export (Felber et al., 1989). Rev (regulator of expression of viral proteins) is a 16-19 kDa, predominantly nucleolar, phosphoprotein. It regulates the mRNA-export by binding to the cis-acting Rev-responsive element (RRE) present on all unspliced and partially spliced mRNAs. Therefore, the RRE must be present in the *sense* orientation within the transcripts.

The accessory protein Vpx is only encoded by viruses of the HIV-2/SIVsmm/SIVmac lineage (HIV-2, SIVmac, SIVsmm, SIVmnd-2, SIVrcm, SIVdrl). This 17 kDa protein is packaged to high levels in the virion through the interaction with the C-terminal p6 domain of the Gag polyprotein (Henderson et al., 1988; Pancio and Ratner, 1998; Wu et al., 1994). It is required for an efficient virus replication in macrophages and in dendritic cells (Fletcher et al., 1996; Hirsch et al., 1998; Srivastava et al., 2008) and essential for the lentiviral vector transduction of primary human monocytes (Wolfrum et al., 2007). Its function is part of efficient reverse transcription in monocyte-derived cells (Srivastava et al., 2008) and to the nuclear import of the viral preintegration complex (Belshan and Ratner, 2003; Fletcher et al., 1996).

The remaining accessory proteins, Vif, Vpu, Vpr, and Nef, are not essential for lentiviral vector transduction, hence they will not be described in more detail. The functions are well reviewed by E. Freed, and M. Martin (Freed and Martin, 2007).

2.1.2 Lentiviral vectors

Retroviral vectors integrate their viral genome into the genome of the host. Thus, a stable, long-term expression of a transgene can be achieved. The γ-retroviral based vectors like MLV cannot transduce non-dividing cells. On the contrary, lentiviral vectors efficiently

transduce non-dividing cells and are therefore of special interest for research and clinical applications.

Structure

The first lentiviral vector was constructed by Luigi Naldini and others in 1996 (Naldini et al., 1996b). Since then, lentiviral vector development has been often modified in order to improve the efficiency and safety of the system. The initial design of lentiviral vectors provides for the separation of the necessary viral elements, rendering the produced vectors replication-incompetent. The vector RNA to be packaged into the vector particles is separated from the structural genes (*gag, pol*) which are important for the particle formation itself, and from the envelope-encoding sequence. This results in a transfer-, a packaging-, and an envelope-construct, respectively. For vector production the different constructs are usually used for 293T-cell transfection, where 48 h post transfection the vectors can be harvested from the supernatant. Subsequently, the titer can be analyzed and the vectors used for target cell transduction (Figure 4).

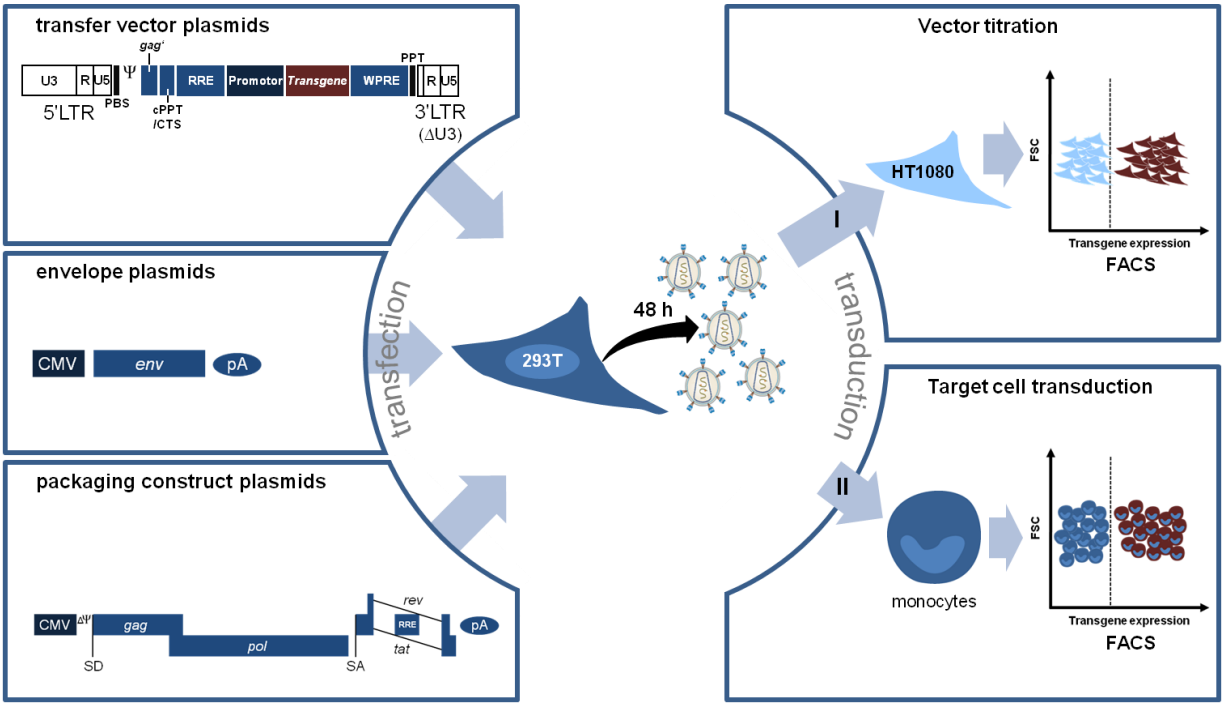

Figure 4: Transient vector production. The transfer- packaging- and envelope-construct are transiently transfected into 293T cells. Two days post transfection, vector particles are harvested and titrated on HT1080 cells (I). Subsequently, they can be used for target cell transduction (e.g. monocyte transduction) (II).

Envelope construct

In general, the native lentiviral envelope is exchanged for the vesicular stomatitis virus G (VSV-G) protein (Naldini et al., 1996b). Pseudotyping with VSV-G allows transduction of a wide range of target cells and tissues and redirects, in contrast to the receptor mediated entry with wild-type envelope, vector entry through to the endocytic pathway (Aiken, 1997).

Using the very stable VSV-G as envelope allows the concentration of the viral vectors by ultracentifugation. Although VSV-G occasionally mediates an immune response in patients which leads to a clearance of the vectors, VSV-G pseudotyping is most widely used as it yields very high transduction efficiencies.

Packaging construct

The packaging construct encodes from the *gag* and *pol* genes all structural and enzymatic proteins that are required for vector particle production and efficient transduction of target cells, with the exception of the envelope protein. Additionally to the Gag/Pol expression, the first generated packaging constructs coded for both regulatory proteins, Tat and Rev, and for all accessory proteins (Naldini et al., 1996a; Naldini et al., 1996b). The viral full-length mRNA, which encodes for the trans-elements, is usually packaged into vector particles and transferred to the target cell. To prevent this, the LTRs, PBS- and Ψ-sites were removed. The expression is therefore normally driven by a heterologous constitutive promoter (CMV or RSV) and ended by polyadenylation signals from the SV40 and insulin gene. These so-called first-generation packaging constructs were improved to second-generation constructs by the deletion of all accessory proteins (Figure 4) (Zufferey et al., 1997) and, further, to third-generation vectors where the *tat* gene was deleted and the *gag/pol* and *rev* genes were split onto separate plasmids (Dull et al., 1998). Further improvements to increase the biosafety of the packaging constructs have been achieved, i.e. a codon-optimized Rev-independent Gag/Pol expression (Kotsopoulou et al., 2000) or the separation of the *gag/pol* genes on two different plasmids (Kappes et al., 2003; Wu et al., 2000).

Transfer vector

The lentiviral transfer vector encodes for the transgene mRNA. Independent of the generation status, the RNA contains all elements necessary for its packaging, reverse transcription, nuclear import, and integration. Besides, it harbors an expression cassette for transgene expression under control of an internal promoter.

The basic transfer vector consists of a 5' UTR, spanning the 5' LTR, the primer binding site, the splice donor (SD), the packaging signal, the rev-responsive element, the splice acceptor (SA), the transgene expression cassette, and the 3'UTR containing the PPT and the 3'LTR (Naldini et al., 1996a; Naldini et al., 1996b). Different changes within the transfer vector led to an increase in vector titer, transduction efficiency, and transgene expression. In addition, it improved the safety of the vectors. Through the addition of a cPPT and CTS a 2-10fold increase in transduction efficiency was achieved (Zennou et al., 2000). During reverse transcription the viral RNA, with the exception of the PPT and cPPT region, is degraded by the RNase H. The resulting two locations prime the plus strand synthesis for the proviral

DNA. The synthesis from the PPT is terminated at the CTS which generates a DNA flap (triple helix structure) necessary for efficient replication and important for nuclear import (De Rijck and Debyser, 2006).

The woodchuck hepatitis virus posttranscriptional regulatory element

The transgene expression was improved by the incorporation of the woodchuck hepatitis virus posttranscriptional regulatory element (WPRE) downstream of the transgene. The WPRE stabilizes the mRNA through secondary structures resulting in a five-fold increased gene expression (Hlavaty et al., 2005; Zufferey et al., 1999). As it codes for enhancer-promoter elements and for the first 60 amino acids of the woodchuck hepatitis virus X protein, concerns about a possible oncogenic activity were expressed (Kingsman et al., 2005). To exclude those safety concerns, a modified WPRE which lacks the potential oncogenic sequences but maintains its ability to enhance transgene expression was developed (Schambach et al., 2006a).

Vectors derived from the simian immunodeficiency SIVsmmPBj

The PBj strain of simian immunodeficiency virus from sooty mangabeys (Cercocebus atys) (SIVsmm) (Fultz et al., 1989), has been shown to replicate *in vitro* in non-stimulated primate PBMCs (Fultz, 1991). As this feature is unique for SIVsmmPBj, compared even to closely related viruses like HIV-2, SIVmac251, it was used to generate SIVsmmPBj-derived two-plasmid system lentivectors. These replication-incompetent vectors enabled an efficient transduction of primary human monocytes (Mühlebach et al., 2005). The ability to transduce monocytes was found to be connected to the viral accessory protein Vpx (Wolfrum et al., 2007). The PBj-derived two-plasmid lentivector was further enhanced to a basic three-plasmid system. It includes the envelope construct pMD.G2 (9.2), the packaging-construct pPBj-pack (9.4), and the transfer vector pPBj-trans (Wolfrum, 2005). This system was used as the origin for further vector enhancements in this thesis.

2.1.3 Risk associated to lentiviral vector transduction

The method for generating retroviral and lentiviral vectors is greatly influenced by possible risks linked to vector gene therapy, such as insertional mutagenesis, vector mobilization, generation of replication competent lentivirus (RCL), and germ-line transmission of vector sequences. In contrast to retroviral vectors, lentiviral vectors show a different integration preference into active transcription units as opposed to regulatory gene regions (Lewinski et al., 2006; Schroder et al., 2002; Wu et al., 2003). Although there is evidence that this different integration preference of lentiviral vectors minimizes the risk of cellular proto-oncogene upregulation in comparison to MLV vectors (Cattoglio et al., 2007; Montini et al.,

2006), the risk of lentiviral mediated insertional mutagenesis is present and has to be further investigated. Safety concerns had a great impact on the design of lentiviral vectors. Several different modifications of the transfer vectors are used to increase their safety profile. They are described in the following paragraphs.

Self-inactivating lentiviral vectors

The generation of self-inactivating (SIN) lentiviral vectors has improved the vector systems substantially (Miyoshi et al., 1998; Zufferey et al., 1998). Here, the promoter and enhancer sequences within the U3 region of the 3'-LTR were deleted. In the process of reverse transcription, this promoter/enhancer deficient U3 region of the 3'-LTR replaces the U3 region of the 5'-LTR in the proviral DNA and thus prevents an RNA transcription. Therefore, only the transgene is expressed by the internal promotor. This shut-off of full-length vector mRNA averts vector mobilization upon superinfection with wild-type virus. Furthermore, the deletion of enhancer and promoter sequences reduces the risk of insertional mutagenesis, homologous recombination, and vector mobilization.

Insulators

The safety of lentiviral vector systems can be improved with insulators. These boundary elements can prevent enhancer-promoter interactions if placed between those elements and protect transgene cassettes from silencing and positional effects. For this, chromatin insulators can be integrated into the U3 region of the transfer vector (Recillas-Targa et al., 2004). The most widely used insulator is the chicken b-globin insulator (cHS4).

Ubiquitously acting chromatin opening elements

The ubiquitously acting chromatin opening elements (UCOEs), like the UCOE from the human HNRPA2B1-CBX3 locus (A2UCOE), consist of methylation-free CpG islands and dual divergently transcribed housekeeping promoters but lack enhancer sequences. They are shown to be resistant to transcriptional silencing and to produce a consistent, ubiquitous, and stable transgene expression due to the obviation of chromosomal position effects (Antoniou et al., 2003; Ramezani et al., 2003). These features could be transferred to a lentiviral vector context. This resulted in a vector with a stable gene expression which is hardly effected by insertion-site position effects and is implied to have a far lower insertional mutagenesis activation potential (Zhang et al., 2007)

2.1.4 Gene Therapy

The general principle of *ex vivo* gene therapy to correct genetic disorders looks very simple. A relevant cell type is isolated from the patient, gene modified *ex vivo* using viral vectors, and

reintroduced into the patient (Figure 5). Important targets for gene therapy are hematopoietic stem cells (HSCs) as a functional correction of these results in a correction of all blood and immune cells in the body. However, basically all long-lived cells can be gene corrected.

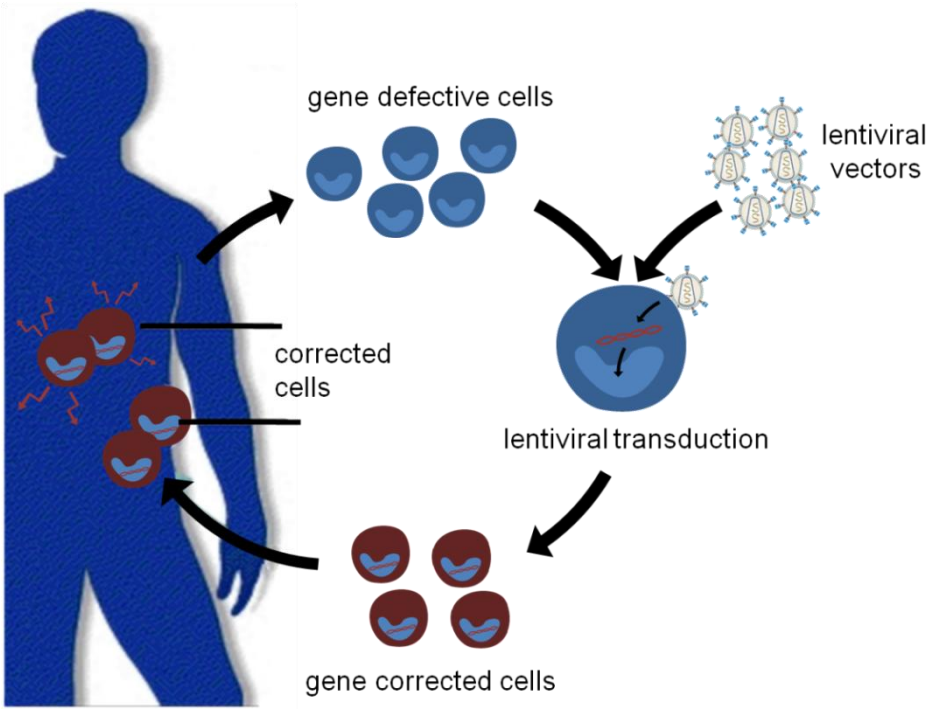

Figure 5: Correcting genetic diseases by *ex vivo* gene therapy. Gene defective cells are harvested and transduced with lentiviral vectors encoding the potentially therapeutic transgene. The gene-corrected cells are then reintroduced into the patient.

Retroviral vectors in gene therapy

In the most prominent gene therapy trials using retroviral vectors, they were employed to treat hematopoietic disorders such as adenosine deaminase-deficient severe combined immunodeficiency (ADA-SCID) (Aiuti et al., 2009), X-linked severe combined immunodeficiency (SCID-X1) (Cavazzana-Calvo et al., 2000; Hacein-Bey-Abina et al., 2002), and X-linked chronic granulomatous disease (xCGD) (see Chpt. 2.3) (Ott et al., 2006). Although all of these retroviral gene therapy trials were great successes, certain risks associated with gene therapy became visible. One major concern, i.e. insertional mutagenesis, persists. As viral vectors integrate with little preference into the host genome, host genes can be directly affected or indirectly activated. In the case of the SCID-X1 trial, insertional mutagenesis led to cancer in several patients (Check, 2005; Hacein-Bey-Abina et al., 2003) and for xCGD-patients a clonal dominance was observed (Grez, 2008). Another problem was the observed gene-silencing in the xCGD patients (Schultze-Strasser, unpublished data).

Lentiviral vectors in gene therapy

The main advantages of lentivirus-derived vectors over retroviral vectors are the ability to transduce different non-dividing cells, a more robust gene expression, and the size-flexibility in the design of the expression cassette (Schambach and Baum, 2008). Although to date retroviral vectors were used in more than 20% of the approved, ongoing, or completed clinical gene therapy trials (317 out of 1472), only the small number of 18 trials employed lentiviral vectors (as of Sept. 2008) (www.wiley.co.uk/genetherapy/clinical/). Many of those are currently in an early phase I/II. Only a few clinical trials are reported on so far:

The first clinical trial with lentiviral vectors was performed on individuals suffering from the acquired immunodeficiency syndrome (AIDS) caused by HIV-1 (Dropulic and June, 2006; Levine et al., 2006). In this case $CD4^+$-T-cells were transduced *ex vivo* using HIV-1-derived vectors to express an HIV Env antisense RNA. After i.v. injection the viral load remained unaffected, but the T-cell count remained stable or even increased. After 36 months no evidence for insertional mutagenesis could be seen.

Two clinical trials have been started using HIV-1-derived vectors for patients suffering from β-thalassemia and X-linked adrenoleukodystrophy (ALD) in 2006 and 2007, respectively. To date only conference reports are available. For ALD, two children have been treated with gene-corrected HSCs and are doing well (Cartier et al., 2007).

Lentiviral vectors generated from the equine infectious anemia virus (EIAV) were used for treatment of Parkinson's disease. The EIAV vector encodes for three basic dopamine biosynthetic enzymes, and is currently tested in a phase I/II clinical trial for evaluation of biosafety and efficiency in patients (Jarraya et al., 2008).

2.2 Monocytes

Monocytes play an important role in immune defense, inflammation, and tissue remodeling. These functions are fulfilled by means of phagocytosis, antigen processing and presentation, and cytokine production. Monocytes stem from a common hematopoietic progenitor, the macrophage and dendritic cell (DC) precursor (MDP). Apart from monocytes, MDPs are the common precursors of macrophages and the two main DC-subsets, i.e. splenic DCs (cDCs) and plasmacytoid DCs (pDCs) (Figure 6) (Fogg et al., 2006; Naik et al., 2006; Varol et al., 2007).

Monocyte subsets

In humans, two major subsets of circulating monocytes can be distinguished by their expression of CD14 (a component of the lipopolysaccharide receptor complex) and CD16

(an FcγRIII immunoglobulin receptor). The major monocyte population, representing 80% - 90% of the circulating monocytes, are $CD14^{high}CD16^{-}$ monocytes (referred to as $CD14^{+}$ monocytes). The minor $CD14^{low}CD16^{+}$ monocyte population (referred to as $CD16^{+}$ monocytes) only contributes to 10% - 20% of the circulating monocytes.

Murine monocytes can be identified by the surface marker CD115 (a receptor for macrophage colony stimulating factor), CD11b, the FSC-SSC FASC-profile, and the expression of Gr1 (Geissmann et al., 2003). Gr1 is an epitope which is expressed on Ly6G and Ly6C antigens (Fleming et al., 1993). It is therefore also present on granulocytes, pDCs, and on 40% of the NK cells. In comparing human and murine monocyte populations, the following similarities are found: The $CX3CR1^{low}CCR2^{+}Ly6C^{+}$ population (referred to as $Gr1^{+}$-monocytes) is most similar to the $CD14^{+}$ monocytes and the $CX3CR1^{+}CCR2^{-}Ly6C^{low}$ population (referred to as $CX3CR1^{+}$-monocytes) best resembles the $CD16^{+}$ monocytes. Both subsets of murine monocytes are present to equal quantities (Geissmann et al., 2003). The $CX3CR1^{+}$-monocytes are a product of the $Gr1^{+}$-monocytes (Sunderkötter et al., 2004; Varol et al., 2007).

Monocyte function

The $Gr1^{+}$- and $CD14^{+}$-monocytes (the so-called inflammatory monocytes) are recruited to inflamed tissue and lymph nodes and produce high levels of TNF-α and IL-1. Upon microbial infection they egress from the bone marrow to the bloodstream and differentiate into TNF-α/iNOS-producing DCs (Tip-DCs). The main function of these monocyte-derived inflammatory DCs is to kill bacteria rather than to regulate T cell functions (Auffray et al., 2009). In contrast to $Gr1^{+}$- and $CD14^{+}$-monocytes the $CX3CR1^{+}$-and $CD16^{+}$-monocytes, termed resident monocytes, patrol the blood vessels. In the case of damage and infection, they rapidly invade the tissue followed by initiation of an innate immune response, i.e. the recruitment of inflammatory cells, and by their differentiation into macrophages (Auffray et al., 2007). While the antigen presentation is a classical feature described for monocytes, it has been found to be less efficient in monocytes than in DC subsets (Banchereau and Steinman, 1998).

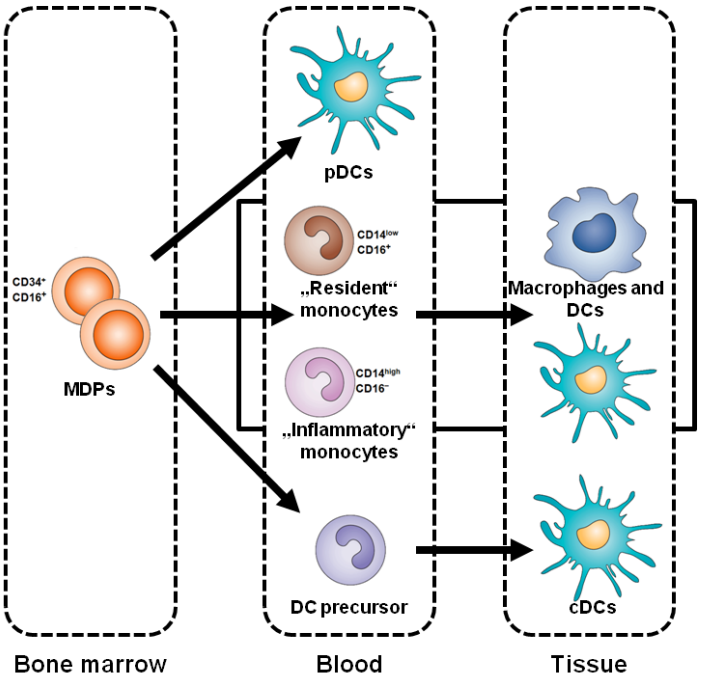

Figure 6: Origin and hematopoietic differentiation of myeloid antigen-presenting cells. (MDP, dendritic cell precursor; DC, dendritic cell; pDC, plasmacytoid DC; cDC, splenic DCs)

2.3 Chronic granulomatous disease

Chronic granulomatous disease (CGD) is a rare disease with approximately one case per 200-500 thousand individuals. Patients with CGD suffer from severe, life-threatening infections and chronic inflammation due to an inability of phagocytes (neutrophils, eosinophils, monocytes and macrophages) to generate reactive oxygen species (ROS), such as superoxide, hydrogen peroxide and hydroxyl radicals, to mediate phagocytic oxidative killing. O_2^-, the precursor of ROS, is produced by the NADPH oxidase, a multi-protein enzyme complex. The enzyme is inactive in resting phagocytes, but becomes activated by the interaction of the phagocytic cells with pathogens and by their subsequent uptake. A genetic alteration in one of the NADPH subunits, either $gp91^{phox}$, $p67^{phox}$, $p47^{phox}$, or $p22^{phox}$ (phox: phagocytic oxidase), results in a non-functional NADPH-oxidase, causing the disease. The most common form (50-70%) is linked to a deficiency of the $gp91^{phox}$ subunit, resulting from a mutation in the *CYBB* gene encoding $gp91^{phox}$ (Johnston, 2001). The *CYBB* gene is located on the x-chromosome; hence, the $gp91^{phox}$ defect leads to the so-called X-linked chronic granulomatous disease (xCGD).

NADPH oxidase and ROS

The NADPH oxidase consists of six hetero-subunits. The catalytic core, a heterodimeric flavocytochrome b_{558}, is formed by the membrane proteins $gp91^{phox}$ and $p22^{phox}$. Only after

the appropriate stimuli, the enzymatic activity is activated by the translocation of the other NADPH subunits $p67^{phox}$, $p47^{phox}$, and $p40^{phox}$, and the small GTPase Rac, from the cytosol to the membrane. The activated NADPH-complex can perform an electron transfer from the co-enzyme NADPH to oxygen, resulting directly in superoxide. It is also described to activate microbicidal azurophil granule proteases, such as cathepsin G and elastase (Rada et al., 2004; Reeves et al., 2002), as well as microbicidal neutrophil extracellular traps (Fuchs et al., 2007) (Figure 7). The reactive oxygen species have also been shown to be involved in functions other than oxidative killing. These include metabolism, cell death, apoptosis, regulation of inflammation, induction of host defense genes, and oxidative signaling (Bylund et al., 2005; Kimura et al., 2005).

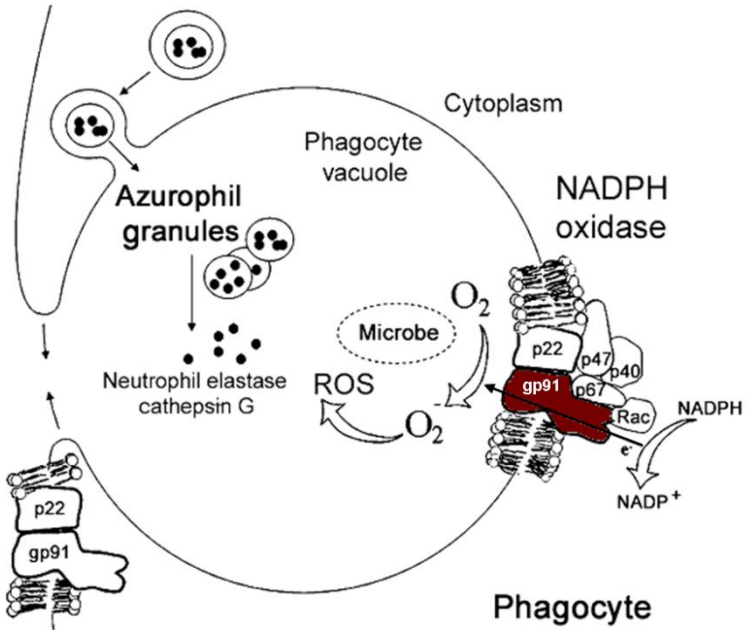

Figure 7: Phagosome formation and oxidative killing of microbes (bacteria and fungi) by phagocytic cells. (Modified from Seger, 2008)

The CGD individuals suffer from a range of infections, mainly pneumonia, abscesses of the skin, tissues, and organs, suppurative arthritis, osteomyelitis, and bacteremia/fungemia. The most common organisms causing diseases are the fungi from *Aspergillus* species and *Candida albicans*, and the bacteria *Staphylococcus aureus* and *Burkholderia cepacia* complex bacteria (Mouy et al., 1989; Winkelstein et al., 2000). In addition to the infections, CGD patients frequently have exuberant and persistent tissue granuloma formation - clinical manifestations of chronic inflammation. As a result of these recurring and severe infections, CGD individuals have an average life expectancy of 18 years +/- 2.6 years (Wolach et al., 2008).

Treatment of CGD

The general medication for CGD is a lifelong prophylaxis against infections. The antibiotic trimethoprim-sulfamethoxazole is administered to decrease the frequency of bacterial infections, itraconazole to prevent fungal infections, and IFN-γ is used to reduce severity of infections. In acute phases, the treatment depends on the type and severity of the infection and includes antibiotic treatment, antifungal therapy, or surgical interventions. In selected CGD patients with life-threatening bacterial and fungal infections a white cell transfusion (granulocyte transfusion) has been performed (von Planta et al., 1997). Although the allogenic cell transfusion is generally well tolerated, adverse events often arise and the risk of alloimmunization to HLA antigens may complicate later allogeneic stem cell transplantation (Stroncek et al., 1996). Interestingly, a small amount of wild-type neutrophils is able to synergize with CGD neutrophils in extracellular *Aspergillus* hyphae killing (Rex et al., 1990).

In order to cure CGD, hematopoietic stem cell transplantation (HSCT) is possible if a human leukocyte antigen identical donor is available. A study of 27 patients who received a marrow graft after conditioning from HLA-identical sibling donors showed an overall cure in 81% of the patients. Severe side effects and graft-versus-host disease were exclusively observed in patients with ongoing infections at the time of transplantation (Seger et al., 2002). Hence, at best infections should be under control before starting to condition for HSCT (Seger, 2008). In the absence of a potential stem cell donor, HSCT is considered to be very risky due to graft failure and a delayed immune reconstitution, but has been performed twice (Kikuta et al., 2006).

In such cases, stem cell gene therapy might become more and more an option for xCGD. As a small amount of corrected neutrophils (~ 5-10%) appears to be highly beneficial (Dinauer et al., 2001; Mills et al., 1980) and the expression of only small amounts of $gp91^{phox}$ is needed for sufficient superoxide production (Bjorgvinsdottir et al., 1997), gene therapy seems well feasible. The problem is that corrected cells lack a selective growth advantage (Stein et al., 2006). Recent gene therapy trials have been performed on one patient in Zurich (2002) and two patients in Frankfurt (2004) using gene-modified $CD34^{+}$-cells (Ott et al., 2006). In the two patients in Frankfurt a high gene marking in peripheral blood leukocytes between 10% and 30% was achieved 3-4 months after transplantation, leading to the elimination of pre-existing bacterial and fungal infections. Later, in both patients the activation of the growth-promoting genes MDS1/EVI1, PRDM16 and SETBP1 caused by insertional activation led to an increase of the gene-corrected cells up to 50-60% of all peripheral blood granulocytes with an existing clonal dominance (Grez, 2008). Although the presence of the transgene remained high in both patients, the expression of $gp91^{phox}$ decreased to almost undetectable

levels caused by methylated gene-silencing (Schultze-Strasser, unpublished data). One of the patients died from a severe sepsis 2.5 years after gene therapy (Alexander et al., 2007).

2.4 Objective

In contrast to other lentiviral vectors, SIVsmmPBj-derived vectors have been proven to efficiently transduce primary human monocytes. This capacity was linked to the *vpx*-gene of PBj, one of this lentivirus' accessory genes. As monocytes constitute a potential target for gene therapy, enhanced PBj vectors suitable for clinical applications had to be developed, and their capacity for functional transfer of therapeutic genes demonstrated.

In the first part of this thesis, the aim was to clarify whether vectors derived from other *vpx*-carrying lentiviruses also reveal the capacity for monocyte transduction. Therefore, lentiviral vectors derived from other viruses of the HIV-2/SIVsmm/SIVmac lineage were to be investigated. The monocyte transduction capacity of HIV-2 and SIVmac vectors was to be tested in comparison to PBj and HIV-1 vectors, and the contribution of the respective *vpx*-genes analyzed.

The main focus of the thesis was on the enhancement of monocyte-transducing lentiviral vectors meeting the required standards for clinical applications concerning gene transfer efficiency and safety. On the basis of the preliminary vector systems available, the goal was to generate high titer vectors revealing a high safety profile. Since available packaging constructs already hold a satisfactory stage of development, the emphasis was laid on the optimization of transfer vectors. Therefore, all elements required for efficient gene transfer had to be inserted and as many needless sequences as possible deleted from the transfer constructs. The vectors should best be designed as self-inactivating (SIN) vectors in order to avoid activation of adjacent cellular genes after integration into the target cell´s genome.

Finally, the new vectors' suitability for future gene therapy approaches was to be demonstrated. The inherited human xCGD was chosen as disease model since a transfer of the correct version of the mutant gene *gp91^{phox}* into monocytes may offer a clinical benefit for patients. In this thesis, the goal was to lay a foundation for analyzing *gp91^{phox}* gene therapy of monocytes. Since the use of rare patient´s monocytes is not advisable at this early stage of development, it was decided to study the efficiency of *gp91^{phox}*-gene transfer in a murine model, using monocytes of healthy human donors only for the development of methods to demonstrate gp91^{phox}-dependent functions like oxidative burst and killing of pathogens. In

murine models including *gp91^{phox}*-knockout mice, the functional *ex vivo* transfer of the *gp91^{phox}*-gene into murine monocytes, as well as the *in vivo* half-life of transplanted monocytes in the bloodstream and their biodistribution were to be investigated to predict the suitability of this novel gene therapy approach.

3 Material and Methods

3.1 Material

3.1.1 Chemicals and consumables

Unless noted otherwise, all chemicals used were obtained in p.a. quality from the companies Merck, Sigma-Aldrich, or Roth. The consumables for cell culture and molecular biology were obtained from the companies BD™, Eppendorf, Gipco, Greiner, Nunc, or Sarstedt.

3.1.2 Enzymes and antibiotics

enzymes	source
restriction endonucleases	New England Biolabs
T4-DNA-ligase	New England Biolabs
Taq-High-Fidelity-DNA-Polymerase	Invitrogen
Klenow-polymerase	New England Biolabs
Antarctic Phosphatase	New England Biolabs

antibiotics	source
ampicillin	Roche
penicillin	Biochrom AG
streptomycin	Biochrom AG

3.1.3 Kits

kits	source
QIAprep Spin Miniprep Kit	Qiagen
EndoFree Plasmid Maxi Kit	Qiagen
DNeasy Blood and Tissue Kit	Qiagen
QIAquick Gel Extraction Kit	Qiagen
QIAquick PCR Purification Kit	Qiagen
Monocyte Isolation Kit II, human	Mitenyi Biotech
QuikChange Site-Directed Mutagenesis Kit	Stratagene
BURSTTEST (PHAGOBURST)	ORPEGEN Pharma
Cytofix/Cytoperm Fixation/Permeabilization Solution Kit	BD Biosciences

3.1.4 Plasmids

name	characterization	source
expression plasmids		
pVpxPBj	Expression plasmid of unmodified Vpx of SIVsmmPBj	Nina Wolfrum, Paul-Ehrlich-Institut
pVpxHIV-2	Expression plasmid of unmodified Vpx of HIV-2	this thesis
pVpxMAC	Expression plasmid of unmodified Vpx of SIVmac	this thesis
pVpxHIV-2-nFLAG	Expression plasmid of unmodified Vpx of SIVsmmPBj carrying a n-terminal FLAG-tag	this thesis
pHA-VpxPBjsyn	Expression plasmid of codonoptimized Vpx of SIVsmmPBj carrying a n-terminal HA-tag	André Berger, Paul-Ehrlich-Institut
pVpxPBjsyn (9.1)	Expression plasmid of codonoptimized Vpx of SIVsmmPBj	this thesis
pVpxHIV-2syn	Expression plasmid of codonoptimized Vpx of HIV-2	Andre Berger, Paul-Ehrlich-Institut
pcDNA3.1(+)	Commercially available backbone for expression plasmids, contains a MCS downstream a CMV promoter, ampicillin resistance	Invitrogen
pMD.G2 (9.2)	VSV-G expression plasmid	D. Trono, Tronolab, Switzerland
two-plasmid vector systems		
pPBj-ΔEeGFP	Genome of SIVsmmPBj1.9 containing a 1 kb deletion in the *env* gene. Expresses eGFP under the control of a CMV promoter.	(Mühlebach et al., 2005)
pPBj-4xKOeGFP	Genome of SIVsmmPBj1.9 containing a 1 kb deletion in the *env* gene and point mutations in the start-ATGs of *vif*, *vpx*, *vpr*, and *nef*. Expresses eGFP under the control of a CMV promoter.	Julia Kaiser, Paul-Ehrlich-Institut
pHIV-1-NL4-3	Genome of HIV-1 (NL4-3) containing a 1.2 kb deletion in the *env* gene. Expresses eGFP under the control of a CMV promoter.	(Mühlebach et al., 2005)
pHIV-2-RodA	Genome of HIV-2 (Rod A) containing deletion in the *env* gene. The eGFP is inframe within the *nef* gene and therefore expressed under control of the viral LTR.	(Reuter et al., 2005)
packaging constructs		
pCMVΔR8.9 (9.3)	HIV-1 packaging plasmid	U. Blömer, University Hospital Kiel, (Zufferey et al., 1997)
pSIV3+	SIVmac packaging plasmid	F.-L. Cosset, University of Lyon, (Negre et al., 2000)
pPBj-pack (9.4)	SIVsmmPBj packaging plasmid	Nina Wolfrum (Wolfrum 2005
pHIV-2d4 (9.5)	HIV-2 packaging plasmid	Carsten Münk, Paul-Ehrlich-Institut

SIVsmmPBj-derived transfer vectors		
pPBj-trans	SIVsmmPBj-derived transfer vector encoding *eGFP* under control of the CMV promoter, contains second exons of *tat* and *rev,* deficient for CTS-element	(Wolfrum, 2005)
pPBj-trans-SIN	Based on pPBj-trans, the second exons of *tat* and *rev* are deleted, SIN-configuration	this thesis
pPBj-trans-cSIN	Based on pPBj-trans-SIN, 1 kb *pol*-deletion and reintroduced cPPT/CTS-element	this thesis
pPBj-SEW-SIN	Based on pPBj-trans-SIN encoding *eGFP* under control of the SFFV promoter, contains WPRE	(Högner, 2007), diploma thesis
pPBj-SEW-cSIN	Based on pPBj-trans-cSIN and pPBj-SEW-SIN, encoding *eGFP* under control of the SFFV promoter, contains WPRE, SIN-configuration	this thesis
pPBj-SR-SEW-cSIN (9.6)	Based on pPBj-SEW-cSIN, SV40/RSV-element replaces U3 in 5'LTR	this thesis
pPBj-MCS (9.7)	SIVsmmPBj-derived transfer vector with MCS derived by Fusion-PCR	this thesis
pPBj-SEW	Based on pPBj-MCS. encoding *eGFP* under control of the SFFV promoter, contains WPRE	this thesis
pPBj-g'-SEW	Based on pPBj-SEW, integrated stop-codon 10 triplets downstream the *gag* start-ATG	this thesis
pPBj-SR-SEW	Based on pPBj-SEW, SV40/RSV-element replaces U3 in 5'LTR	this thesis
pPBj-SR-g'-SEW (9.8)	Based on pPBj-g'-SEW and pPBj-SR-SEW, integrated stop-codon 10 triplets downstream the *gag* start-ATG, SV40/RSV-element replaces U3 in 5'LTR	this thesis
HIV-2-derived transfer vectors		
pHIV-2-MCS (9.9)	HIV-2-derived transfer vector with MCS derived by Fusion-PCR	this thesis
pHIV-2-SEW	Based on pHIV-2-MCS encoding *eGFP* under control of the SFFV promoter, contains WPRE	this thesis
pHIV-2-g'-SEW	Based on pHIV-2-SEW, integrated stop-codon 11 triplets downstream the *gag* start-ATG	this thesis
pHIV-2-SR-SEW	Based on pHIV-2-SEW, SV40/RSV-element replaces U3 in 5'LTR	this thesis
pHIV-2-SR-g'-SEW (9.10)	Based on pHIV-2-g'-SEW and pHIV-2-SR-SEW, integrated stop-codon 11 triplets downstream the *gag* start-ATG, SV40/RSV-element replaces U3 in 5'LTR	this thesis
pHIV-2-SgW (9.11)	Based on pHIV-2-MCS, encoding $gp91^{phox}$ under control of the SFFV promoter, contains WPRE	this thesis

HIV-1-derived transfer vectors		
pHR-CMV-GFP	Genome of HIV-1 containing a deletion in the *env* gene, encoding *eGFP* under control of the CMV promoter	U. Blömer, University Hospital Kiel, (Miyoshi et al., 1998)
pHIV-1-SgpSw (9.12)	HIV-1 transfer-vector encoding *gp91^{phox}* under control of the CMV promoter, contains WPRE, SIN-configuration	Manuel Grez, Georg-Speyer-Haus
pHIV-1-SEW (9.13)	HIV-1 transfer-vector encoding *eGFP* under control of the SFFV promoter, contains WPRE, SIN-configuration	Manuel Grez, Georg-Speyer-Haus
SIVmac-derived transfer vectors		
pGAE-SFFV-WPRE	SIVmac transfer-vector encoding *eGFP* under control of the SFFV promoter, contains WPRE, SIN-configuration	Dorothee von Laer, Georg-Speyer-Haus
MLV-derived transfer vectors		
pSER11S91-SW	SIVmac transfer-vector encoding *eGFP* under control of the SFFV promoter, contains WPRE, SIN-configuration, SV40/RSV-element replaces U3 in 5'LTR	A. Schambach, Hannover Medical School (Schambach et al., 2006b)

3.1.5 Oligonucleotides

All oligonucleotides were synthesized from the company Eurofins MWG Operon.

name	5'→3' sequence	restriction site
BPK 1	tgagaattctaggtagtaagcgatgtcagatcccag	EcoRI
BPK 2	atcctcgagctattatgctagtcctggaggggagg	XhoI
BPK 3	tgagaattctagagtgcaacaaaatgacagac	EcoRI
BPK 4	atcctcgagctattagaccagacctggaggggagg	XhoI
BPK 5	ggtggaattcgagccatgagcgaccccagagagagaatc	EcoRI
BPK 6	tcactcgagtcattaggccagtccaggaggggagg	XhoI
BPK 7	tcaagcttcgaattctgcagtcga	EcoRI
BPK 8	gtaggtaggctatctgaactctgctttacttgtacagctcgt	
BPK 9	acgagctgtacaagtaaagcagagttcagatagcctacctac	
BPK 10	tgactgaatacagagcgaaatgttttatgtcttctatcactg	
BPK 11	cagtgatagaagacataaaacatttcgctctgtattcagtca	
BPK 12	ggtggcggccgctctagaactagggcgactaggagagat	NotI
BPK 13	gcaggttggcgcccgaacag	KasI
BPK 14	aactgccattagtactatagtccaaatctgtccaattcattt	
BPK 15	aaatgaattggacagatttggactatagtactaatggcagtt	
BPK 16	aaggcaattggagtaatctctactaatttgtaatctcccaactccaatcgttccacagct ggtctctgcc	MfeI
BPK 17	tgaggcgcctgaactagtgaaggcctgaaataacctctgaaag	KasI, SpeI
BPK 18	tgccagcctctccgcagagtgagtttattgtatcgagctaggca	
BPK 19	tgcctagctcgatacaataaactcactctgcggagaggctggca	
BPK 20	tcttccctgacaagacggagttt	

name	5'→3' sequence	restriction site
BPK 21	acggtatcgataagcttctg	HindIII
BPK 22	ttgttctgtggtgatcatattgactaatctttctgctggagtcatatcccctattcctccccttc ttttaaaattctcatcatggagctaaaactgaaagaa	
BPK 23	gtcaatatgatcaccacagaacaagaaatacaattccaacaatcaaaaaattcaaa atttaaaaattttcgggtctgattggagttgggagattacaa	
BPK 24	taataaatcccttccagtccccccttttctttttataaaatgatcaaccggtggatcctgca gaattctcatttggccatggtacagtagt	
BPK 25	gggactggaagggatttattacagtgatagaagacataaaatgacatttcgctctgtat tcagt	
BPK 26	ggtggcggccgctctagaac	NotI
BPK 27	ttgatatcgaattcctgcag	EcoRI
BPK 28	tcagaattctcatcgacggtatcgatcaggcg	EcoRI
BPK 29	gcgagaaactccgtcttgtgagggaagaaagcag	
BPK 30	ctgctttcttccctcacaagacggagtttctcgc	
BPK 31	tgactcgaggtccgtggcctgaaataacctct	XhoI
BPK 32	tgccagcctctccgcagagtgagtttattgtatcgagctaggca	
BPK 33	tgcctagctcgatacaataaactcactctgcggagaggctggca	
BPK 34	gctctcactctccttcaagt	KasI
BPK 35	tgaaagcttgtcgactgagaggatgtattacagtgagagaa	HindIII, SalI
BPK 36	gttctgtggtgatcatattgattaatctttctgatggagtcatatcccctattcccccccttctt ttaaaattcatgctcatcataccattggatctaaaactgtaagaa	
BPK 37	caatatgatcaccacagaacaagagatacaattcctccaagccaaaaattcaaaat taaaaaattttcgggtctatttcagagtgagtgtgttcgtgctagggttc	
BPK 38	aaacatcccttccagtcccccccttgtttttattaaatgttcactcgaggtaccggtcaatt gctagcccctcccagtcaggtgctaagga	
BPK 39	ggggactggaagggatgttttacagtgaaagaagacataaaatcttcggtcgctctg cggagaggctgg	
BPK 40	ccgcggcggccgctcaaccg	SacII, NotI
BPK 41	tgacaattgtgaagattttatttagtctccag	MfeI
BPK 42	tcacaattgcgacggtatcgatcaggcgg	MfeI
BPK 43	gaaactccgtcttgagagggtaaaaagcagatgaattagaa	
BPK 44	ttctaattcatctgctttttaccctctcaagacggagtttc	
BPK 45	ttgctcacatgttctttcct	PciI
BPK 46	ttcagaggttatttcaggccctctcagtcgacaagcttat	
BPK 47	ataagcttgtcgactgagagggcctgaaataacctctgaa	
BPK 48	cctagctcgatacaataaactcgctctgcggagaggctgg	
BPK 49	ccagcctctccgcagagcgagtttattgtatcgagctagg	
BPK 50	ctgttcaggcgccaacctgc	KasI
BPK 51	tgacaattgtgagggaatgaaagaccccacct	MfeI
BPK 52	tcaaccggttcaaattcgacaacaccacggaa	AgeI

3.1.6 Bacterial strains and culture media

Name	genotype	source
E. coli TOP 10 F'	F´{*lacI*^{q} Tn10 (Tet^{R})} *mcr*A, D(*mrr-hsd*RMS-*mcr*BC) F80 *lac*ZDM15 D*lac*X74 *deo*R *rec*A1 *ara*D139 D(*ara-leu*)7697 *gal*U *gal*K *rps*L (Str^{R}) *end*A1 *nup*G	Invitrogen
E. coli GM2163	*dam*13::*Tn*9(Cam^{R}) *dcm*-6 *hsd*R2 *leu*B6 *his*G4 *thi*-1 *ara*-14 *lac*Y1 *gln*V44 *gal*K2 *gal*T22 *xyl*A5 *mtl*-1 *rps*L136(Str^{R}) *tsx*78 *mcr*A *mcr*B1 *fhu*A31 *rfb*D1 R(zgb210::Tn10) TetS *end*A1	New England Biolabs
E. coli Stable2	F^{-} *mcr*A D(*mrr-hsd*RMS-*mcr*BC) *rec*A1 *end*A1 lon gyrA96 *thi*-1 *sup*E44 *rel*A1l^{-}D (*lac-pro*AB)	Invitrogen
S. aureus	ATCC25923	Julia Brachert, Paul-Ehrlich-Institut

Luria-Bertani (LB) medium	
Bacto-Trypton	1.0% (w/v)
yeast extract	0.5% (w/v)
NaCl	1.0% (w/v)
pH 7.0	

S.O.C. medium (Invitrogen)	
Tryptone	2.0% (w/v)
yeast extract	0.5% (w/v)
NaCl	10 mM
KCl	2.5 mM
$MgCl_2$	10 mM
$MgSO_4$	10 mM
glucose	20 mM

3.1.7 Cell lines and culture media

name	Genotype	source
HEK-293T	human embryonic kidney cell line genetically engineered to express the large T antigen	ICLC HTL04001
HT1080	human fibrosarcoma cell line	ATCC CCL-121
PLB-985	human acute myeloid leukemia cell line	Manuel Grez, Georg-Speyer-Haus
xCGD-PLB-985	human acute myeloid leukemia cell line with a disrupted *CYBB* gene by homologous recombination (Zhen et al., 1993)	Manuel Grez, Georg-Speyer-Haus

Culture medium for HEK-293T and HT1080 cells

Dulbecco`s modified Eagle medium (DMEM) obtained from Biochrom AG supplemented with 10% fetal calf serum (FCS; Biochrom AG), 2 mM L-glutamine (Biochrom AG), 100 units/ml streptomycine, and 50 µg/ml penicillin.

Culture medium for PLB-985 and xCGD-PLB-985 cells

RPMI 1640 medium obtained from Biochrom AG supplemented with 10% FCS, 2 mM L-glutamine, 100 units/ml streptomycine, and 50 µg/ml penicillin.

Culture medium for murine and human monocytes

Dulbecco`s modified Eagle medium (DMEM) obtained from Biochrom AG supplemented with 10% AB serum (Sigma-Aldrich), 2 mM L-glutamine (Biochrom AG), 1x non-essential amino acids (NEAA) (Gibco), 100 units/ml streptomycine, and 50 µg/ml penicillin.

3.1.8 Mouse strains

strain name	Discription	source, provided by
C57BL/6	C57BL/6 is the most widely used inbred mouse strain	The Jackson Laboratory
B6.SJL-*Ptprc*^{a} *Pepc*^{b}/BoyJ (CD45.1 mice)	Congenic strain which carries the antigen CD45.1 expressed on all hematopoietic cells except mature erythrocytes and platelets. Background strain: C57BL/6	The Jackson Laboratory, Manuel Grez
B6.129S6-*Cybb*^{tm1Din}/J (xCGD mice)	Mice with a null allele of the *Cybb*^{tm1Din} gene involved in X-linked CGD, which encodes the 91 kD subunit of the oxidase cytochrome b. (Pollock et al., 1995) Background strain: C57BL/6	The Jackson Laboratory, Manuel Grez
BALB/cAJic-RAG2^{null} IL-2Rg^{null} (Rag-2/gc$^{-/-}$ mice)	Mice lacking T cells, B cells, and NK cells Background strain: BALB/c	Markus Manz, Dorothee von Laer
C57BL/6-Tg(CAG-GFP)1Osb/J (GFP mice)	Mice expressing *eGFP* that makes all of the tissues, with the exception of erythrocytes and hair, appear green under excitation light.(Okabe et al., 1997) Background strain: C57BL/6	Dorothee von Laer

3.2 Methods of molecular biology

3.2.1 Cultivation of bacteria

Liquid culture

Bacteria were grown in LB medium supplemented with 0.1 mg/ml ampicillin (LB_{Amp}) either at 37°C over night or at 25°C for 60 - 72 h and 200 rpm in a bacteria shaker (Innova® 4200, New Brunswick Scientific).

Culture plate

The cultivation on LB_{Amp} plates (1% (w/v) Bacto-Trypton, 0.5% (w/v) yeast extract, 1% NaCl, 50 µg/ml ampicillin, 1.5% (w/v) agar agar) or standard-1-agar plates (1.5% (w/v) Bacto-Peptone, 0.3% (w/v) yeast extract, 0.6% NaCl, 0.1% (w/v) D (+)-Glucose, 1.2% (w/v) agar agar) were performed by applying bacteria onto the plates using inoculation spreader (Sarstedt) and subsequent incubation at 37°C or 25°C in a bacteria incubator (Innova® 4200, New Brunswick Scientific) until bacteria colonies were visible. The overgrown plates were stored for up to one month at 4°C.

3.2.2 Cloning processes

Restriction

All DNA restrictions were performed using commercially available type II restriction endonucleases from New England Biolabs (NEB) according to the manufacturer's instructions. For a preparative restriction 3 µg and for an analytical restriction 500 ng DNA were used.

Standard restriction:

500 ng or 3 µg	DNA for analytical or preparative purpose
1 µl or 1.5 µl	restriction enzyme for analytical or preparative purpose
2 µl	10x buffer (corresponding NEB buffer 1-4)
2 µl	10x BSA
ad 20 µl	Aqua bidest

The reaction was incubated for 1 h at 37°C in a thermoblock (Thermomixer comfort, Eppendorf). In case of a double digest the optimal buffer for the double digest was chosen to the manufacturer's instructions.

DNA Polymerase I, Large (Klenow)

The Klenow polymerase is a proteolytic product of E. coli DNA polymerase I which retains polymerization and 3'→ 5' exonuclease activity, but has lost 5'→ 3' exonuclease activity.

Therefore, the Klenow polymerase was used to fill-in 5´ overhangs or for the removal of 3´ overhangs to form blunt ends.

Standard Klenow-reaction:

30-50 µl	restricted DNA, purified by gel extraction or PCR purification
1 µl	Klenow
10 µl	NEBuffer 2
3,3 µl	dNTPs (1 mM)
ad 100 µl	Aqua bidest

The reaction was incubated for 15 min at 25°C in a thermoblock (Thermomixer comfort, Eppendorf).

Antarctic Phosphatase

The Antarctic Phosphatase catalyzes the removal of 5´ phosphate groups from DNA and RNA. Since phosphatase-treated fragments lack the 5´ phosphoryl termini required by ligases, they cannot self-ligate. This property was used to decrease the vector background in cloning strategies.

Standard Antarctic Phosphatase reaction:

50 µl	restricted DNA
6 µl	Antarctic-Phosphatase-Buffer 2 (10x)
1 µl	Antarctic-Phosphatase
ad 60 µl	Aqua bidest

The reaction was incubated for 15-60 min at 37°C in a thermoblock (Thermomixer comfort, Eppendorf).

Ligation

For ligation, the T4-DNA-ligase, which catalyses the formation of phosphodiester bonds between the fragments under consumption of ATP, was used. The Ligation was applied for fragments exhibiting complementary overhangs (sticky-end ligation) or blunt ends (blunt-end ligation).

Standard ligation:

3:1	Insert:Vector ratio
0.1-1.0 µg	Total DNA
1.0 or 0.1 units	Ligase for blunt-end or for sticky-end
ad 20 µl	Aqua bidest

The reaction mix was incubated at 16°C over night in a thermomixer (Thermomixer comfort, Eppendorf).

3.2.3 Generation and transformation of competent bacteria

Transformation of *E. coli* (TopF10, GM2163, Stable2) is the method of choice to amplify plasmid DNA through cellular replication. For this purpose, bacteria have to be prepared for the uptake of foreign DNA.

For the generation of chemically competent bacteria 2.5 ml of an overnight culture were used to inoculate 100 ml LB medium, which were subsequently incubated at 37°C and 180 rpm in a bacteria shaker (innova™ 4200, New Brunswick scientific). Cells were grown to an OD_{550} of about 0.5 - 0.55 reaching the logarithmic growth phase. Then the culture was incubated on ice for 5 min, divided into two portions and pelleted at 4,000 rpm for 10 min at 4°C (Multifuge 3SR, Heraeus). Next, the pellets were each resuspended in 20 ml TFB1 buffer (sterile filtrated solution of 30 mM KOAc, 100 mM $RbCl_2$, 10 mM $CaCl_2$, 50 mM $MnCl_2$, 15% glycerine, pH adjusted to 5.8 with HAc), incubated on ice for 5 min and once again pelleted as above. Subsequently the bacteria were resuspended each in 2 ml TFB2 buffer (sterile filtrated solution of 10 mM MOPS, 75 mM $CaCl_2$, 10 mM $RbCl_2$, 15% glycerine, pH adjusted to 6.5 using KOH-solution) and incubated on ice for 15 min. Afterwards the suspension was portioned á 100 µl into 1.5 ml reaction tubes and frozen at -80°C.

To transform the chemically competent *E. coli* bacteria, they were thawed on ice and approximately 50 ng DNA or 10 µl of a ligation reaction (3.2.2) were added to one aliquot. After further incubation on ice for 30 min, a heat shock at 42°C for 45 sec was performed in a thermoblock (Eppendorf). Then 500 µl of pre-warmed (37°C) S.O.C. medium were added to the sample before it was incubated at 600 rpm for 60 min at 37°C in a thermoblock (Eppendorf). Then the bacteria suspension was applied to LB_{Amp} plates (2.2.1) and incubated at 37°C over night or at 25°C for 72 h.

3.2.4 Plasmid preparation

Plasmid preparation from transformed bacteria was performed using the QIAprep® Spin Miniprep kit or the EndoFree® Plasmid Maxi kit according to the manufacturer's instructions. These kits use an anion-exchange tip where plasmid DNA selectively binds under low-salt and pH conditions. RNA, proteins, metabolites, and other low-molecular-weight impurities are removed by a medium-salt wash, and pure plasmid DNA is eluted in high-salt buffer. The DNA is concentrated and desalted by isopropanol precipitation and collected by centrifugation.

For purification of low amounts of DNA (Miniprep), 3 ml LB_{Amp} medium were inoculated with one bacteria clone in a 13 ml tube (Sarstedt) and incubated over night at 37°C or for 48 h at 25°C. The bacteria broth was transferred to a 15 ml conical tube (Greiner bio-one) and pelleted at 2,400 rpm for 10 min at RT in a centrifuge (Multifuge 3SR, Heraeus). The

resulting pellet was used for the preparation of plasmid DNA according to the manufacturer's instructions of the QIAprep® Spin Miniprep kit.

For extraction of larger amounts of DNA (Maxiprep) 250 ml LB_{Amp} medium were inoculated and cultivated over night at 37°C or for 48 h at 25°C in 500 ml glass bottles (Schott Duran). The bacteria broth was transferred to a 250 ml tube (Nalgene) and centrifuged at 6,000 rpm for 10 min at RT (Beckman J2-21). The resulting pellets were used for the preparation of plasmid DNA according to the manufacturer's instructions of the EndoFree® Plasmid Maxi kit (Quiagen).

Finally, the concentration of the isolated plasmid DNA was determined photometrically (GeneQuant pro, Amersham Biosciences) at absorption A_{260}.

3.2.5 Agarose gel electrophoresis

Agarose gel electrophoresis allows the separation of DNA molecules by their size. For this purpose 1% agarose gels were used, by default. For their preparation, the corresponding amount agarose (Biozym Scientific GmbH) was dissolved in 1x TAE buffer (40 mM Tris-Acetat, 1 mM EDTA) by heating the emulsion in a microwave oven. Before the gel was casted into a tray, 0.1 µg/µl ethidium bromide was added. The ethidium bromide intercalates into DNA strands and can be visualized under UV light. After the polymerization of the gel it was covered in 1x TAE buffer and loaded with the samples. The DNA samples were mixed with 6x loading buffer (0.25% brome phenol blue, 0.25% xylenxyanol, 30% glycerin in aqua bidest). As marker, 1.0 µg of a 1 kb DNA ladder (NEB) was used. The DNA fragments were separated by applying 80 V or 120 V for approx. 45 min in an Xcell SureLock™ electrophoresis cell (Invitrogen). The DNA fragment were visualized on a transilluminator (Intas Science Imaging Instruments GmbH) and documented or extracted from the gel (3.2.6).

3.2.6 Gel extraction of DNA fragments

After electrophoretic separation, the DNA fragment of interest was cut out of the gel and transferred into a 1.5 ml micro tube (Sarstedt). The following purification of the DNA from the agarose gels was performed using the Gel Extraction Kit (Quiagen) according to the manufacturer's instructions. This kit is based on binding of DNA to silica gel membranes in the presence of a high concentration of chaotropic salt. After impurities are washed away the pure DNA was eluted using 50 µl of aqua bidest.

3.2.7 Nucleic acid sequencing

Nucleic acid sequencing was performed at the company Eurofins MWG Operon. For this purpose, DNA samples containing approximately 1 µg plasmid DNA were lyophilized in a Speedvac sc 100 (Savant) and sent via regular mail together with appropriate primers of 10 pmol/µl to the company.

3.2.8 Polymerase chain reaction (PCR)

PCR allows the amplification of specific DNA sequences from different origins, such as plasmid, genomic or complementary DNA. The amplified fragment can be used for further molecular biological methods. In this thesis, the PCR was performed with the DNA-dependent High-Fidelity Taq Polymerase (Invitogen). With the appropriate buffers, oligonucleotides (primers), deoxynucleotides and cycling conditions, the DNA polymerase amplifies a DNA fragment (template) bordered by the forward and reverse primer in an exponential manner. A typical PCR cycle contains a denaturizing step at 94°C, leading to the dissociation of the double stranded template. The following hybridization step allows primer annealing to the complementary sequences on the single stranded template. The exact hybridization temperature TH is depends on the G/C-A/T content of the primers. It can be calculated roughly corresponding to the Wallace rule (Suggs et al., 1981): TH = 4x(G+C) + 2x(A+T) - 5. After hybridization, DNA elongation is performed at the temperature optimum of the used DNA-polymerase. By repeating this cycle sequence, the template is amplified in an exponential manner.

Standard PCR-reaction

2 µl	Plasmid DNA template (5 ng/µl)
1 µl	dNTP (10 mM)
1 µl	Forward primer (5 pm/µl)
1 µl	Reverse primer (5 pm/µl)
5 µl	Buffer (10x) mit $MgCl_2$
0.5 µl	High-Fidelity Taq Polymerase (2.5 U/µl)
ad 50 µl	Aqua bidest

Standard-PCR-protocol:

denaturation	2 min	94°C	
denaturation	30 sec	94°C	30x
primer hybridization	1 min	58°C	
elongation	60-90 sec	72°C	
elongation	7 min	72°C	
	∞	4°C	

The length of the primer elongation step depends on the length of the amplification product and was adjusted if necessary. In some cases a temperature gradient was used to determine

the optimal primer hybridization temperature. All PCR reactions were performed using DNA Engine (PTC-200) Peltier Thermal Cycler (Bio-Rad) and were subsequently analyzed by agarose gel electrophoresis (3.2.5) for analytic or preparative purposes. In the case of a Fusion-PCR (3.2.9) the isolated PCR amplification product was used as PCR-template itself. Depending on the detected strength analyzed by agarose gel electrophoresis, 2-10 µl (of a 50 µl elution volume) were used.

3.2.9 Fusion-PCR

The Fusion-PCR is a variation of the normal PCR method (3.2.8). It permits to join two pieces of DNA that share bases of homology at their linear ends. In general, the method consists of two separate PCR amplification steps. In a first step, the DNA fragments to be joined are generated by PCR. For this, primers were designed that share 20 bases of homology with both PCR-fragments. The first 20 bp hybridize with the template of the first PCR-reaction, while the second 20 bp are homologous to the template of the second PCR reaction. Hence, two complementary primer sequences of 40 bp were constructed resulting in the reverse primer for the first PCR-reaction and the forward primer for the second PCR-reaction.

The two generated PCR-fragments were verified on an agarose gel and subsequently used as templates in a Fusion-PCR reaction. In this reaction, both templates hybridized at their complementary parts during the PCR reaction and can therefore be fused together using the terminal primers from the 1st round PCRs (Figure 8). The general PCR reaction is conducted as described in section 3.2.8.

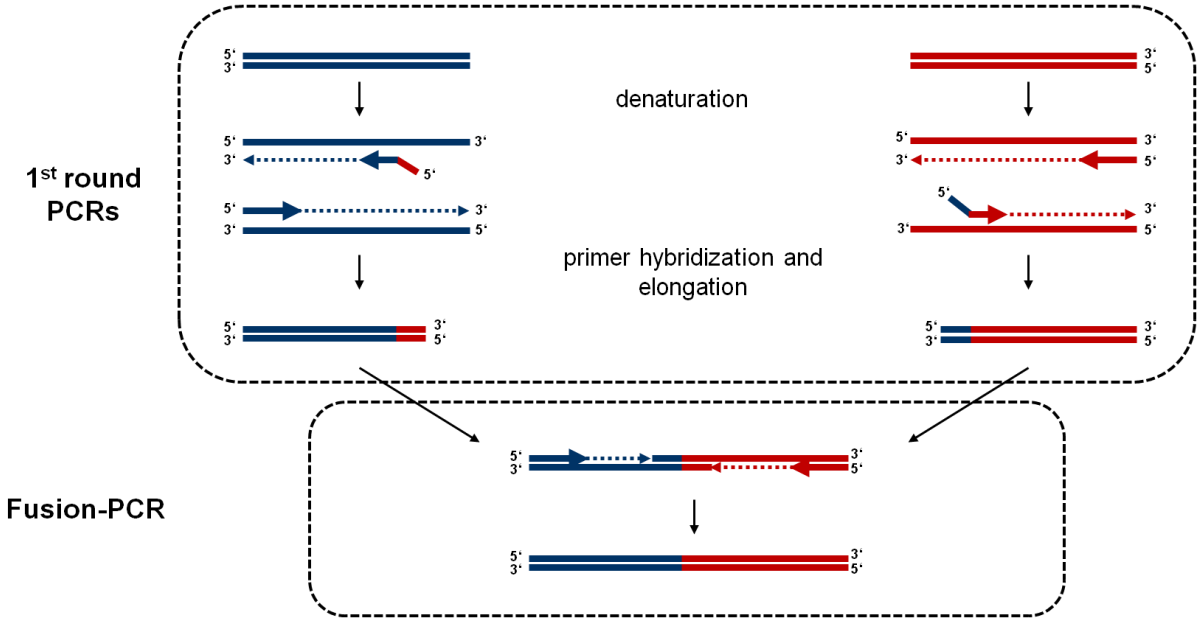

Figure 8: Schematic representation of a Fusion-PCR.

3.2.10 QuikChange™ site-directed mutagenesis kit

The QuikChange™ site-directed mutagenesis kit (Stratagene) was used to introduce point mutations into lentiviral transfer vectors. Within this method a specific mutation is introduced into the vectors using modified oligonucleotide primers containing the desired mutation. The oligonucleotide primers, each complementary to opposite strands of the vector, are extended during PCR by *PfuTurbo* DNA polymerase. This DNA polymerase replicates both plasmid strands with high fidelity and without displacing the mutant oligonucleotide primers producing a mutated plasmid containing staggered nicks. Subsequently, the parental DNA template is digested by DpnI endonuclease which is specific for methylated and hemimethylated DNA. The nicked vector DNA containing the desired mutations is then transformed into competent bacteria.

The QuikChange™ site-directed mutagenesis kit (Stratagene) was used according to the manufacturer's instructions.

3.2.11 *Staphylococcus aureus* killing assay

The human and murine monocytes used for the killing assay were isolated as described (3.3.4, 3.3.5). For the preparation of *S. aureus* (ATCC25923) a cryotube containing *S. aureus* with a concentration of 3-5x10^8 bacteria/ml was thawed at RT until a small clump of ice was left and transferred into a 50 ml conical tube containing LB-medium at 37°C. The bacteria were incubated for 10 min at 200 rpm in a bacteria shaker (Innova® 4200, New Brunswick Scientific), centrifuged (5 min, 2,400 rpm in a Multifuge 3SR, Heraeus) and resuspended in 10 ml DMEM (supplemented with human 10% AB-Serum (Sigma-Aldrich), 1x NEAA (Gipco), and 2 mM L-glutamine (Biochrom AG)). The bacteria suspension was diluted once more 1:5 with DMEM in case murine monocytes were used.

The desired amount of monocytes (in 75 µl), the bacteria (10 µl or 20 µl) and 5 µl PMA (16.2 µM) were mixed in wells of a 96well plate (Nunc). For each desired monocyte-to-bacteria ratio and time-point, one separate well was set up. Samples were taken after 0 min, 60 min, 120 min, and 180 min incubation at 37°C. 10 µl of the sample were diluted 1:1000 with aqua bidest and 25 µl spread on an agar plate. The number of colonies was counted 15-24 h later.

3.3 Cell culture and virological methods

3.3.1 Cultivation of cell lines

Cell lines were cultivated in the appropriate medium (3.1.7) in an incubator (BBD 6220, Heraeus) at 37°C, 6.0% CO_2 and saturated water atmosphere and were passaged twice a week. For this purpose, adherent cells were washed once with PBS and detached with PBS-EDTA (PBS (Biochrom AG), 100 mM EDTA) before an appropriate fraction of the resulting suspension was seeded into a new culture flask with fresh medium.

3.3.2 Freezing and thawing of cultured cells

Freezing

Adherent cells were washed once with PBS, detached by trypsinising (PBS (Biochrom AG), 100 mM EDTA, 0.25% Trypsin-Melnick) and resuspended in the appropriate medium before they were, like suspension cells, centrifuged (1000 rpm for 10 min at 4°C in a Multifuge 3SR, Heraeus) to pellet the cells. These were then resuspended in 4°C cold freezing medium (DMEM or RPMI with 20% FCS, 10% DMSO, 2 mM L-glutamine), aliquoted á $1.5x10^6$ cells into precooled cryotubes and frozen in a 5100 Cryo 1°C Freezing Container (Nalgene) at -80°C. After 24 h the cells were transferred into liquid nitrogen.

Thawing

Cryotubes were thawed at RT until a small clump of ice was left. Then the cell suspension was immediately transferred into a 50 ml falcon tube with 40 ml prewarmed medium. To exclude the cytotoxic DMSO, cells were subsequently centrifuged (1000 rpm for 10 min at RT, Multifuge 3SR, Heraeus), resuspended in fresh medium (containing 20% FCS) and seeded into appropriate cell culture flasks. 24 h later the medium was exchanged to fresh medium (3.1.7).

3.3.3 Isolation of human peripheral blood mononuclear cells (PBMC)

Human PBMCs were isolated from freshly drawn blood, treated with an anti-coagulant heparin or citrate, by density centrifugation using Histopaque®-1077 (Sigma-Aldrich). For this purpose, 15 ml cold Histopaque (4°C) were overlaid with 25 ml of a 1:1 mixture of human blood and PBS (Biochrom AG) in a 50 ml conical tube (Greiner bio-one), By centrifugation 400×g for 30 min at 20°C in a swinging-bucket (without break; Multifuge 3SR, Heraeus) the red blood cells and granulocytes were pelleted. Above the Histopaque solution the

lymphocytes, monocytes and macrophages were concentrated within the whitish interface ("lymphocyte-ring"). The interfaces of maximal four conical tubes were pooled into a new 50 ml conical tube already containing approx. 5 ml PBS using a 5 ml pipette (Greiner bio-one). The tubes were filled up to 50 ml with PBS. The cells were centrifuged at 300×g for 10 min at 20°C (Multifuge 3SR, Heraeus) and the supernatant carefully removed. Next, remaining erythrocytes were lysed through incubation in 10 ml 0.86% ammonium chloride solution at 37°C for 5-10 min, depending on the amount of red blood cells. Then, the cells were washed twice with PBS as described above. Finally, they were resuspended in 30 ml MACS-buffer, counted in a Neubauer counting chamber and used for monocyte isolation.

3.3.4 Isolation of primary human monocytes

Primary human monocytes were isolated from fresh human PBMCs with the Monocyte Isolation Kit II (Mitenyi Biotech) following the manufacturer's instructions. With this kit, untouched monocytes were isolated by depleting B cells, T cells, natural killer (NK) cells, dendritic cells and basophils. For this purpose, the unwanted cells are indirectly magnetically labeled using a cocktail of biotin-conjugated antibodies against CD3, CD7, CD16, CD19, CD56, CD123 and Glycosphorin A as well as biotin MicroBeads. By retaining the magnetically labeled cells on a MACS® column in a magnetic field, the unlabeled monocytes are isolated to a high purity as they pass through the MACS® column.
Depending on subsequent experiments, the freshly isolated monocytes were either cultivated in RPMI-monocyte medium (3.1.7) or kept on ice in cold PBS (4°C) for a short period of time.

3.3.5 Isolation of murine monocytes from BM

A number of necessary mice were sacrificed and the tibias and femurs flushed with PBS (Biochrom AG) (4°C) using a 0.8 mm syringe (HSW). The bone-marrow cells from different numbers of mice were pooled in a 50 ml conical tube, centrifuged (300×g, 10 min, 4°C) and resuspended in 10 ml PBS. The cells were overlaid on 5 ml sucrose solution (Histopaque 1083, density 1.083 g/ml, Sigma-Aldrich), and centrifuged for 30 min at 400×g at RT in a 15 ml conical tube. The mononuclear cell interface was collected with a 1 ml pipette (Eppendorf) in a 50 ml conical tube and washed by filling the tube up to 50 ml with PBS and centrifugation (300×g, 10 min, 4°C). Remaining erythrocytes were lysed through incubation in 5 ml 0.86% ammonium chloride solution at 37°C for 5-10 min. The cells were washed once more with PBS and resuspended in 10 ml MACS-buffer, counted in a Neubauer counting chamber and used for monocyte isolation. Therefore, the cells were centrifuged (300×g, 10 min, 4°C), resuspended in 100 µl MACS-buffer and incubated with a mixture of FITC-conjugated antibodies (10 µl per $1x10^7$ cells) against T cells (CD90.2), B cells (CD45R

(B220)), NK cells (CD49b (DX5)), and erythrocytes (Ter119) (Mitenyi Biotech) for 10 min at 4°C. The antibodies were chosen on the bases of the murine monocyte isolation of F. Swirski and co-workers (Swirski et al., 2006). The cells were washed by filling the tube up to 50 ml with MACS-buffer and centrifugation (300×g, 10 min, 4°C). The resuspended cells were incubated once more with αFITC-antibody MicroBeads (Mitenyi Biotech) (10 µl per $1x10^7$ cells) for 10 min at 4°C, washed and resuspended in 500 µl MACS-buffer. The cells were then run through an LD-negative selection column (Mitenyi Biotech). The negative (putative monocyte) fraction was collected, and cells were counted.

The following antibodies were used for murine monocyte isolation:

name	dilution	source
FITC conjugated rat α-mouse CD90.2 mAb	-	Miltenyi Biotec
FITC conjugated rat α-mouse CD45R (B220) mAb	-	Miltenyi Biotec
FITC conjugated rat α-mouse CD49b (DX5) mAb	-	Miltenyi Biotec
FITC conjugated rat α-mouse Ter-119 mAb	-	Miltenyi Biotec
MicroBeads conjugated αFITC mAb	-	Miltenyi Biotec

3.3.6 Production and concentration of vector particles

Vector particles were generated by transient transfection of HEK-293T cells. Depending on the lentiviral vector system two, three or four plasmids were used for transfection. The plasmid DNA was introduced into the cells by calcium phosphate transfection. The procedure is based on slow mixing of HEPES-buffered saline (HBS) containing sodium phosphate with a $CaCl_2$ solution containing the DNA. A DNA-calcium phosphate co-precipitate forms, which adheres to the cell surface and is taken up by the cell, presumably by endocytosis.

Three days before transfection, $4.6x10^6$ HEK-293T cells were seeded into a T175 flask. One hour before transfection the medium was replaced by 9 ml pre-warmed (37°C) medium supplemented with chloroquine (DMEM supplemented with 10% FCS, 2 mM L-glutamine, 100 units/ml streptomycine, 50 µg/ml penicillin, and 25 µM chloroquine).

Depending on the vector system different amounts of plasmid DNA were used to set up the transfection reagents for four T-175 flasks:

Two-plasmid vector systems: 262.8 µg vector DNA, 131.4 µg pMDG.2

Three-plasmid vector systems: 100 µg transfer vector, 100 µg packaging construct and 33 µg pMD.G2. Additionally, 33 µg of unmodified Vpx-expression plasmid or 16.5 µg of codonoptimized Vpx-expression plasmids were used.

To the plasmid DNA 600 µl 2.5 M $CaCl_2$ solution was added and the tube filled up with H_2O (Sigma-Aldrich W-3500) to 6 ml. While vortexing 6 ml 2x HBS Buffer (281 mM NaCl; 100 mM HEPES; 1.5 mM Na_2HPO_4, pH 7.12) was added dropwise. Afterwards the solution was

vortexed for an additional minute. Then, the 3 ml precipitate was added to the cells of one T175 flask. After 8 h and 24 h the medium was replaced by 25 ml and 10 ml fresh DMEM medium, respectively. Forty-Eight hours after transfection, the cell supernatant, containing the pseudotyped lentiviral vector particles, was harvested and replaced by 10 ml fresh DMEM. The supernatants of four T175 flasks, transfected with the same expression-plasmids, were combined, centrifuged (3,500 rpm, 5 min), and filtered (0.45 µm filter, Sortorius Stedim Biotech GmbH). The filtered supernatant was concentrated by centrifugation at 25,000 rpm, at 4°C for 2 h in an ultracentrifuge (Optima™ L-70k Ultrazentrifuge, Beckman) through a 20% (w/v) sucrose cushion in pollyallomer centrifuge tubes (Beckman). The pellet was resuspended in 200 µl FCS-free RPMI-medium (Biochrom AG). Vector particle aliquots were stored at -80°C.
The vectors were also harvested and prepared the same way at 72 h and 96 h post transfection. The third vector preparation was used to generate vector lysates (3.4.1).

3.3.7 Transfection of cells in six well plates

Transfection of cells in six well plates was performed by calcium phosphate or Lipofectamine™ LTX (Invitrogen) transfection. Twenty-four hours before transfection, $8x10^5$ 293T cells were seeded into a single well of a six well plate.
This low scale calcium phosphate transfection was used to analyze the best plasmid ratios of transfer vector to packaging construct in the generation of vector particles. One hour before transfection, the medium was replaced by 800 µl fresh medium supplemented with chloroquine. Not more than 5 µg plasmid DNA was mixed with 7 µl $CaCl_2$ filled up with H_2O (Sigma-Aldrich W-3500) to 62.5 µl. While vortexing 62.5 µl 2x HBS buffer was added dropwise. Afterwards the solution was vortexed for an additional minute. Then, the 125 µl precipitate was added to the cells. After 8 h and 24 h the medium was replaced by 2 ml and 1 ml fresh DMEM medium, respectively.
The Lipofectamine™ LTX (Invitrogen) transfection was used together with PLUS™ reagent (Invitrogen) for all other 6well transfections. The Lipofectamine™ LTX transfection reagent [µl] to, PLUS™ reagent [µl] to DNA [µg] ratio used was 4:1:2. The transfection was performed according to the manufacturer's instructions.

3.3.8 Titration of vector particles

For the titration of *eGFP*-transferring vector particles about $3x10^4$ HT1080 cells were seeded into a single well of a 24well plate (Nunc). On the next day, the vector particle stocks were serially diluted in 1:10 steps with medium and a total of 315 µl of the dilutions added per well. In advance the old medium was removed from the cells. After incubation for 4 - 6 h, the

transduction reaction mix was exchanged for 1 ml of fresh medium (3.1.7). After 5 days, the titers were calculated by determining the percentage of eGFP-fluorescent cells by FACS-analysis (LSR II System, BD). The counted cells per well were multiplied by the dilution factor and the factor 3.17 (used 315 µl x 3.17 = 1 ml) to obtain transducing units per milliliter (TU/ml). For vector titer calculation, dilutions, in which about 5-20% of the cells were transduced, were chosen.

The titration of *gp91^{phox}*-transferring vector particles was performed by transduction of 2x10^5 xCGD-PLB-985 cells. Therefore, vector particle stocks were serially diluted in 1:10 steps and a total of 250 µl of the dilutions added to 250 µl suspension cells per well. After 5 days, the titers were calculated by determining the percentage of 7-AAD negative, *gp91^{phox}*-expressing cells using 7-AAD (BD Biosciences) and FITC conjugated mouse α-human flavocytochrome b_{558} mAb (MoBiTec), respectively, by FACS-analysis (LSR II System, BD).

3.3.9 Transduction of primary monocytes

For the transduction of murine and human monocytes, the cells were taken into cell culture directly after isolation. If not indicated otherwise, 2x10^5 or 5x10^5 monocytes per well of a 48well plate were transduced one day post isolation. Therefore, the monocytes were washed once with PBS and the desired amount of vector particles, diluted in 200 µl DMEM medium (supplemented with human 10% AB-Serum (Sigma-Aldrich), 1x NEAA (Gipco), and 2 mM L-glutamine (Biochrom AG) added onto the cells. After incubation for 6-8 h, the transduction reaction mix was exchanged by 500 µl of fresh medium. After 5 days the monocytes were analyzed depending on the transgene.

3.3.10 Fluorescence activated cell sorting (FACS)

FACS analysis allows assaying cell populations for eGFP-expression or surface expression of proteins. The method makes use of scattered light and fluorescence of eGFP or fluorophore labeled antibodies. The cells are excited with a laser beam and the fluorescence is detected. FACS analysis was performed on the LSR II system (BD Bioscience). For this purpose, adherent cells were detached by incubation with PBS-EDTA solution (PBS (Biochrom AG), 100 mM EDTA). Approximately 2x10^5 - 5x10^5 cells were pelleted by centrifugation at 3,500 rpm, 4°C, 5 min (Multifuge 3SR, Heraeus). Then they were washed with 5 ml PBS and centrifuged (3,500 rpm, 4°C, 5 min). The cells were resuspended in PBS and incubated with 1 µl FcR Blocking reagent (Miltenyi Biotech) for 10 min at 4°C in the dark. Afterwards, the cells were incubated with 1-3 µl of the appropriate antibody/antibodies for 15 min at 4°C in the dark. After antibody incubation, the cells were washed with 5 ml FACS washing buffer (PBS, 1% FCS, 0.1% (w/v) NaN_3) and finally fixed in 100-600 µl FACS-Fix

(PBS, 1% paraformaldehyde). For the detection of eGFP-positive cells, they were directly fixed after the first washing step. To determine the rate of unspecific staining by the antibodies, cells were incubated with isotype controls conjugated with the same fluorofore as the applied antibody. The samples were either used directly for FACS analysis or stored up to three days at 4°C in the dark.
FACS-data were analyzed either with the FACSDiva™ software (BD Bioscience) program or FlowJo (version 7) (Tree Star, Inc.).

The following antibodies were used for FACS analysis:

name	dilution	source
PE conjugated rat α-mouse CD90.2 mAb	1:10	Miltenyi Biotec
PE conjugated rat α-mouse CD45R (B220) mAb	1:10	Miltenyi Biotec
PE conjugated rat α-mouse CD49b (DX5) mAb	1:5	Miltenyi Biotec
PE conjugated mouse α-mouse NK1.1 mAb	-	Miltenyi Biotec
PE conjugates rat α-mouse Ly6G	1:10	BD Biosciences
PE conjugated mouse α-mouse CD45.1 mAb	-	eBiosciences
PE Mouse IgG2a Isotype Control	-	Miltenyi Biotec
PE rat IgG2b Isotype Control	-	Miltenyi Biotec
PE rat IgM Isotype Control	-	Miltenyi Biotec
PE-Cy7 conjugated rat α-mouse CD11b mAb	-	BD Biosciences
PE-Cy7 Rat IgG2b, k Isotype control	-	BD Biosciences
APC conjugated rat α-mouse CD11b	1:20	Miltenyi Biotec
APC rat IgG2b Isotype Control	-	Miltenyi Biotec
Vio-Blue conjugated rat α-mouse Gr1 mAb	-	Miltenyi Biotec
Pacific Blue® Rat IgG2b Isotype Control	-	eBiosciences
PerCP-Cy5.5 conjugated mouse α-mouse CD45.2 mAb	-	eBiosciences
PerCP-Cy5.5 Mouse IgG2a, K Isotype Control	-	eBiosciences
FITC conjugated mouse α-human flavocytochrome b_{558}	-	MoBiTec
FITC mouse IgG1 Isotype control	-	Miltenyi Biotec
APC conjugated mouse α-human CD14	-	Miltenyi Biotec
APC mouse IgG2a Isotype control	-	Miltenyi Biotec

3.3.11 Determination of *in vivo* biodistribution of murine monocytes

Murine bone-marrow monocytes were isolated from GFP mice (C57BL/6-Tg(CAG-GFP)1Osb/J) as described (3.3.5). After the isolation, $4x10^7$ monocytes were resuspended in 400 µl PBS (Biochrom AG) and drawn up with a 1 ml syringe (HSW). 200 µl of the suspension (equated $2x10^7$ monocytes) were transplanted into the tail vein of one of two recipient Rag-2/$\gamma c^{-/-}$ mice (BALB/cAJic-RAG2^{null} IL-2Rg^{null}), a mouse strain that lacks T cells, B cells, and NK cells. For control, two other Rag-2/$\gamma c^{-/-}$ mice received 200 µl PBS. The transplantation procedure was performed by Janine Kimpel (Georg-Speyer-Haus, Frankfurt). Five hours prior to the injection the mice received a sublethal dose of five gray radiated

(Biobeam2000, Eckert & Ziegler BEBIG GmbH). One and four days after the injection one transplanted Rag-2/γc$^{-/-}$ mouse and one of the control mice were sacrificed. From both mice tissue of the liver, spleen, bone marrow, kidney, blood-samples, lymph nodes and fluid of the abdominal cavity was collected. The cells of the different organs were singularized using a 40 µm cell strainer (BD Falcon), the erythrocytes lysed by 0.86% ammonium chloride and the tissues analyzed for eGFP-positive cells by FACS spectrometry. As different tissue cell types have a different autofluorescence a positive control was prepared for each tissue sample by mixing 1x10^6 eGFP-monocytes with the negative cell population. Therefore, monocytes of another GFP mouse were isolated.

3.3.12 Intracellular flavocytochrome b_{558} staining of murine monocytes

For the intracellular flavocytochrome b_{558} staining of murine monocytes, 2x10^5 or 5x10^5 cells were transferred into FACS-tubes (Sarstedt), and incubated with 3 ml Pharmlysis (BD Biosciences) for 10 min in the dark. The cells were subsequently centrifuged (5 min at 1400 rpm (Multifuge 3SR, Heraeus), and washed with PBS (resuspended in PBS and centrifugation for 5 min at 1400 rpm). If, next to the intracellular stain, also cell surface molecules were detected, the cells were incubated with 1 µl mouse FcR Blocking reagent (Miltenyi Biotech) and the corresponding mAb for 15 min at 4°C in the dark. Following the incubation, the cells were washed once with PBS, vortexed and mixed with 500 µl Cytofix/Cytoperm solution (BD Biosciences) for 15 min in the dark. Subsequently, the cells were washed with, 1 ml Perm/Wash and incubated with 3 ml Perm/Wash for 10 min in the dark. Then, the cells were centrifuged (5 min at 1400 rpm) and incubated with 1 µl mouse FcR Blocking reagent (Miltenyi Biotech) and the FITC conjugated mouse α-human flavocytochrome b_{558} mAB (MoBiTec) for 30 min in the dark. After the incubation, the cells were centrifuged (5 min at 1400 rpm) once more, resuspended in 3 ml Perm/Wash and incubated for 5 min in the dark. Then, the cells were centrifuged (5 min at 1400 rpm), vortexed, resuspended in 200 µl Cytofix/Cytoperm solution (BD Biosciences), and analyzed by FACS (3.3.10)

3.3.13 Analysis of murine monocyte half-life in bloodstream

Murine bone-marrow monocytes were isolated from C57BL/6 mice as described (3.3.5). After the isolation, 1.9x10^8 monocytes were resuspended in 422 µl PBS (Biochrom AG) and drawn up with a 1 ml syringe (HSW). 200 µl of the suspension (equated 9x10^7 CD45.2 monocytes) were injected into the tail vein of each of the two recipient CD45.1 mice (B6.SJL-*Ptprc*^{a}

Pepc^{b}/BoyJ), a congenic mouse strain which carries the differential B cell antigen CD45.1. The transplantation procedure was performed by Christian Brendel (Georg-Speyer-Haus, Frankfurt). As control one CD45.1 mouse was left untransplanted. The weight of the mice was 26.3 g, 28.0 g, and 27.5 g, respectively. 4 h, 24 h, 47 h, 73 h, 94 h, and 117 h after transplantation, blood samples were taken from the tail vein of each animal. Therefore, a small cut was made into the tail of the mouse to derive a small droplet of blood, which was collected in capillary tube (Microvette® CB 300, Sarstedt). If necessary, the caused wound in the tail of the mouse was closed by a caustic agent (ARGENTRIX® Einmal-Höllenstein-Ätzstift, Ryma Pharm).

The blood samples were transferred into FACS-tubes (Sarstedt) and treated with Pharm Lyse™ (BD Biosciences) to remove erythrocytes and most of the neutrophils. The samples were subsequently stained with antibodies (Gr-1-Vio-Blue, CD11b-PE-Cy7, CD45.1-PE, and CD45.2-PerCP-Cy5.5) and analyzed by flow cytometry on a FACSCanto™ II system (BD Biosciences) (3.3.10).

The half-life was calculated by a nonlinear regression (curve fit) using a one phase exponential decay with the program GraphPad Prism 4. For this, the plateau constrain was set constant equal to zero.

3.3.14 Phagocytosis assay

Phagocytosis is the ingestion of solid particles by endocytosis. The phagocytosis capacity of cells can be quantified by different ways. In contrast to using FITC-labled yeast cells (Rohloff et al., 1994), DQ-BSA (Invitrogen) was used. DQ-BSA is a derivative of bovine serum albumin (BSA) that is labeled to such a high degree with BODIPY TR-X, that the dye is strongly selfquenched. After uptake by phagocytotic cells, the proteolysis of the BSA results in dequenching of the dye. The fluorescence can be monitored easily by FACS. This way, the endocytosis capacity of phagocytes can be monitored.

To measure the DQ-BSA uptake of monocytes, 1x10^{6} freshly isolated monocytes were incubated for 2 h with 5 µg (1 mg/ml) DQ-BSA (Invitrogen) at 37°C. For a negative control, the same amount of monocytes were pre-incubated for 30 min at 4°C and subsequently incubated for 2 h with 5 µg (1 mg/ml) DQ-BSA at 4°C. Following the DQ-BSA incubation, the cells are washed once with PBS, detached and transferred into FACS-tubes (Sarstedt). The cells were washed with 5 ml FACS washing buffer (PBS, 1% FCS, 0.1% (w/v) NaN_3), and finally fixed in 400 µl FACS-Fix (PBS, 1% paraformaldehyde). The cells were analyzed by FACS on the LSR II system (BD Biosciences) for the uptake of DQ-BSA.

3.3.15 Phagoburst assay

The quantification of the oxidative burst activity of monocytes was measured with the BURSTTEST kit (ORPEGEN Pharma). It determines the percentage of phagocytic cells which produce reactive oxidants and their enzymatic activity.

Therefore, $5x10^5$ isolated human monocytes from heparinized whole blood (3.3.4) or $5x10^5$ murine monocytes from bone marrow (3.3.5) were resuspended in 100 µl DMEM-medium supplemented with 10% AB serum (Sigma-Aldrich), 2 mM L-glutamine (Biochrom AG), and 1x NEAA (Gibco) in a FACS-tube (Sarstedt). The cells were activated with 20 µl PMA (1:200 stock solution) for 10 min at 37°C in a water bath (GFL). A sample without stimulus (20 µl washing-solution) served as negative background control. Upon stimulation, monocytes (as granulocytes) produce reactive oxygen metabolites which destroy bacteria inside the phagosome. The reactive oxidants during the oxidative burst were monitored by the addition and oxidation of DHR 123. Therefore, 20 µl of a substrate solution was added to the samples, vortexed and incubated for 10 min at 37°C in a water bath. At the end of the incubation, 100 µl FACS-FIX (PBS, 1% w/v paraformaldehyde) was added and the evaluation of oxidative burst activity performed by flow cytometry (3.3.10).

3.4 Methods of protein biochemistry

3.4.1 Preparation of cell- and vector lysates and Bradford assay

Preparation of cell lysates

To analyze the expression of intracellular proteins, the cells (transfected in a 6well by Lipofectamine™ LTX transfection (3.3.7)) were washed ones with 5 ml PBS (Biochrom AG), detached and transferred into a 1.5 ml reaction tube. The cells were pelleted by centrifugation (12,000 rpm, 4°C, 1 min) and resuspended in 200 µl ice-cold RIPA lysis buffer (25 mM Tris pH 8.0, 137 mM NaCl, 1% Glycerin, 0.1% SDS, 0.5% Na-deoxycholate, 1% NonidentP40 and 40 µl/ml protease inhibitor cocktail (Roche)). After incubation for 5-30 min at 4°C, the lysates were centrifuged at 13,000 rpm, 4°C for 10 min (Heraeus Fresco) to get rid of the cell debris. The supernatant was transferred into a new 1.5 ml reaction tube and either directly used for Bradford assay or frozen at -20°C. To determine the protein concentration in cell lysates by Bradford the Quick StartTM Bradford Dye reagent from Bio-Rad was used. Therefore, 5 µl of the cell lysate was added to 1 ml Breadford in a cuvette. After 5 min, the absorption was detected at 595 nm using a spectrophotometer (GeneQuant II, RNA/DNACalculator, Pharmacia Biotech).

Preparation of vector lysates

For the preparation of vector lysates, concentrated vector particles (3.3.6) were resuspended in 1 ml RPMI (Biochrom AG) and layerd over a 10 ml 20% w/v sucrose cushion in a polyallomer ultracentrifuge tube (Beckman). After centrifugation at 35,000 rpm (4°C) for 1.5 h (Optima™ L-70k Ultrazentrifuge, Beckman) the pellet was resuspended in 100 µl RIPA lysis buffer (25 mM Tris pH 8.0, 137 mM NaCl, 1% Glycerin, 0.1% SDS, 0.5% Na-deoxycholate, 1% NonidentP40 and 40 µl/ml protease inhibitor cocktail complete (25x)). The amount of 20 µl vector lysate was generally used for Western blot analysis.

3.4.2 SDS-polyacrylamide-gelelectrophoresis

The SDS-polyacrylamide-gelelectrophoresis (SDS-PAGE) allows the separation of protein mixtures according to the molecular weight of the proteins. The basic principle includes binding of multiple molecules of the anionic detergent sodium dodecyl sulfate (SDS) via hydrophobic interactions causing the denaturation of the protein. That way, irrespective of their native charges, the denatured proteins acquire an excess of negative charge on their surface and can thus be applied to electrophoresis. For this purpose, the samples were loaded on polyacrylamid gels, which act like molecular sieves.

To denature the proteins and allow binding of SDS, the samples were mixed with the appropriate amount of 4x Roti® load (Carl Roth GmbH) and heated for 5 min at 95°C. Then, they were loaded on NuPage 4-12% Bis-Tris gels (Invitrogen) within an Xcell SureLock™ electrophoresis cell (Invitrogen) and filled with NuPage running buffer (Invitrogen). As protein standard 5 µl of the SeeBlue® Plus2 pre-stained marker (Invitrogen) was used. SDS-PAGE was performed at 200 V until the dye front had left the resolving gel.

3.4.3 Western blot analysis

The Western blot technique is a method which enables the transfer of proteins onto protein-binding surfaces such as nitrocellulose membranes (Towbin et al., 1979). This transfer, also termed blot, enables the specific visualization of proteins of interest by immunostaining. Usually, proteins which have been separated by SDS-PAGE are applied to Western blot analysis. The transfer of the proteins from the SDS polyacrylamid gels onto PVDF membranes (Millipore Corporation) was performed electrophoretically within a Xcell SureLock™ electrophoresis cell (Invitrogen) according to the manufacturer's instructions. In advance, four 3 mm Whatman filter papers (Schleicher & Schuell) were shortly incubated in NuPage transfer buffer (Invitrogen). The PVDF membranes were activated for 1 min in methanol. After blotting at 200 mA for approx. 90 min, unspecific binding sites were blocked with blocking solution (PBS, 5% milk powder (AppliChem), 0.5% Tween 20) for 1 h at RT.

For specific protein staining, antibodies diluted in blocking solution have been used. Staining was performed either for 1 h at RT or over night at 4°C. Then, the membranes were rinsed once with 0.5% PBST (PBS, 0.5% Tween 20) and washed three times for 10 min at RT with 0.1% PBST (PBS, 0.1% Tween 20) before they were incubated for 1 h at RT with the appropriate horseradish peroxidase (HRP) conjugated secondary antibodies diluted in blocking solution. After washing as described above, detection of the proteins was performed using ECL- or ECLPlus-reagent (GE Healthcare) according to the manufacturer's instructions. The reagents contain a HRP substrate that emits light during conversion into the product by the HRP conjugated secondary antibodies. Hence, the signal can be visualized using chemiluminescence films (Amersham Biosciences). The latter ones were exposed to the substrate-incubated membrane/s for 5 sec to 30 min depending on the signal intensities.

The following antibodies were used for Western blotting:

primary antibody	**dilution**	**source**
rabbit αTubulin mAb	1:200	Cell Signaling Technology, Inc.
mouse αVSV mAb	1:1000	Sigma-Aldrich
mouse αVpxHIV-2 mAb	1:50	NIH AIDS Research and Reference Reagent Program, Rockville, USA
secondary antibody	**dilution**	**source**
HRP conjugated sheep α-mouse Immunoglobulins	1:7,500	GE Healthcare
HRP conjugated donkey α-rabbit Immunoglobulins	1:7,500	GE Healthcare

For the detection of VSV-G or tubulin ECL-reagent (GE Healthcare), and for the detection of Vpx ECLPlus-reagent (GE Healthcare) was used.

4 Results

This thesis shows that vectors derived from the HIV-2/SIVsmm/SIVmac lentivirus lineage enable primary human monocyte transduction. Therefore the generation of novel PBj- and HIV-2-transfer vectors for the generation of 3rd generation lentiviral vector-systems is described. One possible clinical application for PBj/HIV-2-vector driven monocyte transduction - the correction of *gp91^{phox}*-deficient monocytes from xCGD-patient for autologous cell transfusion - was conceived and human and murine monocytes were investigated for their potential to be used in such a setting.

4.1 HIV-2-derived lentivectors are able to transduce primary human monocytes

In previous work it could be shown that vectors derived from SIVsmmPBj are able to transduce primary human monocytes efficiently, where HIV-1 vectors fail (Mühlebach et al., 2005). Our lab could demonstrate that the viral protein Vpx is solely necessary to facilitate this transduction of monocytes (Wolfrum et al., 2007). As HIV-1-derived lentivectors do not code for the accessory *vpx* gene, these vectors are incapable of efficient human monocytes transduction. Besides SIVsmmPBj also other prominent lentiviruses, namely HIV-2 and SIVmac, contain a *vpx* gene. Therefore, an HIV-2-derived two-plasmid-system was obtained for comparison to PBj vectors in its ability to transduce primary human monocytes.

4.1.1 Comparison of HIV-1-, SIVsmmPBj- and HIV-2-derived lentiviral vector transduction of primary human monocytes

In order to investigate, whether HIV-2-derived lentiviral vectors are able to transduce primary human monocytes, the vectors from an HIV-2 two-plasmid system (HIV-2-RodA) were generated. The monocyte transduction capacity of HIV-2 vectors was compared to that of HIV-1- (HIV-1-NL4-3) and PBj-derived (PBj-ΔEeGFP) two-plasmid systems. The vectors were generated by transient transfection of 293T cells with one of the vector constructs HIV-2-RodA, HIV-1-NL4-3 or PBj-ΔEeGFP (Figure 9A) and the VSV-G expression plasmid pMD.G2. The vector particle containing supernatant was harvested two days post transfection, concentrated over a 20% sucrose cushion and used for titration on HT1080 cells (3.3.8). The titers reached were $1.0x10^9$ TU/ml, $4.4x10^8$ TU/ml, and $6.2x10^7$ TU/ml for HIV-2-RodA, PBj-ΔEeGFP, and HIV-1-NL4-3, respectively.

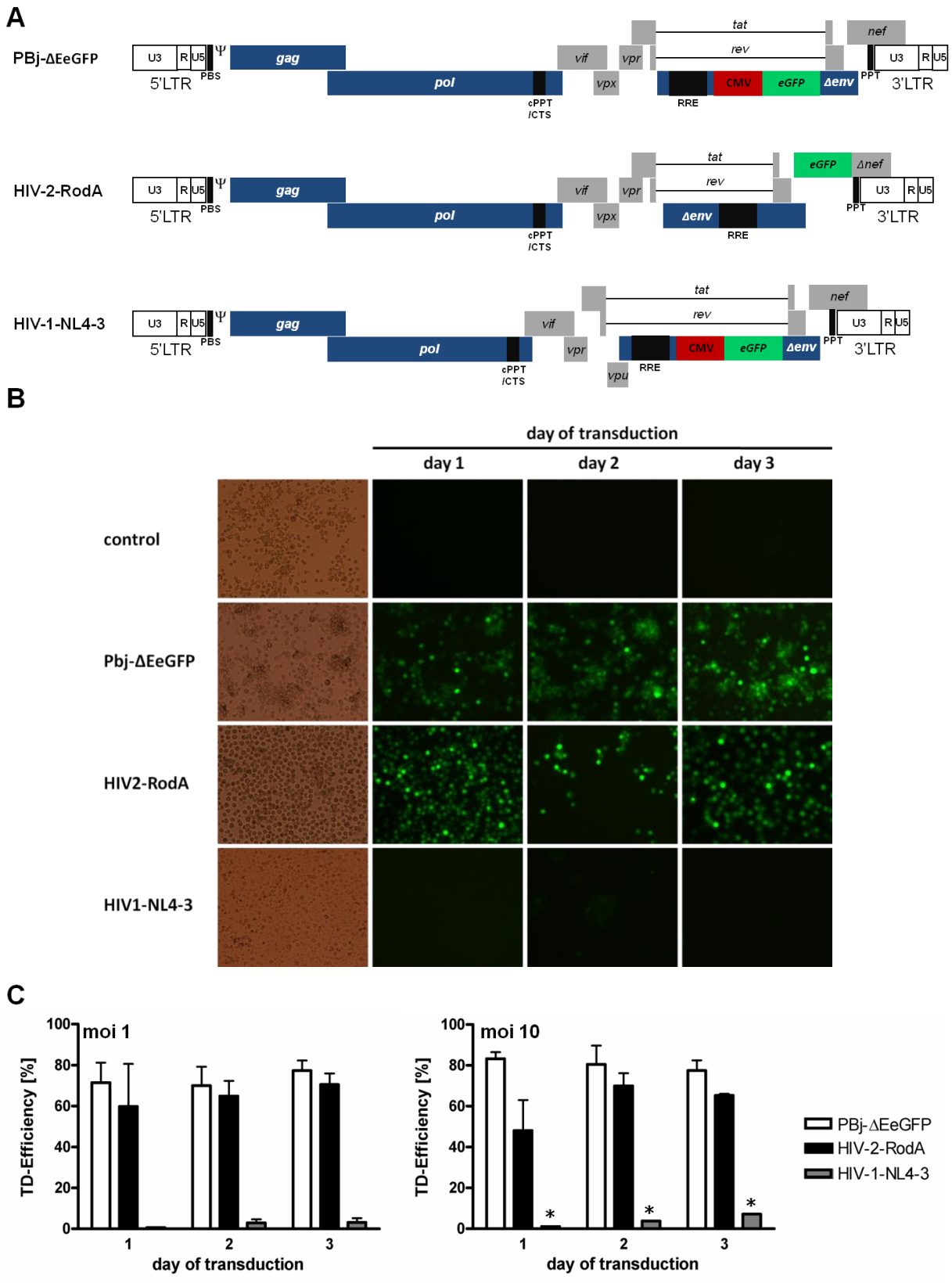

Figure 9: Transduction efficiency of various lentiviral vectors on primary human monocytes. Primary human monocytes of three different donors were transduced with PBj-ΔEeGFP-, HIV-2-RodA- or HIV-1-NL4-3-vectors at day one, two or three after isolation using the indicated moi. **(A)** Schematic representation of the indicated vectors. **(B)** eGFP-expression of transduced monocytes (moi 1) of one representative donor shown by fluorescent microscopy (20 x magnifications). **(C)** Transduction rates of αCD14^{+}-APC-stained monocytes determined by FACS-analysis. The star (∗) indicates that data of only one donor is shown as the monocytes of the two other donors died.

Monocytes of three different donors were isolated from whole blood samples via MACS and taken into cell-culture (3.3.4). One, two or three days after isolation the monocytes were transduced using the different vector-systems at the moi of one or ten. Seven days post transduction they were analyzed for transgene expression by FACS and fluorescent microscopy (Figure 9). For FACS-analysis, the cells were stained with αCD14-APC. This way only the specific transduction efficiency of HIV-2-RodA, PBj-ΔEeGFP, and HIV-1-NL4-3 for $CD14^+$-monocytes transduction was determined. The transduction efficiencies for HIV-2-derived vectors of approx 60% - 70% at an moi of one and ten were in the range of those for PBj-derived vectors. Only HIV-2-RodA showed a 30% reduced transduction of monocytes at an moi of ten at day one after isolation in comparison to PBj-ΔEeGFP transduced cells. The transduction with HIV-1-NL4-3 was not feasible at either moi as expected. For the transduction at moi of ten, only one donor was FACS-analyzed as the monocytes of both other donors died.

The monocyte transduction experiments confirmed the assumption that vectors derived from HIV-2 are able to transduce monocytes.

4.1.2 Monocyte transduction with Vpx-supplemented SIVsmmPBj-4xKOeGFP vectors

Generation of Vpx-expression plasmids

As VpxPBj is the determining factor facilitating the monocyte transduction of PBj-derived vectors (Wolfrum et al., 2007) and HIV-2-derived vectors are able to transduce monocytes (Figure 9), it can be assumed that VpxPBj homologues like VpxHIV-2 and VpxMAC also facilitate monocyte transduction. To confirm this assumption, expression plasmids for Vpx of HIV-2-RodA and SIVmac were generated. The *vpx* genes of HIV-2 and SIVmac were PCR-amplified out of the templates HIV-2-RodA and SIV-3+ (Negre et al., 2000; Reuter et al., 2005) using the primer pairs BPK1 / BPK2 and BPK3 / BPK4, respectively. The PCR amplificates were inserted into the pcDNA3.1(+) backbone via the restriction sites EcoRI and XhoI. The expression plasmids were used for transfection of 293T cells. Two days after transfection cell lysates were prepared and examined for Vpx-expression by Western blot using a αVpxHIV-2 monoclonal antibody. The Vpx-expression of VpxPBj and VpxHIV-2 was very weak and VpxMAC expression was not detectable (Figure 10). In order to achieve an enhanced protein expression, codonoptimized Vpx-expression plasmids for PBj (VpxPBjsyn) and HIV-2 (VpxHIV-2syn) were used. The VpxHIV-2syn expression plasmid was available in the lab whereas the VpxPBjsyn expression plasmid had to be constructed by removing the HA-tag of an available HA-tagged VpxPBjsyn plasmid. For this purpose the VpxPBjsyn fragment was PCR-amplified out of the template HA-VpxPBjsyn using the primer pair BPK5 /

BPK6. The PCR product was inserted into a pcDNA3.1(+) backbone via the EcoRI and XhoI restriction sites. The codonoptimized Vpx-expression plasmids were used to transfect 293T-cells. Two days after transfection the Vpx expression was analyzed by Western blot. The expression of the codonoptimized proteins VpxPBjsyn and VpxHIV-2syn was strongly enhanced compared to that of VpxPBj and VpxHIV-2.

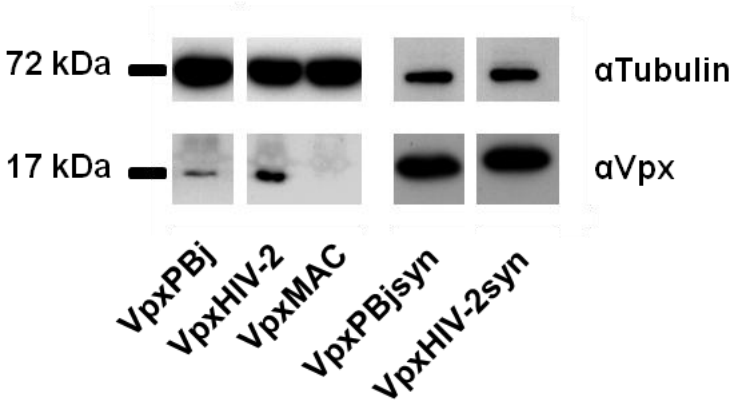

Figure 10: Analysis of Vpx-expression. Western blot analysis of Vpx-expression in 293T cells transfected with the Vpx-expression plasmids indicated using αtubulin- and αVpx-antibodies. For VpxPBj, VpxHIV-2 and VpxMAC exposition times of 1 min for αTubulin and 5 min for αVpx were used, and for VpxPBjsyn and VpxHIV-2syn 5 min for αTubulin and 10 sec for αVpx, respectively.

Vpx mediated monocyte transduction

The different Vpx-expression plasmids were tested in their ability to facilitate the transduction of a PBj-ΔEeGFP-derived two-plasmid-system, deficient for all four accessory genes (*vpr*, *vif*, *nef*, and *vpx*) and therefore termed, SIVsmmPBj-4xKOeGFP (PBj-4xKOeGFP). For this purpose 293T cells were transfected with pPBj-4xKOeGFP and VSV-G expression plasmids necessary for vector production. The transfection was supplemented with no (control) or one of the respective Vpx-expression plasmids. Two days later the vector containing cell supernatants were harvested and concentrated over a 20% sucrose cushion by ultracentrifugation. The collected vectors were titrated on HT1080 and used for transduction of freshly isolated monocytes at an moi of one or five (Figure 11). The transduction efficiencies were determined five days post transduction by FACS-analysis. Prior to the analysis the cells were stained with αCD14-APC antibodies, hence only the transduction efficiencies of the $CD14^+$-cell population was taken into account.

As expected, the PBj-4xKOeGFP (-) vector, generated in absence of Vpx, was not able to transduce monocytes efficiently. In contrast, all but one vector generated in the presence of Vpx allowed a dose-dependent transduction. Thereby, the codon-optimized Vpx were most efficient. Only the unmodified Vpx of HIV-2 failed to facilitate monocyte transduction (Figure 11).

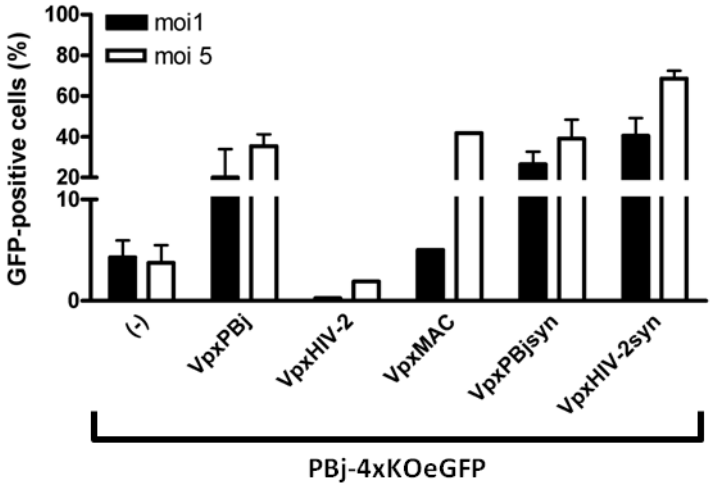

Figure 11: Vpx dependent transduction of primary human monocytes. The transduction efficiency of PBj-4xKOeGFP-derived vectors supplemented with the indicated Vpx in $CD14^{+}$-monocytes was analyzed by FACS**.**

Vpx incorporation in vector particles

The corresponding vector-lysates of the latter 4xKOeGFP-vectors used for monocyte transduction were tested for Vpx incorporation by Western-blot analysis (Figure 12). Except for the well detectable codonoptimized VpxPBjsyn and VpxHIV-2syn, the unmodified VpxPBj, VpxHIV-2 and VpxMAC were not detected using αVpxHIV-2 monoclonal antibody. Vector particles generated in the presence of the stable, but non-functional n-terminally Flag-tagged VpxHIV-2 were used as positive control. The used particle amount was visualized by αVSV antibodies. For VpxHIV-2nFLAG, VpxPBj, VpxHIV-2 and VpxMAC exposition times of 2 min for αVSV and 5 min for αVpx were used and for VpxPBjsyn and VpxHIV-2syn exposition times of 15 sec for αVSV and 2 min for αVpx.

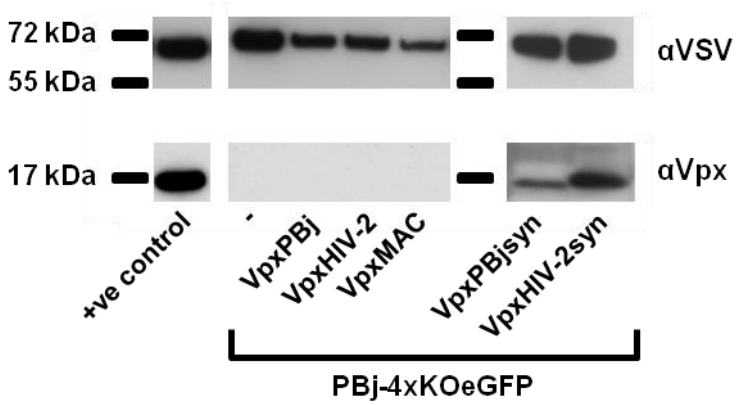

Figure 12: Incorporation of different Vpx proteins into PBj-4xKOeGFP vector particles. Western blot analysis of vector lysates of PBj-4xKOeGFP vectors supplemented with the Vpx indicated. The VSV-G- and Vpx-protein expression is visualized.

Obviously, the amount of Vpx packaged into vector particles is not correlated with the efficiency of monocyte transduction.

4.2 Construction of novel HIV-2- and PBj-derived lentiviral vector systems

In the first section it was shown that next to SIVsmmPBj-derived vectors, HIV-2-derived lentiviral vectors are also able to transduce primary human monocytes. In both cases the transduction is facilitated through Vpx. Both systems were used to establish a human and non-human derived three-plasmid vector system. To construct safe lentiviral vector systems, it is necessary to separate the viral genetic information onto different plasmids and minimize their viral DNA content. The separation of the structural *gag/pol* genes from the sequences used for the transfer-DNA-construct and the envelope-construct minimizes the risk of unwanted recombination events.

As previous results demonstrated that it is possible to construct basic HIV-2- and PBj-derived three-plasmid systems (Negre et al., 2000; Wolfrum, 2005), one aim of this thesis was to develop transfer vectors for both systems which allow the production of high titer and safe lentiviral vectors for the transduction of primary human monocytes.

Fully functional packaging constructs were available for both vectors systems (Negre et al., 2000; Wolfrum, 2005). Hence, it was necessary to construct new transfer vectors.

4.2.1 Construction of a PBj-derived transfer vector – the conventional way

The conventional way to generate a lentiviral transfer vector is to remove all needless parts from the wild-type sequence (i.e. *gag/pol* and accessory genes), leaving the *cis*-acting sequences intact, and to introduce necessary modifications (i.e transgene expression cassette) in successive cloning steps. This conventional cloning strategy has been used to gradually enhance the PBj-derived transfer vector **pPBj-trans** (Wolfrum, 2005) (Figure 13A). For most of the cloning steps the Fusion-PCR technique was used (3.2.9), as described on page 31. Correct cloning was confirmed by sequencing of the relevant parts (3.2.7).

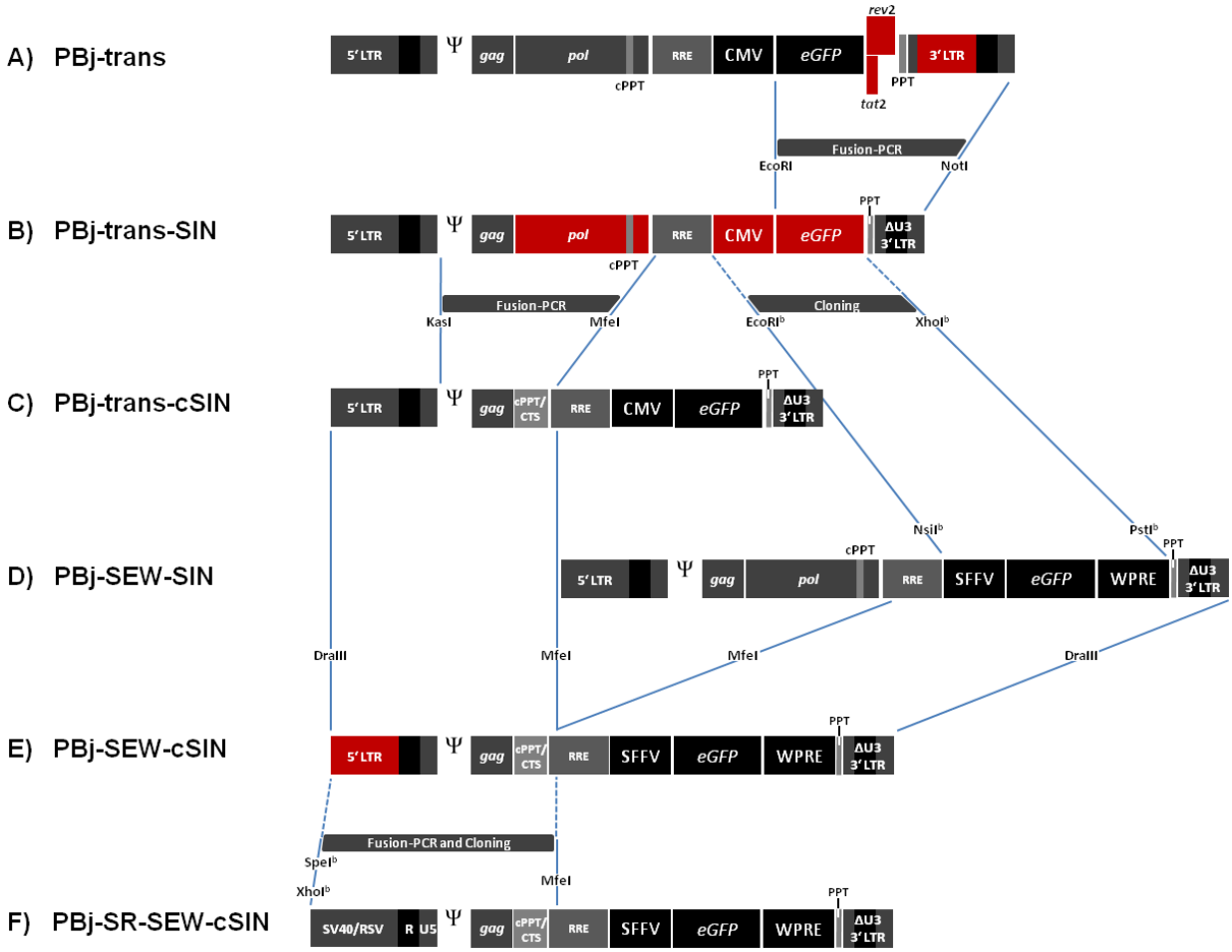

Figure 13: Generation of PBj-derived transfer vector constructs. Schematic representation of the different transfer vector plasmids derived from SIVsmmPBj. The vector elements exchanged in a subsequent cloning step are highlighted in red. The restriction sites and the method used for each step, such as the insertion of fragments after digestion (cloning) or generation of fragments by Fusion-PCR, are shown. Ψ, packaging signal; [b], generated blunt-ends; LTR, long terminal repeat; SD, splice donor; cPPT, central polypurine tract; CTS, central termination sequence; RRE, Rev-responsive element; SA, splice acceptor; CMV, human cytomegalovirus early promoter; SFFV, spleen focus forming virus early promoter; WPRE, woodchuck hepatitis virus post-transcriptional regulatory element.

Construction of a self-inactivating (SIN) vector

In a first step, a SIN vector was generated by deleting the U3 promoter sequences in the 3`LTR. This resulted in the construct **pPBj-trans-SIN** (Figure 13B). For the deletion of the promoter sequences, a Fusion-PCR was performed to generate a SIN-3'-LTR sequence, including the attachment sites and the R- and U5-region. The PPT was included upstream of the SIN-3'-LTR. The Fusion-PCR was performed by fusing three different PCR products derived with the primer pairs BPK 7 / BPK 8, BPK 9 / BPK 10 and BPK 11 / BPK 12 on the PBj-trans template. The restriction sites EcoRI and NotI were included through the primers BPK 7 and BPK 12, respectively. Using these restriction sites allowed the Fusion-PCR fragment to be interchanged with the respective PBj-trans sequence. For this, the EcoRI-NotI fragment was excised from the PBj-trans backbone, and the Fusion-PCR fragment integrated

in a directed ligation. The insertion of the Fusion-PCR fragment also led to the deletion of the useless second exons of *tat* and *rev*.

Integration of the cPPT/CTS element and SFFV-*eGFP*-WPRE expression cassette

In order to assure an accurate reverse transcription of the transfer vector, the central termination sequence (CTS) was reintroduced downstream of the central polypurine tract (cPPT). In the same step, it was possible to remove the remaining part of the *pol* gene (1107 bp) to further minimize the presence of viral sequences. These changes resulted in the construct **pPBj-trans-cSIN** (Figure 13C). To generate the latter, another Fusion-PCR was performed with the fragments derived from PCRs using the primer pairs BPK 13 / BPK 14 and BPK 15 / BPK 16 on the templates pPBj-trans and pPBj-ΔEeGFP, respectively. The Fusion-PCR-fragment containing the corrected cPPT/CTS sequence was integrated into PBj-trans-SIN via the restriction sites KasI and MfeI.

In parallel, the CMV-eGFP expression cassette of pPBj-trans-SIN was replaced by a SFFV-*eGFP*-WPRE expression cassette resulting in **pPBj-SEW-SIN** (Figure 13D). The SFFV-*eGFP*-WPRE expression cassette insert was obtained by excision out of a HIV-1-derived transfer vector (pHIV-1-SEW) through the restriction sites EcoRI and XhoI. In contrast, the CMV-eGFP was excised from the pPBj-trans-SIN backbone via the restriction sites NsiI and PstI. In order to join the backbone and insert fragments, they were processed with Klenow-Enzyme to yield blunt-ends (3.2.2). Consequently, the SFFV-*eGFP*-WPRE expression cassette was integrated into the pPBj-trans-SIN backbone by blunt-end ligation to yield the construct pPBj-SEW-SIN (Högner, 2007).

The combination of both modifications - the deletion of the remaining *pol*-gene sequence leaving a corrected cPPT/CTS sequence in pPBj-trans-cSIN and the insertion of an SFFV-*eGFP*-WPRE expression cassette in pPBj-SEW-SIN - resulted in the construct **pPBj-SEW-cSIN** (Figure 13E). For the construct combination pPBj-trans-cSIN and pPBj-SEW-SIN were cut with MfeI und DraIII and joined in a directional ligation.

Construction of a Tat-independent transfer vector

The U3-region within the 5´LTR was substituted by a chimeric SV40-enhancer/RSV-promoter-(SV40/RSV)-element to obtain a strong, Tat-independent vector RNA expression in the packaging cells (Schambach et al., 2006b). For this purpose a cloning strategy via an intermediate construct was performed.

First, a Fusion-PCR was conducted. For this, the PCR-products using the primer pairs BPK 17 / BPK 18 and BPK 19 / BPK 20 on the SV40/RSV-element containing plasmid SER11S91-SW and the transfer vector pPBj-trans SIN as templates, respectively, were

used. During this, the primer sequence BPK 17 introduced a KasI and a SpeI restriction site at the 5'-end of the Fusion-PCR construct. The primer sequence BPK 20 hybridized downstream of a KasI restriction site at the 3' end of the Fusion-PCR construct. This way, the generated SV40/RSV-R-U5 sequence was inserted downstream of the 5'LTR of PBj-trans-cSIN via the KasI restriction sites (intermediate construct not shown).
Second, from the intermediate construct the integrated SpeI site was used together with an upstream MfeI restriction site to excise the Insert-DNA-fragment containing the SV40/RSV-element, the Ψ-site and the corrected cPPT/CTS-element. This fragment was used to replace the corresponding sequence of pPBj-SEW-cSIN. For this, the corresponding sequence was excised from the pPBj-SEW-cSIN-backbone via the XhoI and MfeI restriction sites. For successful cloning, the insert and backbone fragments were processed with Klenow-Enzyme after the first restriction of SpeI or XhoI, respectively, in order to yield blunt-ends. Only then, the MfeI restriction was performed. In a last step, the insert and backbone were ligated to yield the transfer vector **pPBj-SR-SEW-cSIN** (Figure 13F).

Evaluation of the generated PBj-derived transfer vectors

To compare the functionality of the different generated transfer vectors, VSV-G pseudotyped vector particles were generated by transient transfection of 293T cells with the packaging construct pPBj-pack, the envelope-construct pMD.G, the VpxPBj expression plasmid and one of the respective transfer vectors (3.3.7). The gained vectors were titrated on HT1080 cells (3.3.8) (Figure 14). The introduced modifications within the transfer vector lead to a gradual increase in vector titers. Compared to the starting construct PBj-trans, the final vector system PBj-SR-SEW-cSIN resulted in a nearly 100-fold increase in vector titers before concentration and an additional 10-fold increase after concentration. The enhanced vector construct yielded vector titers above 10^7 TU/ml after concentration (Figure 14A).

Next, vector particles derived from the most sophisticated transfer vector, PBj-SR-SEW-cSIN were compared to vector particles derived from the starting construct PBj-trans and to HIV-1-derived vectors in their ability to transduce primary human monocytes. Both PBj-derived vectors were produced in the presence and absence of the VpxPBj-expression plasmid and used for monocyte transduction at an moi of one. The vector particles produced in the absence of VpxPBj transduced monocytes only at background level as did HIV-1-derived vectors. However, vector particles produced in the presence of VpxPBj resulted in an efficient transduction of monocytes. About 20% of the primary human monocytes could be transduced one day after isolation (Figure 14B).

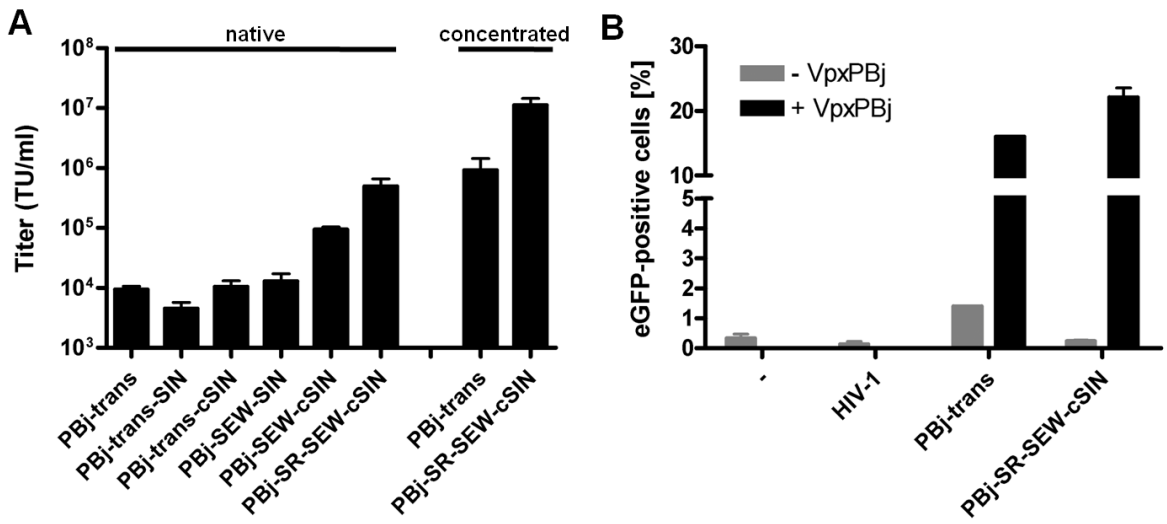

Figure 14: Evaluation of vector particles generated with PBj-derived transfer vectors. (A) Titers reached on HT1080 cells for generated vector particles using the indicated transfer vector before (native) and after concentration. **(B)** Transduction efficiency of primary human monocyte for the indicated lentivectors in presence and absence of VpxPBj using an moi of one.

In summary, a safe SIVsmmPBj-derived vector system, reaching titers of up to $1x10^7$ TU/ml for an efficient monocyte transduction was successfully constructed.

4.2.2 Constructing lentiviral transfer vectors – the new way

The construction of lentiviral derived transfer vectors by gradual enhancing cloning steps is very time consuming. A general transfer vector encompasses normally more than 7000 bp with repetitive sequences, i.e. LTR. Hence, the procedure is prone to mutations occurring throughout the cloning steps. The more cloning steps have to be performed, the more unwanted viral DNA sequences between the necessary vector elements are likely to remain due to unfitting restriction sites. These sequences enhance the homology to the wild-type-virus sequences and needlessly increase the size of the transfer vector. In order to construct a lentiviral transfer vector in a fast way by simultaneously minimizing the non-functional DNA sequences, a novel way to design transfer vectors from a lentiviral origin was conceived. The concept was to generate a transfer vector directly by Fusion-PCR. In order to demonstrate that this concept was in principle possible, it was used in the construction of an HIV-2- and PBj-derived transfer vector (Figure 15). The primers used for the different PCR reactions generating PBj-MCS and HIV-2-MCS are depicted in Table 1. The exact primer sequences are given in section 3.1.5.

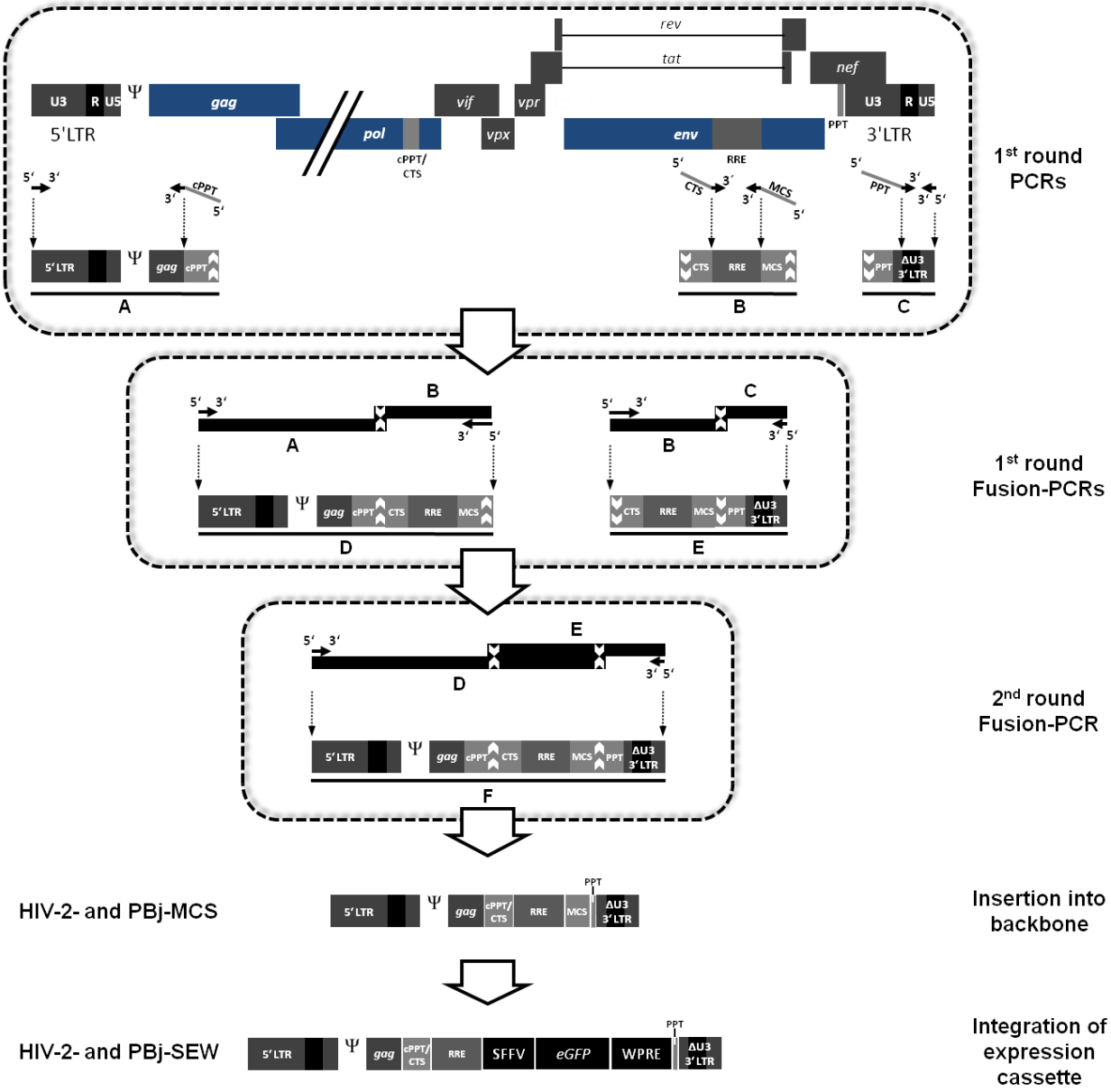

Figure 15: Schematic representation of the new cloning strategy to generate lentiviral transfer vectors. On the basis of HIV-2- and PBj- lentiviral wild-type sequences lentiviral transfer vector scaffolds were generated and further processed to HIV-2-SEW and PBj-SEW transfer vectors, respectively. The primer binding positions are represented by the horizontal, black arrows. The angled, grey extensions of the primers contain the indicated elements. Complementary sequences are indicated by the bold, white vertical arrows. PCR products are depicted A-F. Ψ, packaging signal; LTR, long terminal repeat; cPPT, central polypurine tract; CTS, central termination sequence; RRE, Rev-responsive element; SFFV, spleen focus forming virus early promoter; WPRE, woodchuck hepatitis virus post-transcriptional regulatory element; pA, bovine growth hormone polyadenylation signal.

Table 1: Primers used for the generation of PBj-MCS and HIV-2-MCS.

Generation of PBj-MCS	PCR notation (see Figure 15)	Forward-Primer	Reverse-Primer	Templates
1st round PCRs	A	BPK 21	BPK 22	PBj-ΔEeGFP
	B	BPK 23	BPK 24	PBj-ΔEeGFP
	C	BPK 25	BPK 26	PBj-ΔEeGFP
1st round Fusion-PCRs	D	BPK 21	BPK 24	A, B
	E	BPK 23	BPK 26	B, C
2nd round Fusion-PCR	F	BPK 21	BPK 26	D, E
Generation of HIV-2-MCS	**PCR notation (see Figure 15)**	**Forward-Primer**	**Reverse-Primer**	**Template**
1st round PCRs	A	BPK 35	BPK 36	HIV-1-RodA
	B	BPK 37	BPK 38	HIV-1-RodA
	C	BPK 39	BPK 40	HIV-1-RodA
1st round Fusion-PCRs	D	BPK 35	BPK 38	A, B
	E	BPK 37	BPK 40	B, C
2nd round Fusion-PCR	F	BPK 35	BPK 40	D, E

1st round PCRs

In a first step, the wild-type sequence of a lentivirus was used as template for three different PCR reactions. The PCR product sequences together form the scaffold for the PBj- and HIV-2 transfer vectors. The first PCR reaction (A) stretches out over the 5'LTR, the Ψ sequence and 200 bp of the *gag* gene. The forward primer carried a HindIII restriction site. For the second PCR (B) the primers were placed to flank the RRE. The third PCR reaction (C) was set to amplify the R-U5-region of the 5'-LTR. In this PCR reaction the reverse primer carried a NotI restriction site. All other sequences necessary for a lentiviral transfer vector which could not be PCR amplified were included in the primer extensions (indicated as angled arrow extensions in Figure 15). These sequences included the *cis*-acting elements cPPT, CTS, and PPT as well as a MCS and the attachment sites of the 3'LTR. Hence, the length of the designed primers was up to 100 bp long.

1st and 2nd round Fusion-PCRs

The products of the first three PCRs (A-C) were used as templates for subsequent Fusion-PCRs. The PCR products of A and B as well as B and C were joined by the Fusion-PCRs D and E, respectively. The products of the 1st round Fusion-PCRs (D and E) in turn served as template for a 2nd round Fusion-PCR resulting in the transfer vector scaffold.

Insertion into backbone

The transfer vector scaffolds derived by the Fusion-PCRs were cloned into a plasmid-backbone taken from the pPBj-pack vector. The backbone originated from a pBluescript-plasmid and included an antibiotic resistance gene (ampicillin) and an f1 helper phage origin of replication. For this, the HIV-2- or PBj-derived transfer vector scaffolds and the pPBj-pack vector were cut with the restriction enzymes HindIII and NotI and fused together in a directed ligation to give HIV-2-MCS or PBj-MCS, respectively. These constructs could be used as a foundation for different transfer vectors as they contain an MCS (Figure 16), e.g. to insert an expression cassette of choice. The MCS was integrated into the PBj- or HIV-2 construct with help of the primers BPK 24 or BPK 38, respectively. The MCSs within the respective PBj-MCS or HIV-2-MCS constructs contain four restriction sites designed to be present only once within the vector (single-cutter). In addition, the MCS in HIV-2-MCS also contains a KpnI restriction site which has three additional recognition sites throughout the vector. All restriction sites produce sticky ends.

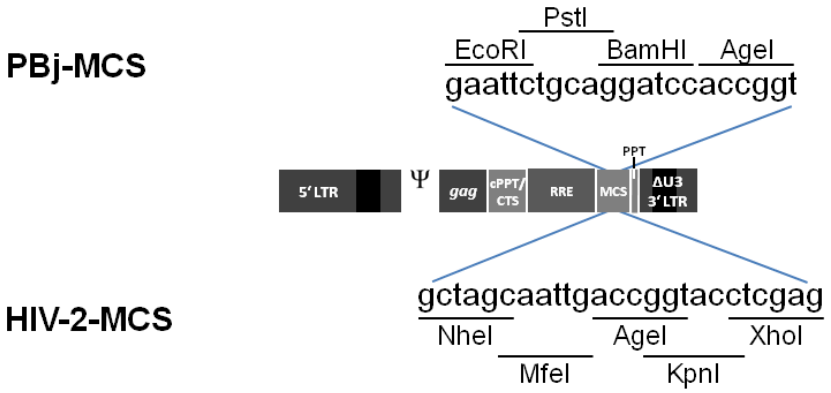

Figure 16: Multiple cloning site of PBj-MCS and HIV-2-MCS.

Integration of a eGFP expression cassette into HIV-2-MCS and PBj-MCS

To prove the functionality of the newly derived vectors, an *eGFP* gene under the control of an SFFV-promoter followed by a WPRE (SFFV-*eGFP*-WPRE) was inserted into HIV-2-MCS and PBj-MCS. For the generation of HIV-2-SEW, the SFFV-*eGFP*-WPRE-expression cassette was amplified out of the SIVmac-derived transfer vector pGAE-SFFV-WPRE using the primers BPK 41 and BPK 42. Both primers contain an MfeI restriction site for subcloning of the PCR product into the HIV-2-MCS vector. The PBj-SEW vector was cloned almost in the same manner. Here, the primers BPK 27 and BPK 28, both containing an EcoRI restriction site, were used to amplify the sequence identical SFFV-*eGFP*-WPRE-expression cassette out of the HIV-1-derived transfer vector template pHIV-1-SEW. Subsequently, the expression cassette was inserted into PBj-MCS via the EcoRI restriction sites (Figure 15).

Titers achieved using the HIV-2-SEW and PBj-SEW transfer vectors

The newly derived transfer vectors HIV-2-SEW or PBj-SEW were used together with the packaging vectors pPBj-pack or pHIV-2d4, respectively, and with the VSV-G expression plasmid pMD.G2 in a transient transfection of 293T cells. The transfection to generate vector particles was performed in 6well plates (3.3.7). The harvested vector particles were titrated on HT1080 cells (3.3.8) (data not shown). Vector particles generated with both, the HIV-2-SEW and the PBj-SEW transfer vectors were able to transduce HT1080 cells. Therefore both transfer vectors were used for high concentrated vector particle production (3.3.6). This way, vector titers about 100fold higher than those for particles generated with the PBj-trans transfer vector were reached. Nevertheless, they were still about 5 - 10fold less than the titer of HIV-1-SEW-derived vector particles (Figure 17). In order to achieve especially high vector titers, large amounts of vector supernatant were concentrated and the gained vectors pooled in small aliquots. This way, vector titers of $5.4x10^8$ TU/ml for HIV-2-SEW and $4.0x10^8$ TU/ml for PBj-SEW compared to titers of $2.0x10^9$ TU/ml for HIV-1-SEW were feasible.

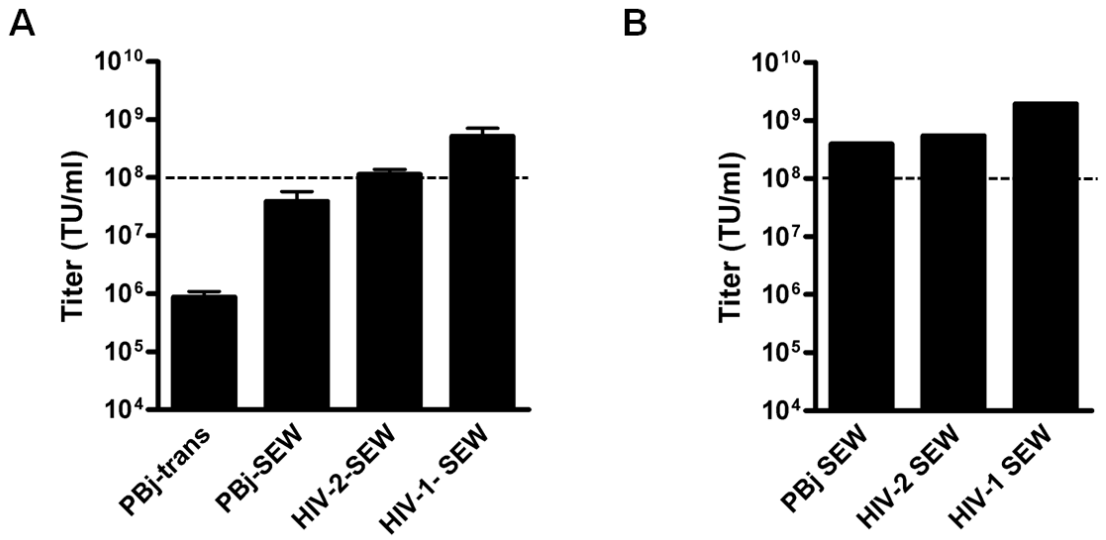

Figure 17: Evaluation of vector particles generated with the novel HIV-2- and PBj-derived transfer vectors. Titers reached on HT1080 cells for generated vector particles using the indicated transfer vector after concentration. **(A)** The mean titers of at least three separate transduction experiments. **(B)** The highest titers reached for PBj-SEW, HIV-2-SEW and HIV-1 SEW vectors.

4.2.3 Enhancing the transfer vectors generated by Fusion-PCR

Introduction of a stop-codon into HIV-2-SEW and PBj-SEW *gag* sequence

As the novel transfer vectors HIV-2-SEW and PBj-SEW still contained the first 200 bp of the *gag* sequence, there was still a potential for an initiation of its translation. Although the truncated *gag* gene would probably not lead to a functional protein, a stop-codon was

introduced downstream the *gag* start-ATG to abrogate any initiated translation resulting in the constructs **HIV-2-g'-SEW** and **PBj-g'-SEW** (Figure 18).

In order to introduce a stop-codon into the *gag* gene of HIV-2-SEW the "aaa"-codon 11 triplets downstream of the start-ATG was changed to "taa", resulting in the sequence 'atgggcgcgagaaactccgtcttgagagggtaa'. For PBj-SEW the "tca"-codon 10 triplets downstream of the start-ATG was changed into a "tga" sequence (atgggcgcgagaaactccgtcttgtgagggaag) to introduce a stop-codon. Both experiments were performed with the QuikChange™ site-directed mutagenesis kit (Stratagene) (3.2.10) using the primer-pairs BPK 43 / BPK 44 for the generation of HIV-2-g'-SEW and BPK 29 / BPK 30 for the generation of PBj-g'-SEW.

Construction of Tat-independent transfer vectors

In a analogous experiment, the U3-region of the 5'LTR was replaced by an SV40/RSV-element to gain a Tat-independent vector RNA expression in packaging cells. For this, the SV40/RSV sequence was PCR-amplified out of the MLV-derived transfer vector SER11S91-SW. It was then fused upstream the R-U5-region of the respective 5'LTR sequence by Fusion-PCR. The subsequent SV40/RSV-R-U5 sequence was cloned into HIV-2-SEW or PBj-SEW resulting in the constructs HIV-2-SR-SEW and PBj-SR-SEW, respectively (Figure 18).

The exact cloning steps are described in the following:

HIV-2-SR-SEW: For the generation of the HIV-2-SR-SEW construct three different PCR sequences were combined by Fusion-PCR to give the SV40/RSV-R-U5 sequence. The different 1st round PCRs were performed using the primer pairs BPK 45/ BPK 46, BPK 47 / BPK 48 and BPK 49 / BPK 50 on the templates HIV-2-SEW, SER11S91-SW, and HIV-2-SEW, respectively. The subsequent Fusion-PCR linked the latter PCR products together. It was performed with the primers BPK 45 and BPK 50. These also introduced the restriction sites PciI and KasI, respectively. The latter were used to integrate the Fusion-PCR construct into the HIV-2-SEW construct, thereby replacing the common 5'LTR sequence with the SV40/RSV-R-U5 sequence.

PBj-SR-SEW: To construct PBj-SR-SEW the 1st round PCRs were performed using the primer pairs BPK 31 / BPK 32 and BPK 33 / BPK 34 on the templates SER11S91-SW and PBj-SEW, respectively. The primers BPK 31 and BPK 34 used for the subsequent Fusion-PCR introduced the restriction sites XhoI and KasI. The latter were used to insert the resulting SV40/RSV-R-U5 sequence into the HIV-2-SEW construct, thereby replacing the native 5'LTR sequence.

Combining the introduced stop-codon and the SV40/RSV-element on one transfer vector

In order to construct an HIV-2- or PBj-derived transfer vector that will contain a stop-codon downstream of the *gag* gene start-ATG as well as an SV40/RSV element within the 5'LTR, both of the latter constructed vectors, which each harbor one of these elements, were combined.

For this purpose, HIV-2-SR-SEW was restricted with PciI and KasI to excise the SV40/RSV-R-U5 sequence. It was then integrated into HIV-2-g'-SEW via the same restriction sites, replacing the native 5'LTR to give **HIV-2-g'-SR-SEW**.

In the same manner PBj-SR-SEW was restricted with KasI and XhoI to excise the SV40/RSV-R-U5 sequence. It was integrated into PBj-g'-SEW replacing the native 5'LTR resulting in **PBj-g'-SR-SEW** (Figure 18).

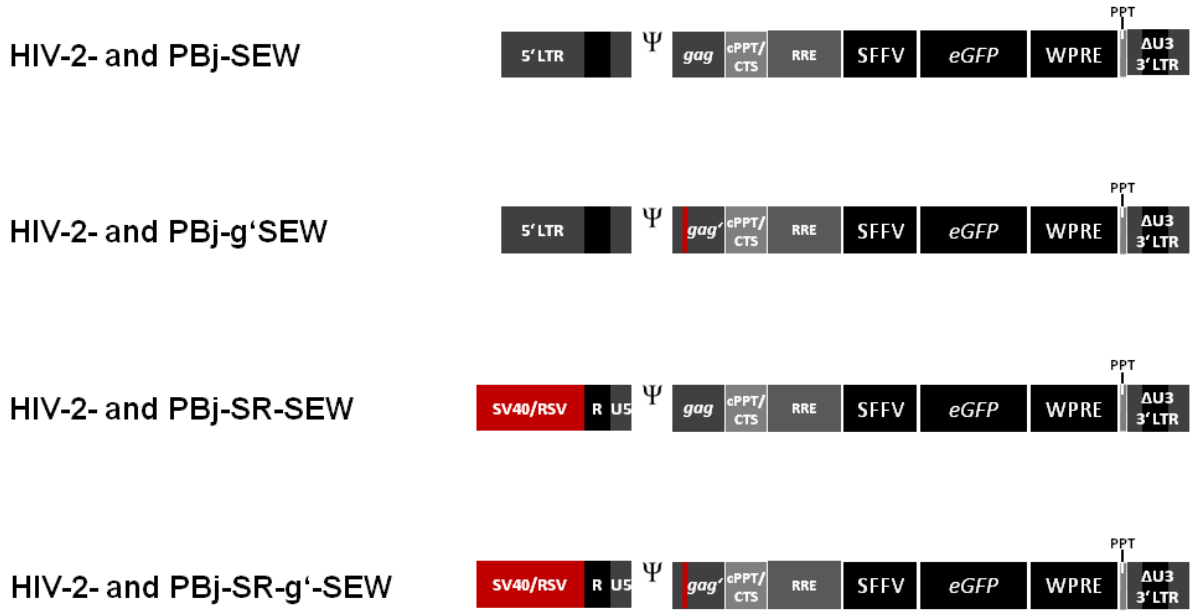

Figure 18: Schematic representation of the final PBj- and HIV-2-derived transfer vectors. The introduced stop-codon and SV40/RSV-element are highlighted in red.

Evaluation of the generated HIV-2- and PBj-derived transfer vector particles

After completing the optimization steps, enhanced HIV-2- and PBj-lentiviral transfer vectors were used to generate vector particles. The vector particles were produced in the presence and/or absence of the codonoptimized Vpx-expression plasmids VpxHIV-2syn or VpxPBjsyn, respectively. The harvested vector particles were concentrated by ultracentrifugation and titrated by HT1080 cell transduction (3.3.8). The difference in vector titers between the constructs is marginal. The PBj-derived vectors resulted in titers around $5x10^7$ TU/ml, where the HIV-2-derived vectors resulted in titers of $1x10^8$ TU/ml (Figure 19).

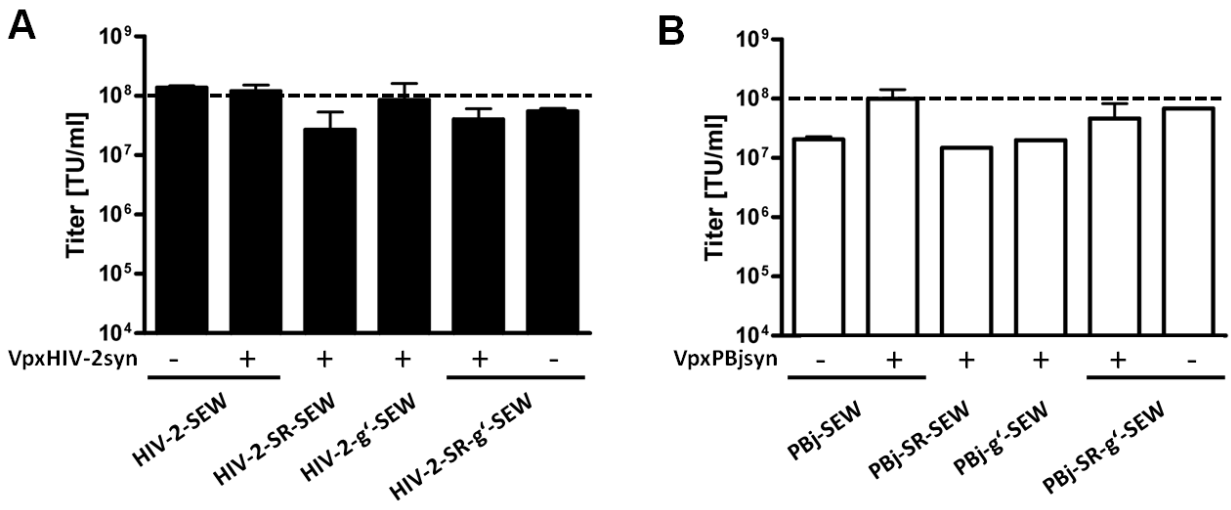

Figure 19: Titers of enhanced HIV-2- and PBj-derived vector particles on HT1080 cells. Titers of **(A)** HIV-2- or **(B)** PBj-based vectors after concentration in the presence or absence of Vpx as indicated.

The consistent titers for the vector particles generated with the different transfer vectors show, that the latter modifications to increase the safety profile of the vector systems, had no negative impact on vector titers.

Monocyte transduction using HIV-2- and PBj-derived vector particles

The constructed HIV-2 and PBj vectors were used for transduction of primary human monocytes. For this, blood monocytes from two donors were isolated by Ficoll-gradient centrifugation followed by a negative MACS selection (3.3.4). The isolated monocytes were cultivated in VLE-RPMI-medium for 24 h and transduced with the novel PBj- and HIV-2-derived lentiviral vectors at an moi of one or ten. The transduction efficiencies were analyzed five days post transduction.

For the HIV-2-derived vectors generated in presence of VpxHIV-2syn, the transduction increased in general from an moi of one to an moi of ten (Figure 20A). The HIV-2-derived vectors with no incorporated VpxHIV-2syn were used as control and transduced the monocytes with low efficiencies. For the transduction experiments with the HIV-2-derived lentivectors the mean transduction was calculated from three to twelve transduction experiments on different donor-monocytes.

All vectors derived from SIVsmmPBj were able to transduce the monocytes efficiently when supplemented with VpxPBjsyn (Figure 20B). The transduction efficiency increased by changing the moi from one to ten for PBj-SEW (VpxPBjsyn), PBj-g'-SEW (VpxPBjsyn), and PBj-SR-g'-SEW (VpxPBjsyn), but decreased for PBj-SEW (-), PBj-SR-SEW-cSIN (VpxPBjsyn), and PBj-SR-g'-SEW (-). The mean transduction efficiency from one to eleven experiments on different donor-monocytes was considered.

As the Vpx-incorporation into the vector particles is crucial for the ability to transduce primary human monocytes, all vectors were tested for their Vpx-incorporation. Therefore, vector lysates of concentrated vector particles were analyzed by Western blotting (Figure 20C). For the detection of Vpx the αVpxHIV-2 monoclonal antibody (αVpx) was used. The antibody is described to be cross-reactive to VpxPBj. As expected, Vpx was detectable for all lentiviral vectors generated by cotransfection of the Vpx-expression plasmid.

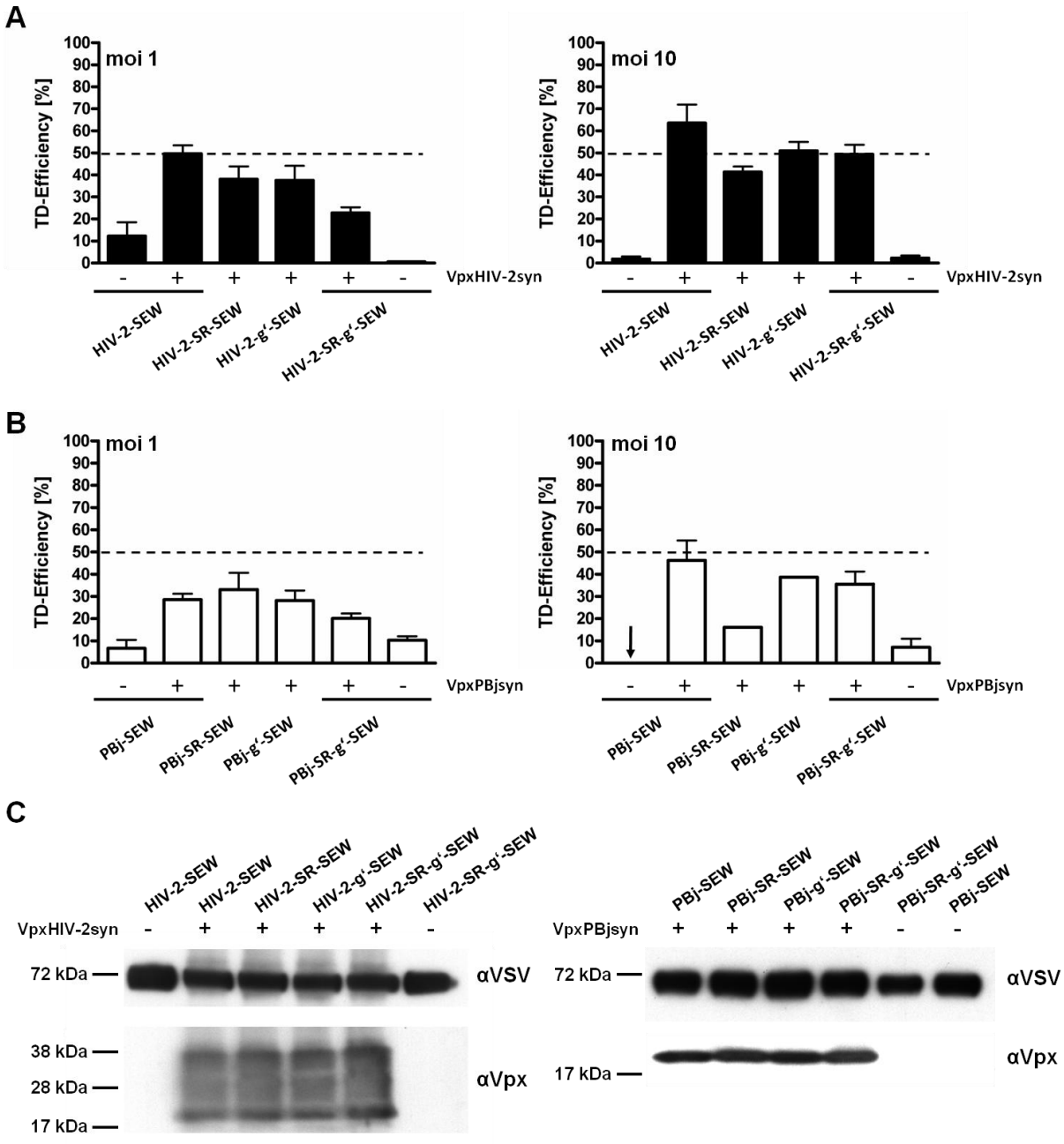

Figure 20: Monocyte transduction and Vpx incorporation of the novel PBj- and HIV-2-derived lentiviral vectors. Efficiency of transduction for **(A)** HIV-2- and **(B)** PBj-derived lentiviral vectors at an moi of one or ten. The vector particles were generated with the indicated transfer vector. **(C)** Western blot analysis for Vpx-incorporation of the generated vector particles used for the transduction experiments.

The transduction experiments confirm that the fast and efficient generation of functional lentiviral transfer vectors by Fusion-PCR is successful. The ability to transduce primary human monocytes was maintained.

Suitability of HIV-2 SEW- and PBj-SEW-derived vector particles for B-cell and neuron transduction

The novel HIV-2- and PBj-derived lentiviral vectors were used to investigate their potential for the transduction of other primary cell types than monocytes. They were used to transduce human unstimulated primary B-cells and murine neuronal brain cells.

Both the HIV-2-SEW- and PBj-SEW-derived lentiviral vectors pseudotyped with VSV-G failed to transduce unstimulated B-cells (data not shown). The inability to transduce unstimulated B-cells was not unexpected as it is described for VSV-G pseudotyped HIV-1-lentivectors in the literature (Funke et al., 2009). The block in unstimulated B cells could not be overcome by either of the PBj- or HIV-2-derived vectors, regardless of homologous Vpx-complementation. The B-cell transduction experiments were performed in cooperation with Sabrina Funke.

For the transduction of murine neuronal cells the primary cells were provided by Brigitte Anliker and Julia Brynza. Briefly, the Cerebella of 5/6-days old mice were isolated as described elsewhere (Rogister and Moonen, 2001), minced and taken into cell culture. After five days in cell culture, the cells were transduced with HIV-1-SEW-derived lentivectors as well as HIV-2-SEW- and PBj-SEW-derived vector particles generated in the presence and absence of VpxHIV-2syn and VpxPBjsyn, respectively, at the moi of ten. The transduction efficiency was analyzed five days post transduction. For this, the cells were stained with NeuN-Cy5, a neuronal cell marker, and 4',6-diamidino-2-phenylindole (DAPI), a nucleus marker, and fixed. The fixed cells were analyzed by Fluorescent Laser Scanning Microscopy (Figure 21). The primary murine neuronal cells could efficiently be transduced with VSV-G pseudotyped PBj-SEW- and HIV-2-SEW-derived lentiviral vectors. Although the cell transduction was not specific for the brain neurons, as also transduced stromal cells were found, the eGFP-expression was particularly strong in those cells. The transduction of the neuronal cells was Vpx independent as also HIV-1-SEW- and HIV-2-SEW-derived vectors in absence of Vpx showed equal transduction efficiency (data not shown).

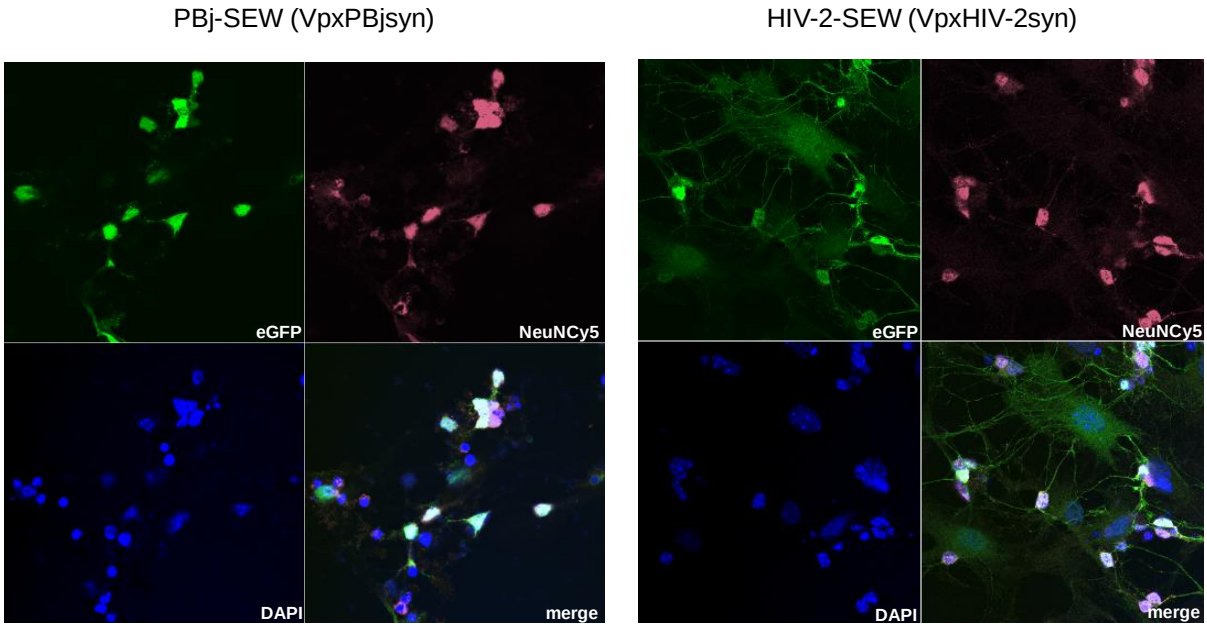

Figure 21: Transduction of murine neuronal cells with an HIV-2- and PBj-derived vector. The cells were analyzed by Fluorescent Laser Scanning Microscopy for eGFP-expression, DAPI-staining and NeuNCy5-staining.

The promising ability of the novel PBj- and HIV-2-derived lentivectors to transduce murine brain neurons will be further investigated *in vivo* in a cooperation with the Institute of Virology at the University of Vienna.

4.3 Analyzing human monocytes as potential target for *gp91^{phox}* gene correction

Patients suffering from X-linked chronic granulomatous disease (xCGD) are highly susceptible to bacterial and fungal infections. The reason is a non-functional NADPH oxidase activity. This leads to the inability of xCGD patients to generate superoxides for monocyte- and granulocyte-mediated killing of intracellular pathogens. It was therefore hypothesized that correcting the underlying *gp91^{phox}* gene defect in patients´ monocytes may provide a possible treatment option. The assumption is that monocytes can be isolated from patients' blood samples, corrected *ex vivo* by lentiviral gene-transfer and given back to the patient. If the corrected monocytes were able to decrease the bacterial and fungal load, the treatment could benefit the patients in various ways. In order to corroborate the assumption, the first step was to investigate human monocytes in their potential to phagocytose, burst and kill *Staphycoccus aureus*, a bacterium most xCGD-patients suffer from severely (Winkelstein et al., 2000).

4.3.1 Flavocytochrome b_{558} is ubiquitously expressed by human monocytes

In a first experiment the ability to isolate a pure monocyte population was evaluated. For this, primary human monocytes were isolated by negative depletion from peripheral blood mononuclear cells (PBMCs) from two different donors (3.3.4). The purity of the isolated monocytes was analyzed by determination of the $CD14^+$-cell population by FACS-analysis using APC-coupled CD14 mAb (Figure 22). For the different donors about 90% and 94% of the isolated cells were monocytes.

In the same step, the isolated monocytes were characterized for their expression of flavocytochrome b_{558}, a membrane bound heterodimer that consists of a smaller α-subunit ($p22^{phox}$) and a larger ß-subunit ($gp91^{phox}$). As the flavocytochrome b_{558} is part of the NADPH-oxidase, its detection was an indirect measurement for NADPH-oxidase expression. To determine the expression level of on the surface of human monocytes, the isolated monocytes were stained for flavocytochrome b_{558} and CD14. For the FACS-analysis FITC-coupled α-flavocytochrome b_{558} mAb and APC-coupled α-CD14 mAb were used (3.3.10). For both donors, about 99% of the $CD14^+$-monocytes expressed flavocytochrome b_{558} on their cell surface (Figure 22).

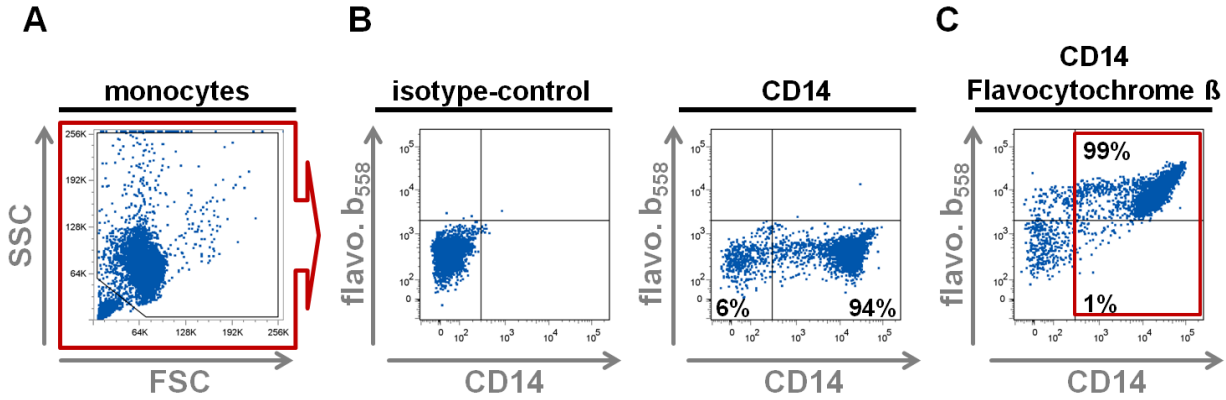

Figure 22: Flavocytochrome b_{558} expression of primary human blood-monocytes. (A) FSC-SSC FACS profile. **(B)** Monocyte purity determined by $CD14^+$-expression in comparison to the isotype control. **(C)** A α-flavocytochrome b_{558}/α-CD14 double-positive cell staining showed that approx. 99% of the blood-monocytes express flavocytochrome b_{558} on their surface. (Representative FACS-data for one donor is shown.)

4.3.2 Phagocytosis and phagoburst ability of human monocytes

Monocytes are described to have a high ability to engulf bacteria and fungi. To assure that the isolated monocytes retained the ability of phagocytosis in cell culture, the endocytosis capacity of the monocytes was analyzed by the DQ-BSA assay (3.3.14). Briefly, the monocytes were isolated and incubated at either 4°C or 37°C for 30 min. Then, DQ-BSA was added for another 2-h incubation period after which the cells were measured for uptake of

the DQ-BSA by FACS. More than 90% of the monocytes phagocytosed the DQ-BSA at 37°C compared to the inactive monocytes at 4°C (Figure 23, left).

A high uptake of bacteria and fungi alone does not account for the ability of monocytes to destroy the pathogens. In order to functionally kill them, the phagocytes have the ability to produce reactive oxygen species (ROS) such as superoxide anions, hydrogen peroxides and hypochlorous acids. The induction of ROS by activated monocytes (oxidative burst) was measured by the phagoburst assay (3.3.15). For this, the isolated blood-monocytes were stimulated with either PMA or washing-solution for ten minutes and their subsequent ROS induction was visualized using the substrate dihydrorhodamine (DHR) 123 by FACS. For donor A and B, 94.3% and 96.4% of the monocytes produced a strong phagoburst, respectively (Figure 23, right).

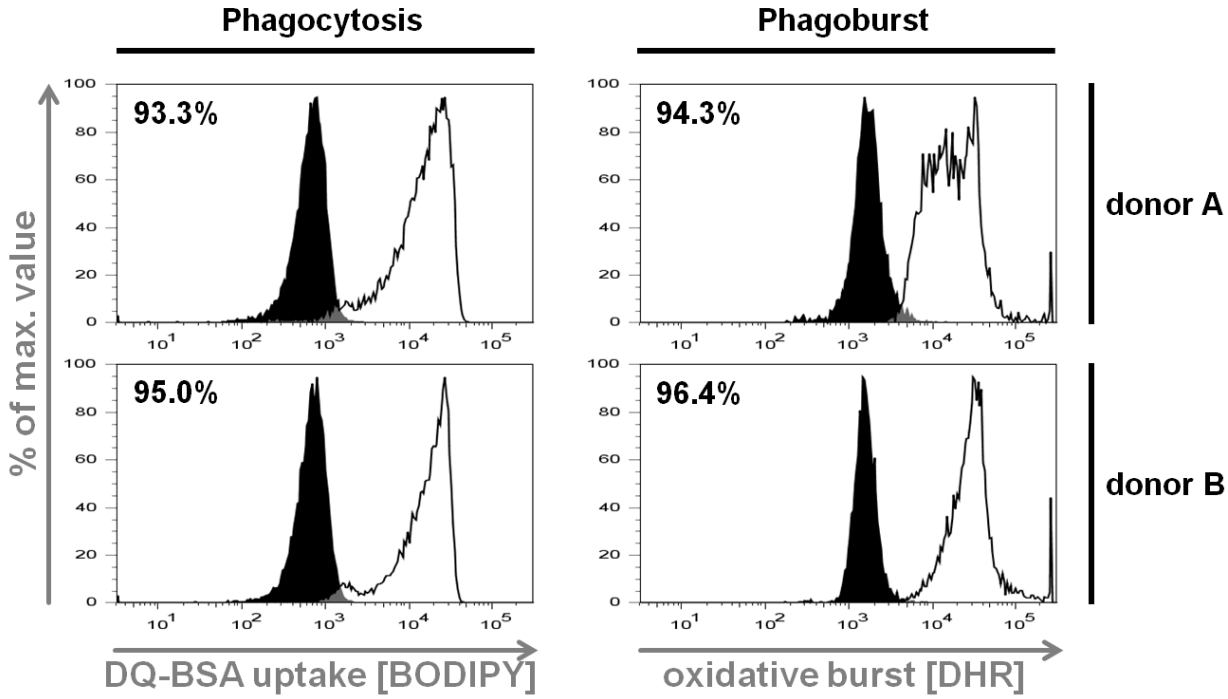

Figure 23: Phagocytosis and Phagoburst of human monocytes. (Left) Phagocytosis capacity analyzed by DQ-BSA uptake of monocytes at 4°C (solid black) or 37°C (white). **(Right)** Phagoburst capacity analyzed by ROS production of unstimulated (solid black) or PMA stimulated (white) monocytes.

4.3.3 *Staphylococcus aureus* killing by human monocytes

The ability of monocytes to kill bacteria has been known for a long time. As *S. aur*eus is one of the major concerns of patients suffering from xCGD (Winkelstein et al., 2000), this bacterium was chosen to demonstrate the killing ability of human monocytes isolated from healthy donors. As no exact standard protocol for such an assay was available, different settings were tested and an own protocol established to measure the killing activity of monocytes (3.2.11).

Briefly, monocytes were isolated from heparinized whole blood (3.3.4) in order to ensure their ability to burst. Following isolation, 0, 1x10^4, 1x10^5, or 1x10^6 monocytes were mixed with two different amounts of *S. aureus* (~3x10^5 or ~1x10^6 bacteria), seeded in a 96well plate and activated with PMA. Thus, in both *S. aureus* killing assays the monocyte-to-bacteria ratios were 0.03, 0.33, 3.35 or 0.01, 0.1, 1, respectively. One single well was set up for each time point and monocyte-to-bacteria ratio. The samples were incubated at 37°C. The bacteria concentration was determined at different time points. For this, 25 µl of a 1:1000-dilution was spread on Agar-plates, incubated at 37°C and the number of colonies was counted 15-24 h later (Figure 24).

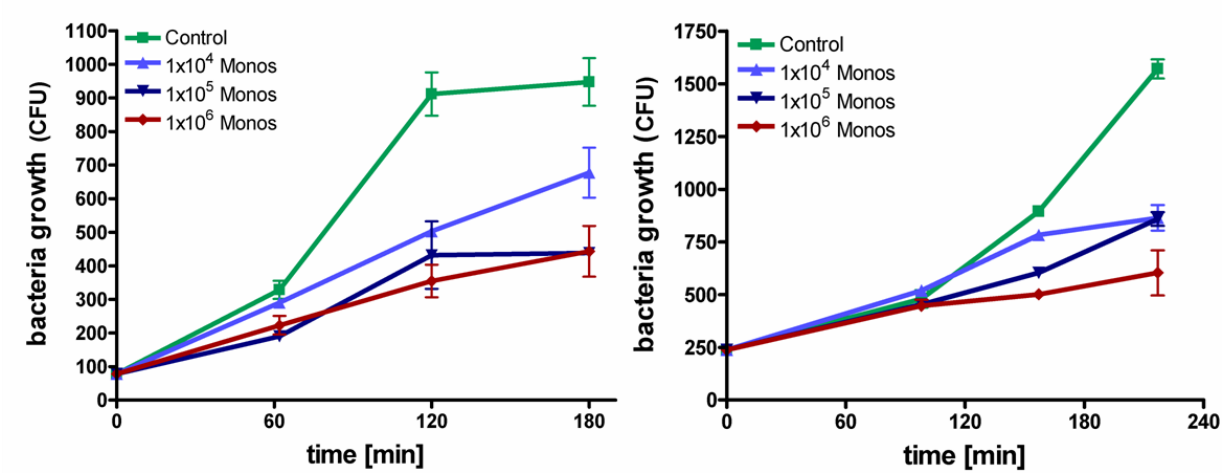

Figure 24: Capacity of human monocytes to kill *S. aureus* bacteria. Growth curves of 3x10^5 **(left)** and 1x10^6 **(right)** bacteria inoculated onto the indicated amount of PMA-activated monocytes. At the indicated time points the bacteria load was analyzed.

Bacterial growth was impaired noticeably with increasing amounts of monocytes. While bacteria in absence of monocytes showed a normal growth curve, the *S. aureus* growth was impaired inversely proportional to the monocyte presence. Even at the lowest monocyte-to-bacteria ratio of 0.01 the bacteria growth was reduced by 45% in comparison to the control after 3 h incubation. Hence, a method to investigate the ability of monocytes to kill bacteria was established. Using this assay, the potency of human monocytes to kill bacteria was confirmed.

4.3.4 HIV-2 based lentiviral transfer vector for *gp91^{phox}* gene-transfer

After the successful demonstration of efficient phagocytosis, oxidative burst, and killing activity of freshly isolated primary human monocytes, a vector for the correction of *gp91^{phox}*-deficient monocytes from xCGD patients was constructed. The newly developed, HIV-2-derived vectors were superior to the PBj-derived vectors (Figure 20). Hence, it was decided to construct a vector for the *gp91^{phox}* gene transfer on the basis of HIV-2.

For this, an expression cassette including the *gp91^{phox}* gene under the control of the SFFV-promoter upstream of a WPRE, depicted SFFV-SgW-WPRE-expression cassette, was inserted into the HIV-2-MCS vector. In contrast to the WPRE used for constructing the eGFP-expressing vectors, this WPRE already contained a mutation which was introduced due to safety concerns (Schambach et al., 2006a). The SFFV-SgW-WPRE-expression cassette was amplified from the HIV-1-based pHIV-1-SgpSw-transfer vector by PCR using the primer-pair BPK 51 / BPK 52 and subsequently cloned into HIV-2-MCS via the restriction sites MfeI and AgeI. The resulting transfer vector, designated HIV-2-SgW, was used for transient transfection of 293T cells together with the packaging plasmid pHIV-2d4, a Vpx-expression plasmid and the VSV-G expression plasmid pMG.G2. The vector particles were harvested, concentrated and titrated on Δ*gp91^{phox}*-PLB-985 cells (Figure 25). This was done by transducing a defined number of Δ*gp91^{phox}*-PLB-985 cells with serial dilutions of the vector. The cells were analyzed for gp91^{phox} expression five days post transduction by a α-flavocytochrome b_{558}-stain. They were also stained with 7-AAD, which stains dead cells (data not shown). Only living, 7-AAD negative cell populations were analyzed for flavocytochrome b_{558} expression (Figure 25). The gp91^{phox} expressing wild-type PLB-985 cells were used as positive control. A 1:5000-dilution of the HIV-2-SgW transfer vector generated vector particles resulted in 18.1% flavocytochrome b_{558}-positive cells. Hence, the HIV-2-SgW vector titer was calculated to be 3.5 x 10^8 TU/ml.

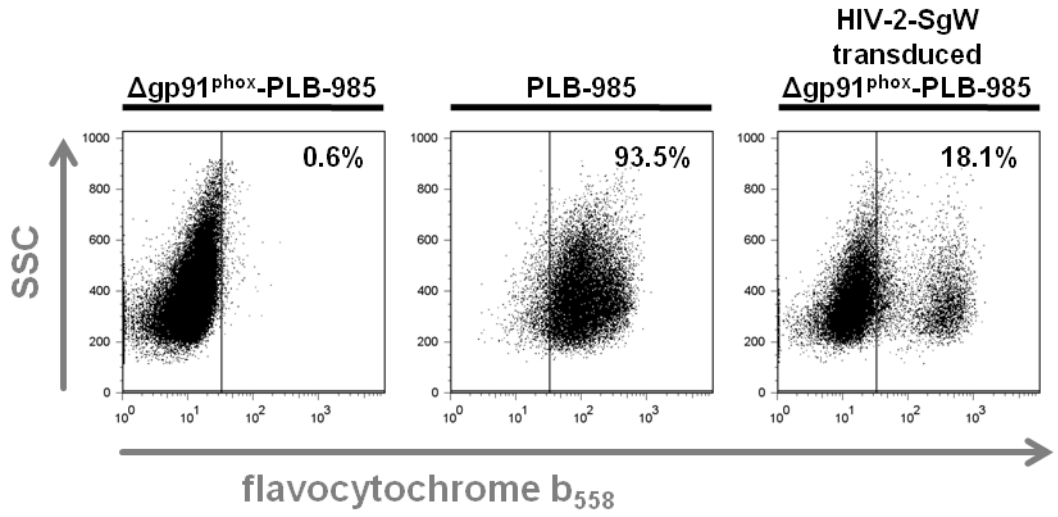

Figure 25: Titration of vector particles generated with the HIV-2-SgW transfer vector on Δ*gp91^{phox}*-PLB-985 cells. Percentage of 7-AAD negative gp91^{phox}-expressing cells measured through a α-flavocytochrome b_{558}-stain by FACS.

4.4 *Gp91^{phox}* gene correction of murine monocytes

The X-linked chronic granulomatous disease is a rare disease. It is difficult to come by patient blood-samples. However, a good mouse model, the xCGD-knockout mouse, is available (Pollock et al., 1995). This model was used to study the correction of the *gp91^{phox}* gene defect in murine monocytes with the help of lentiviral vectors.

4.4.1 Cell-composition of murine bone marrow

As described, the aim was to study the ability of phagocytosis, oxidative burst, and *S. aureus* killing of murine monocytes as well as to correct the *gp91^{phox}* gene-defect in *gp91^{phox}*-defecient murine monocytes with lentiviral vectors. In order to accomplish all of this, large amounts of the cells are necessary. Therefore, it was decided to isolate the cells from bone marrow to isolate high amounts of monocytes. This isolation of murine monocytes from the bone marrow was not yet established in the laboratory. To ensure that enough monocytes are present in the murine bone marrow, the cell-composition of the bone marrow was analyzed in collaboration with Sibylle Wehner (University of Frankfurt). C57BL/6 mice were sacrificed and the femur was isolated. The bone was cut and the bone marrow used for bone-marrow smears on cover-slips. The cover-slips were Pappenheim stained. This method can be used to differentiate between different plasma cells. The Pappenheim stained cells were analyzed with a light microscope (Figure 26).

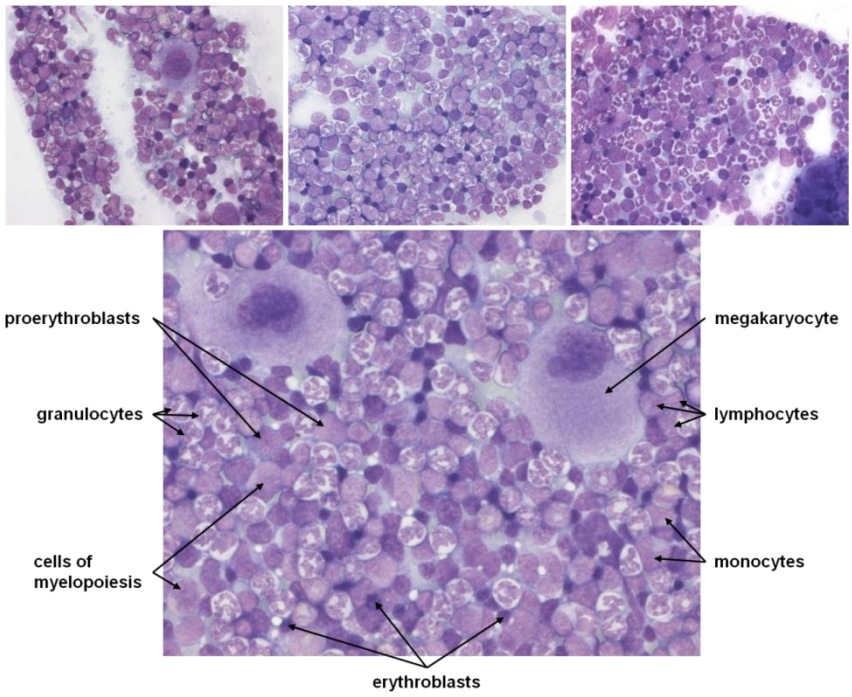

Figure 26: Cellular composition of the murine bone marrow. Pappenheim stained murine bone-marrow smears. Different cell types of the murine bone marrow are indicated (40 x magnification).

Cells of erythropoiesis (proerythroblasts, basophilic- / polychromatic- / eosinophilic erythroblasts), megakariopoiesis (megakarioblasts, megakariocytes) the myelocytopoiesis (myeloblasts, promyelocytes, myelocytes, juvenile myelocytes, band granulocytes, segmented granulocytes), and lymphocytopoiesis (prolymphocytes, lymphocytes) as well as monocytopoiesis (monoblasts, monocytes) can be distinguished.
Although the exact cell composition could not be quantified with the generated bone-marrow smears, the stains revealed a normal hematopoiesis, including the presence of monocytes.

4.4.2 Isolation and purification of functional murine monocytes from bone marrow

Murine monocytes are not as well discernible from other cell types as their human monocyte counterpart, which can be easily identified by CD14-expression. Murine monocytes share common markers (e.g. CD11b and Gr1) with neutrophils. As the work with murine monocytes had not been established in our laboratory, a purification protocol was established and the correct monocyte isolation verified by standard murine monocyte markers. In accordance with the isolation of human monocytes, the murine monocytes were also purified by negative depletion to ensure untouched monocytes (3.3.5). Briefly, murine bone marrow was isolated, resuspended in PBS, layered over Ficoll-Paque® (1.083 density) and subjected to density-gradient centrifugation to enrich the mononuclear cells and to remove granulocytes and erythrocytes, among others. The PBMC-containing interface was collected, washed and stained with FITC-coupled antibodies against B-cells (α-CD45R (B220)), T-cells (α-CD90), NK-cells (α-CD49b (DX5), and erythrocytes (α-Anti-Ter119). A second α-FITC antibody conjugated with magnetic beads enabled a negative depletion by magnetic associated cell sorting (MACS) leaving the isolated monocytes (Figure 27A).
To verify the purification protocol the isolated monocytes were analyzed by FACS-staining. Different PE-coupled antibodies were used to identify contaminations of B-cells (α-CD45R (B220)), T-cells (α-CD90), and NK-cells (α-CD49b (DX5) and NK1.1), respectively. None of these cells could be found in the monocyte population but were detected in the depleted cell fraction (data not shown). The purity of murine monocytes was determined by the CD11b-staining to be approx. 94%. The CD11b antigen is expressed on myeloid cells such as monocytes/macrophages and to a lower extent on granulocytes, NK cells and subsets of dendritic cells. More than half of the $CD11^+$-cells were positive for Ly6G (Figure 27B). The marker for Ly6G is described to be negative for murine blood-monocytes but transiently expressed on monocytes in the bone marrow.
The $CD11b^+/Ly6G^+$ stain to analyze murine monocytes was replaced with a $CD11b^+/Gr1^+$-double positive stain to characterize murine $Gr1^+$-monocytes (also called inflammatory

monocytes). Of the isolated cells from the bone marrow, 92% were CD11b$^+$/Gr1$^+$-double positive (Figure 27C). Although neutrophils also carry the CD11b and Gr1-surface receptor molecules, the granulocytes were excluded from the monocyte population by Ficoll-Paque® density-gradient centrifugation.

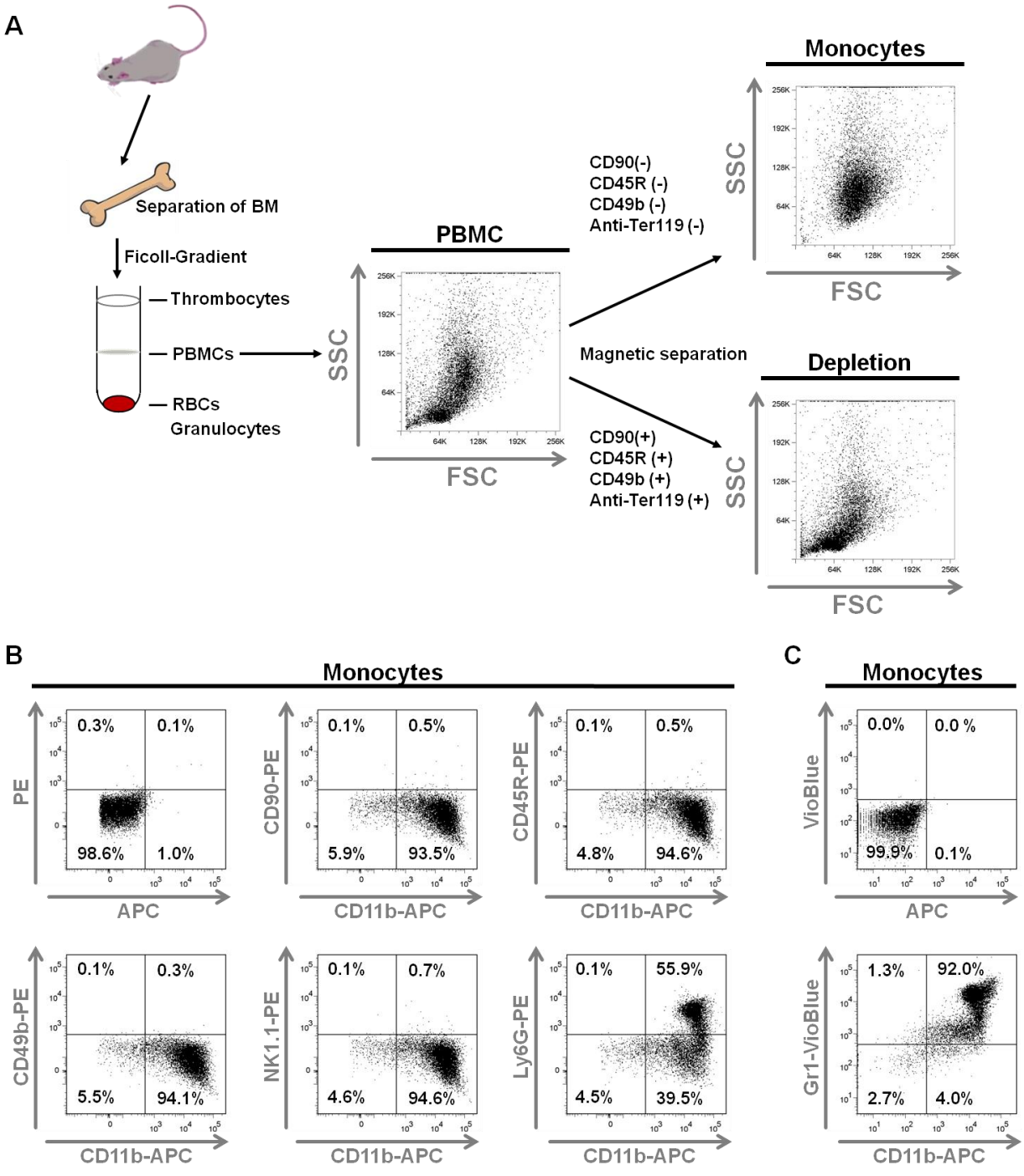

Figure 27: Isolation and characterization of murine monocytes. (A) Schematic representation of monocyte isolation and purification. **(B)** Validation of the monocyte isolation protocol with the indicated antibodies. **(C)** Characterization of purified inflammatory Gr1$^+$-monocytes by their CD11b$^+$/Gr1$^+$-expression profile (CD90: T-cells, CD45R: B-cells, CD49b: NK-cells, Anti-Ter119: Erythrocytes)

After successfully establishing the purification of CD11b/Gr1-positive murine bone marrow monocytes, the cells were used for functional analysis. Like human monocytes, the murine monocytes of C57BL/6 wild-type mice and *gp91*^{phox}-knockout mice were tested for their phagocytosis, phagoburst, and *S. aureus* killing ability.

4.4.3 Phagocytosis ability of murine monocytes

Murine monocytes derived from xCGD-mice and their parental C57BL/6 strain were analyzed for their phagocytosis ability. Therefore, bone-marrow derived monocytes were isolated by negative MACS-depletion (3.3.5). The ability of phagocytosis was determined with the DQ-BSA-assay (3.3.14). Briefly, the cells were incubated for 30 min at 4°C (control) or at 37°C. The DQ-BSA was added for continuous 2-h incubation at the same temperature. Then the uptake of the DQ-BSA, indicative for phagocytosis, was measured by FACS. The phagocytosis capacity of murine wt-monocytes of 93.7% was higher than that of *gp91*^{phox}-knockout mice with 81.8% (Figure 28).

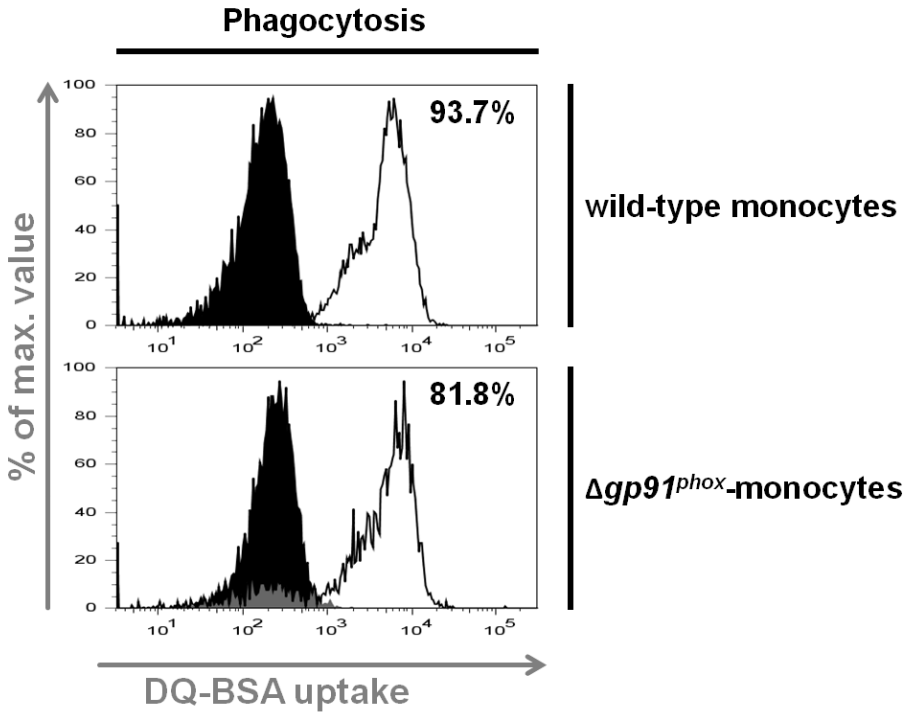

Figure 28: Phagocytosis capacity of murine wt- and Δ*gp91*^{phox}-monocytes. Cells analyzed by the phagocytosis assay incubated at 4°C (solid black) or 37°C (white).

As expected, murine monocytes showed a high phagocytosis ability. Importantly, this ability was not impaired by the lack of gp91^{phox} expression. This can be deducted from the level of the phagocytosis ability in *gp91*^{phox}-deficient monocytes in comparison to that of monocytes from the wild-type C57BL/6 strain.

4.4.4 Phagoburst ability of murine monocytes

Next, freshly isolated wild-type monocytes were compared to *gp91^{phox}*-deficient monocytes for their ability to induce an oxidative burst. For this, the cells were stimulated with PMA or washing solution (control) for ten minutes. To visualize the production of ROS by FACS, the substrate DHR was added to the cells after the stimulation (3.3.15). This way in 93% of the PMA stimulated wild type cells a strong burst was induced. In contrast, it was not possible to detect an oxidative burst for *gp91^{phox}*-deficient cells (Figure 29).

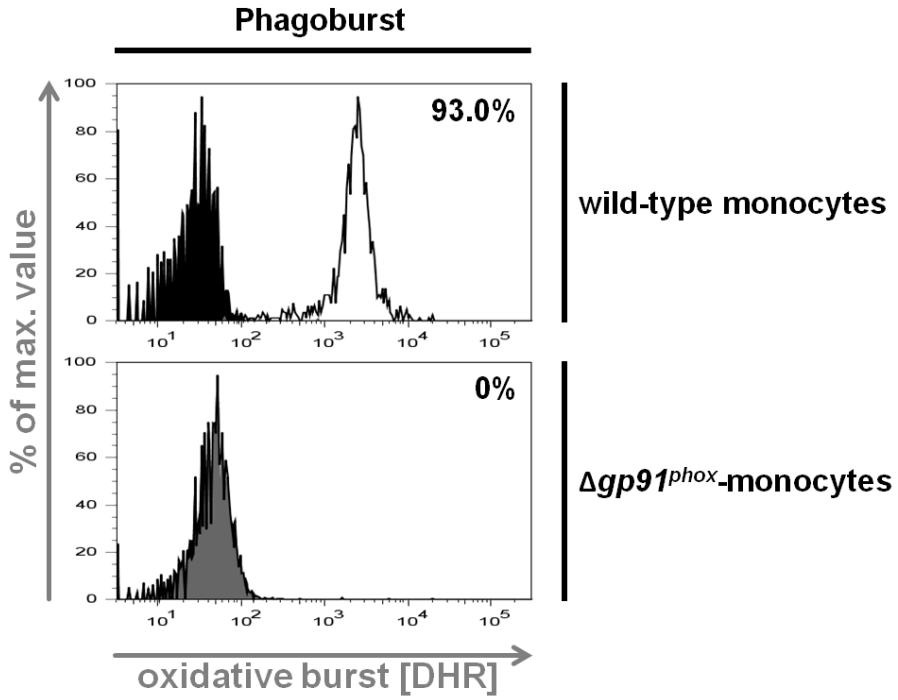

Figure 29: Phagoburst capacity of murine wt- and Δ*gp91^{phox}*-monocytes. Unstimulated (solid black) or PMA stimulated (white) monocytes analyzed by the phagoburst assay.

The phagoburst assay reproduces the published result, and shows a 100% inability of the *gp91^{phox}*-deficient monocytes to produce ROS. The sensitive assay can therefore be further used for the analysis of *gp91^{phox}*-corrected monocytes.

4.4.5 *Staphylococcus aureus* killing by murine monocytes

In order to analyze the capacity of murine monocytes to kill *Staphylococcus aureus* bacteria, the same settings as established for human monocytes were applied (3.2.11). Hence, different amounts of the isolated murine bone-marrow monocytes were plated in a volume of 75 µl in 96well plate-wells. They were mixed with either $6.1x10^4$ or $2.0x10^5$ *S. aureus* bacteria and stimulated with 5 µl PMA. For each ratio multiple wells were set up – one for each reading point. The monocytes were incubated at 37°C and samples taken at different time points to determine the bacteria concentration. For this, a 1:1000 dilution was spread on

Agar-plates, incubated at 37°C and the colonies counted 15-24 h later (Figure 30). In both experiments the $1x10^6$ monocytes resulted in a 16-times and 5-times access of monocytes over bacteria numbers and therefore resulted in a very high bacteria killing rate. The bacteria growth was reduced 90% and 85%, respectively, after 180 min in comparison to the control. At monocyte-to-bacteria ratios of 1.6, 0.5, and 0.05, the resulting bacteria growth rates were reduced 36%, 40%, and 54%, respectively. In one of the experiments, at a monocyte-to-bacteria ratio of 0.16 a killing of *S. aureus* by the monocytes failed and resulted in the same bacteria level as the control after 180 min incubation (Figure 30).

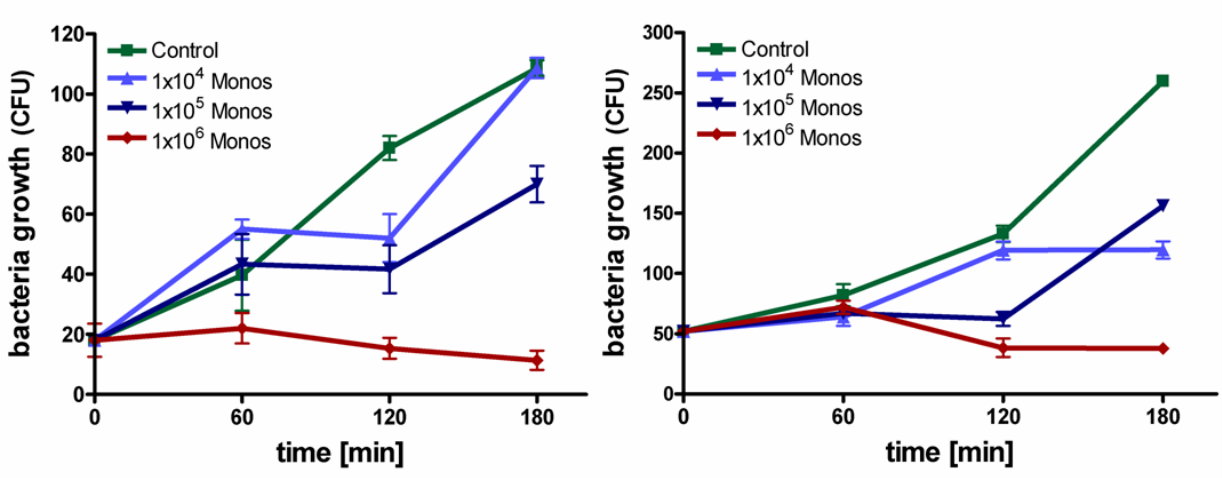

Figure 30: Capacity of murine monocytes to kill *S. aur*eus bacteria. Growth curves of $6.1x10^4$ **(left)** and $2x10^5$ **(right)** bacteria inoculated onto the indicated amount of PMA-activated monocytes. At the indicated time points the bacteria load was analyzed.

4.4.6 Biodistribution of murine monocytes

In order to get an idea where injected monocytes travel within the body, biodistribution studies were performed. To enable the recovery of the injected cells, the monocytes were isolated from the bone marrow of genetically modified mice with endogenous expression of eGFP. An analysis of the isolated monocytes revealed that only 52% were eGFP-positive at the time of injection (data not shown). $2x10^7$ eGFP-monocytes were injected intravenously into the tail vein of two Rag-2/$\gamma c^{-/-}$ mice. This mouse strain is not capable of generating an immune response against transplanted cells due to a lack of B cells, T cells, and NK cells. For control, two other Rag-2/$\gamma c^{-/-}$ mice received 200 µl PBS. Five hours prior to the injection the mice were irradiated (5 gray). In one of the recipient mice the transplantation of the murine eGFP-monocytes worked better. Twenty-four hours after the injection this Rag-2/$\gamma c^{-/-}$ mouse and one of the control mice were sacrificed. From both mice, tissue of the liver, spleen, bone marrow, kidney, blood-samples, and lymph nodes was taken, and fluid from the abdominal cavity was collected. The cells of the different organs were singularized, the

erythrocytes lysed, and the tissues analyzed for eGFP-positive cells by FACS spectrometry. As different tissue cell types have a different autofluorescence a positive control was prepared for each tissue sample by mixing $1x10^6$ eGFP-monocytes with a part of the respective negative tissue cells. Four days post transplantation, the mouse which received less eGFP-monocytes and the second control mouse were sacrificed and their tissues analyzed for GFP-positive cells.

Cells expressing the green fluorescent protein could be detected in the transplanted mice. The highest amount of eGFP-positive cells were found within the blood, the bone marrow, and the spleen in the mouse sacrificed one day after injection. Four days after the injection, eGFP-positive cells were still detectable in the blood and in the bone marrow (Figure 31).

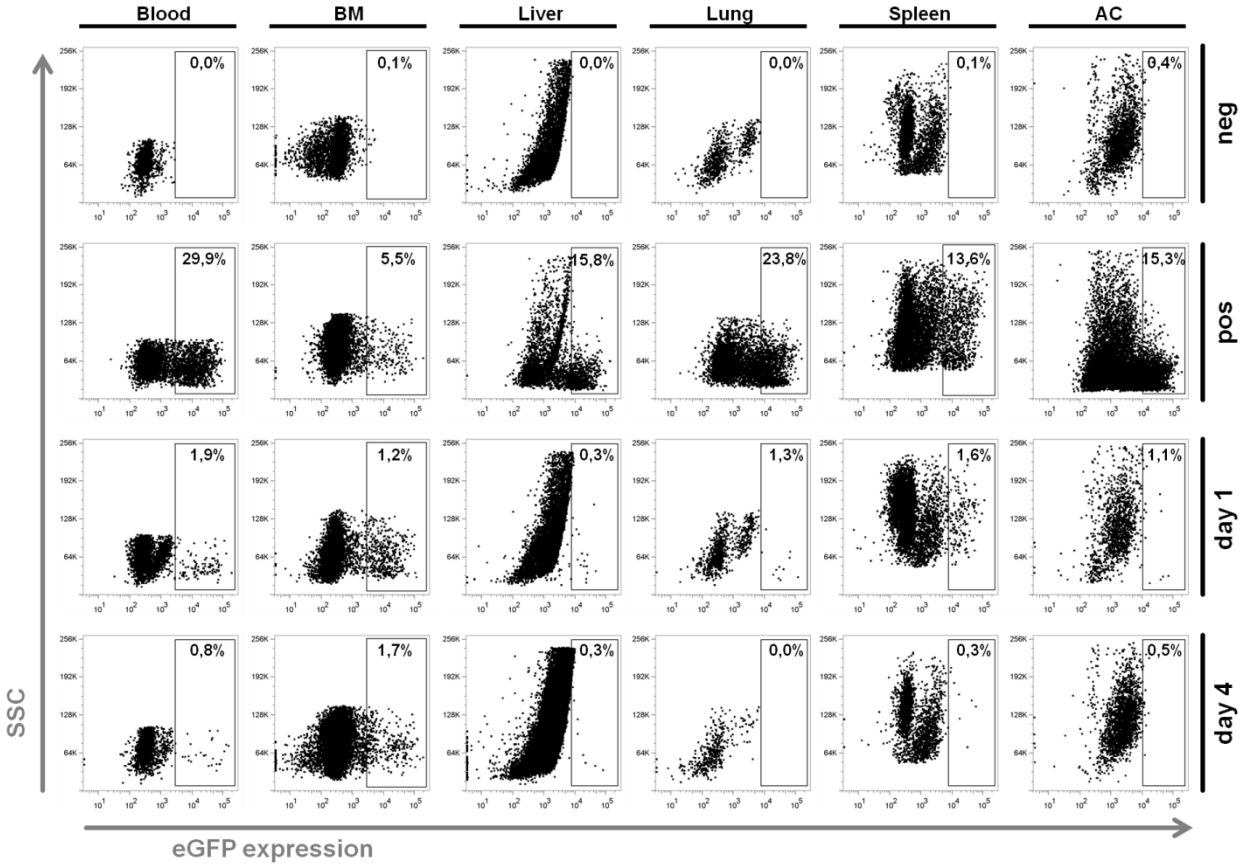

Figure 31: Biodistribution of murine monocytes. EGFP expressing cells detected by FACS in various tissues of Rag-2/γc$^{-/-}$ one and four days after i.v. injection. Non-transplanted Rag-2/γc$^{-/-}$ mouse tissues were used alone as negative control (neg) or mixed with eGFP-monocytes as positive control (pos). (BM, bone marrow; AC, abdominal cavity)

4.4.7 Determination of the half-life of murine monocytes *in vivo*

The idea to use monocytes instead of granulocytes for xCGD gene therapy is based on the described longer half-life of the cells. Granulocytes have a very short half-life of approx. 6 h which makes them all but impossible to use for gene correction. In contrast, the half-life of

murine blood-monocytes is described to be 43.5 +/- 7.9 h (Swirski et al., 2006). These data rely on an indirect radioactivity measurement of [^{111}In]oxine-labeled blood-monocytes. In this thesis the murine monocytes are derived from the bone marrow. The half-life between bone-marrow derived monocytes and blood-monocytes might differ and was therefore analyzed.

To determine the half-life of murine bone-marrow monocytes, C57BL/6 mice were sacrificed and monocytes isolated from the bone marrow. Monocytes isolated from C57BL/6 mice carry the CD45.2 antigen. The amount of $9x10^7$ CD45.2 monocytes were resuspended in PBS and injected into the tail vein of CD45.1 mice immediately after isolation. CD45.1 mice carry the CD45.1 antigen, an alloantigen of CD45.2. Both are expressed on all hematopoietic cells except mature erythrocytes and platelets. The two recipient mice and the control mouse all looked healthy and had weighed 26.3 g, 28.0 g and 27.5 g, respectively. The injection procedure into the tail vein worked flawlessly and the whole volume (200 µl) was injected. Blood samples were taken from the tail vein of the animals at regular intervals of 24 h until day five after injection. The percentage of CD45.2 monocytes within the monocyte population was calculated by FACS. For this the blood samples were treated with Pharm Lyse™ (BD Biosciences) to remove erythrocytes and neutrophils. The samples were subsequently stained with antibodies against Gr-1-Vio-Blue, CD11b-PE-Cy7, CD45.1-PE, and CD45.2-PerCP-Cy5.5. Within the double positive $CD11b^+/Gr1^+$-monocyte population it was possible to distinguish between the CD45.1-monocytes of the recipient mouse from the CD45.2-monocytes of the donor mice. The first blood sample was taken four hours post injection where the amount of calculated CD45.2-monocytes (9.84% and 7.62%) was normalized to 100%. The percentage of CD45.2-monocytes decreased constantly until day five. The blood of a CD45.1-mouse as well as isolated CD45.2-monocytes was used as control. By a nonlinear regression (curve fit) through the time point values, the half-life of murine monocytes in the bloodstream was measured to be 55.2 +/- 5.1 h (Figure 32).

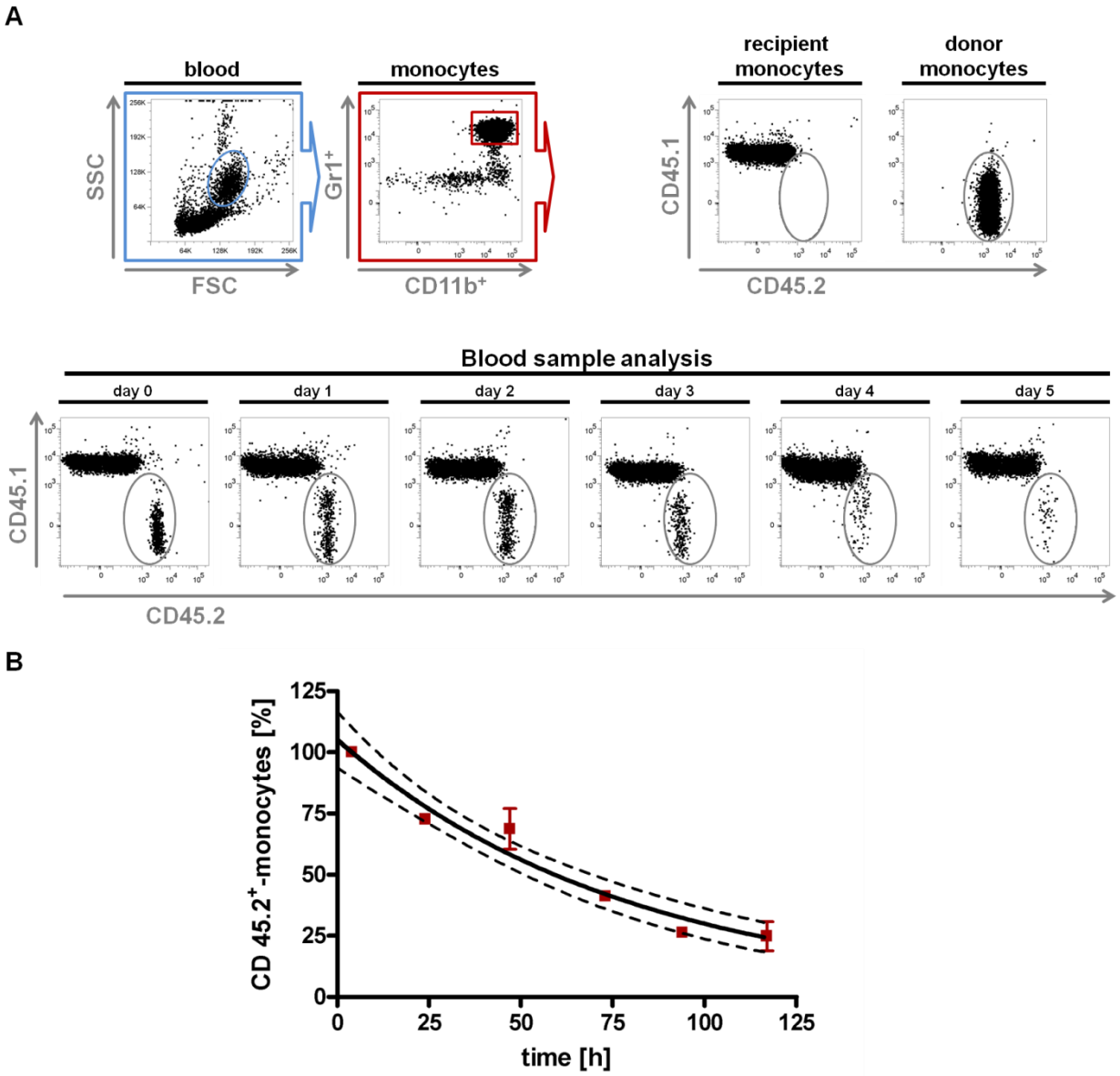

Figure 32: Retention of monocytes in the blood circulation. CD45.2-monocytes were injected i.v. into two recipient CD45.1-mice. The percentage of CD45.2-monocytes was measured from blood withdrawals over a period of five days. **(A)** FACS-measurements (3000 events) for one representative mouse. **(B)** Retention of monocytes analyzed by nonlinear regression. The number of measured CD45.2-monocytes immediately after injection was normalized to 100%.

4.4.8 Gene correction of *gp91^{phox}*-deficient murine monocytes

In a last step the *gp91^{phox}*-deficient monocytes of the knockout mice were corrected by gene transfer with a lentiviral vector. For this purpose, lentiviral vectors derived from PBj (PBj-SEW), HIV-2 (HIV-2-SEW), or HIV-1 (HIV-1-SEW) were compared in their ability to transduce murine monocytes. The vectors were generated by transient transfection of 293T cells. Next to the transfer construct, the packaging-construct, and the envelope-construct, the according VpxPBjsyn or VpxHIV-2syn was used for PBj or HIV-2 transient transfection, respectively. The generated vectors were used for murine monocyte transduction at moi of 1,

10, 30, or 100. PBj- and HIV-2-derived vectors failed to transduce murine monocytes efficiently (data not shown). In contrast, even at an moi of one, 11% and 18% of the cells could be transduced by HIV-1 vectors. Increasing the amount of the vectors also increased the transduction efficiency. A transduction at the moi of 10 or 30 in two separate experiments led to rates of 39.0% and 58.0% or 52.0% and 65.0% positive cells, respectively. A transduction of the cells at an moi of 100 resulted in the highest transduction rate of 70%. Based on these transduction results, further transduction experiments of murine monocytes were conducted with HIV-1-derived lentiviral vectors.

For the lentiviral gene correction of murine *gp91^{phox}*-deficient monocytes, the HIV-1 transfer vector pHIV-1-SgpSw, which harbors the same expression cassette (SFFV-*gp91^{phox}*-WPRE) as HIV-2-SgW-vector systems, was kindly provided by Manuel Grez. For vector production, VSV-G pseudotyped HIV-1 particles were produced by transient transfection of 293T cells using the packaging construct pCMVΔR8.9, the envelope construct pMD.G2, and the pHIV-1-SgpSw transfer vector. The HIV-1 particles were titrated on Δ*gp91^{phox}*-PLB-985 cells (3.3.8). This way, a vector titer of $7.56x10^9$ TU/ml was achieved after concentration.

The produced high-titer HIV-1-SgpSw vectors were used for *gp91^{phox}* gene correction of murine Δ*gp91^{phox}*-monocytes. For this, the murine cells were isolated from the bone marrow of *gp91^{phox}*-knockout mice by negative depletion (3.3.5) and plated in 48well plates for transduction (3.3.9). The monocytes were transduced at the moi of 10, 30, and 100. The transduced monocytes were cultivated for six days and analyzed for their burst activity. The transduction efficiency of HIV-1-SgpSw vectors was determined by a correlation to the transduction with HIV-1-SEW vectors. These two vector systems differ only in their transgene expression by the transfer vector. The VSV-G pseudotyped vector particles themselves are identical. Hence, it was assumed that within one experiment, the transduction of identical isolated cells from the same mouse background with the same moi will yield comparable transduction efficiencies. Based on this assumption, the transduction efficiencies were calculated with vector particles that were generated using the eGFP-transferring HIV-1-SEW transfer vector. A transduction of *gp91^{phox}*-deficient murine monocytes at an moi of 10, 30, and 100 yielded 57.7%, 63.1%, and 64.9% eGFP-positive cells, respectively. In contrast, the phagoburst ability of *gp91^{phox}*-corrected monocytes with HIV-1-SgpSw-derived vector particles was much lower (Figure 33). Prior to the FACS-analysis of the HIV-1-SgpSw transduced monocytes, the cells were incubated with α-Gr1-VioBlue antibodies. The calculated phagoburst for this $Gr1^+$-monocytes was 0.9%, 2.5%, and 10.2% for the transduction at an moi of 10, 30, and 100, respectively. The burst experiments from wild type monocytes show a phagoburst activity of 98.4%.The results show that the burst activity of the

murine monocytes is weak in comparison to the corresponding calculated transduction efficiency.

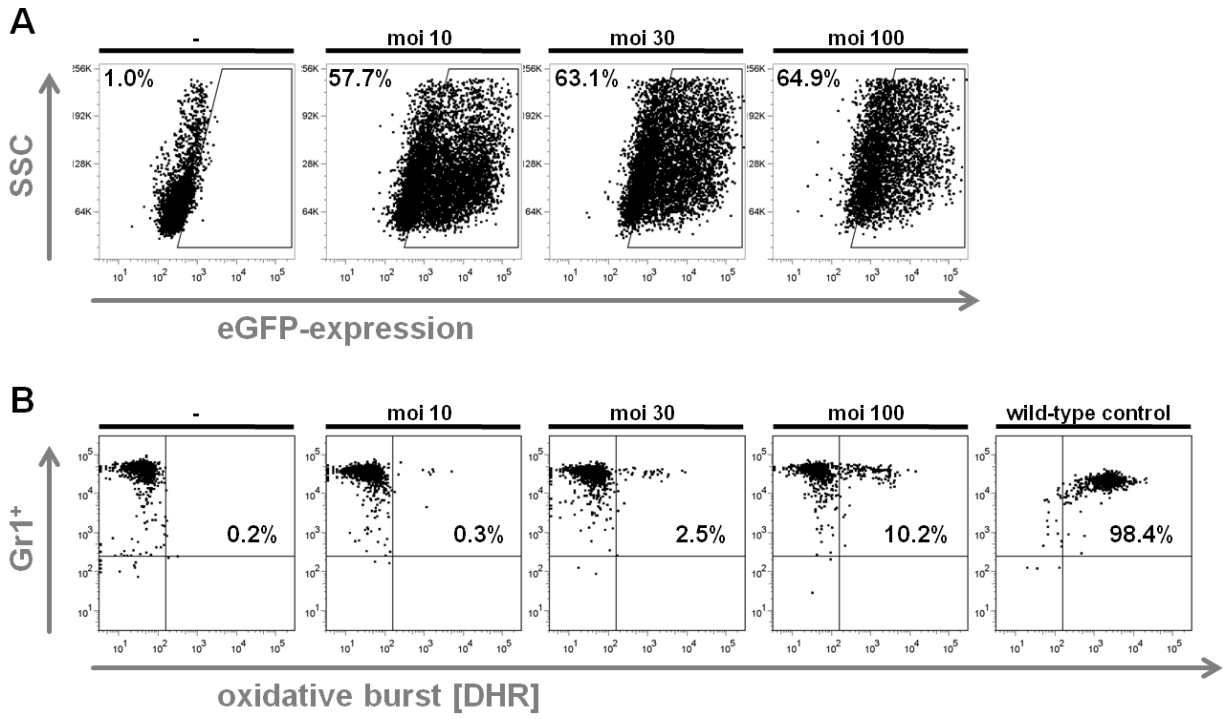

Figure 33: Gene transfer into murine Δ*gp91^{phox}*-monocytes using HIV-1 vectors. (A) EGFP expressing monocytes detected by FACS after transduction with vector particles generated with the HIV-1-SEW transfer vector. **(B)** Phagocytosis capacity of *gp91^{phox}* gene-corrected monocytes after transduction with vector particles generated with the HIV-1-SgpSw transfer vector.

Although the experiment showed that a *gp91^{phox}* gene correction was achieved and resulted in functional ROS-producing monocytes, the number of corrected cells was low. In the following, it was analyzed whether this low correction capacity was due to an inefficient ability to induce an oxidative burst in the corrected cells, as indicated by the high transduction efficiency of eGFP-transferring vectors, or to a reduced transduction ability of *gp91^{phox}*-transferring vectors. For this, the transduction efficiency of HIV-1-SgpSw vectors was not measured indirectly by co-transduction of eGFP-transferring vectors, but directly by detection of the gp91^{phox}-expression in the transduced monocytes. In contrast to the determination of *gp91^{phox}*-expressing PLB-985 cells, the expression in monocytes had to be measured by an intracellular stain because this cell type is known to otherwise yield false-positive signals.

Murine bone-marrow monocytes of *gp91^{phox}*-knockout mice were isolated by MACS negative-depletion as described before (3.3.5) and transduced with HIV-1-SgpSw at an moi of 1, 10, 30, 100, and 500. Five days post transduction the transduced Gr1^{+}-monocytes were analyzed for their oxidative burst activity as well as for their gp91^{phox}-expression. For this, the cells were split. In one fraction of the cells, the oxidative burst activity was analyzed by the phagoburst assay (3.3.15). In the other fraction, the gp91^{phox}-expression was determined by

an intracellular antibody-staining against flavocytochrome b_{558} (3.3.12). In both cases the cells were also stained against $Gr1^+$ with VioBlue conjugated $Gr1^+$-antibodies (Figure 34).

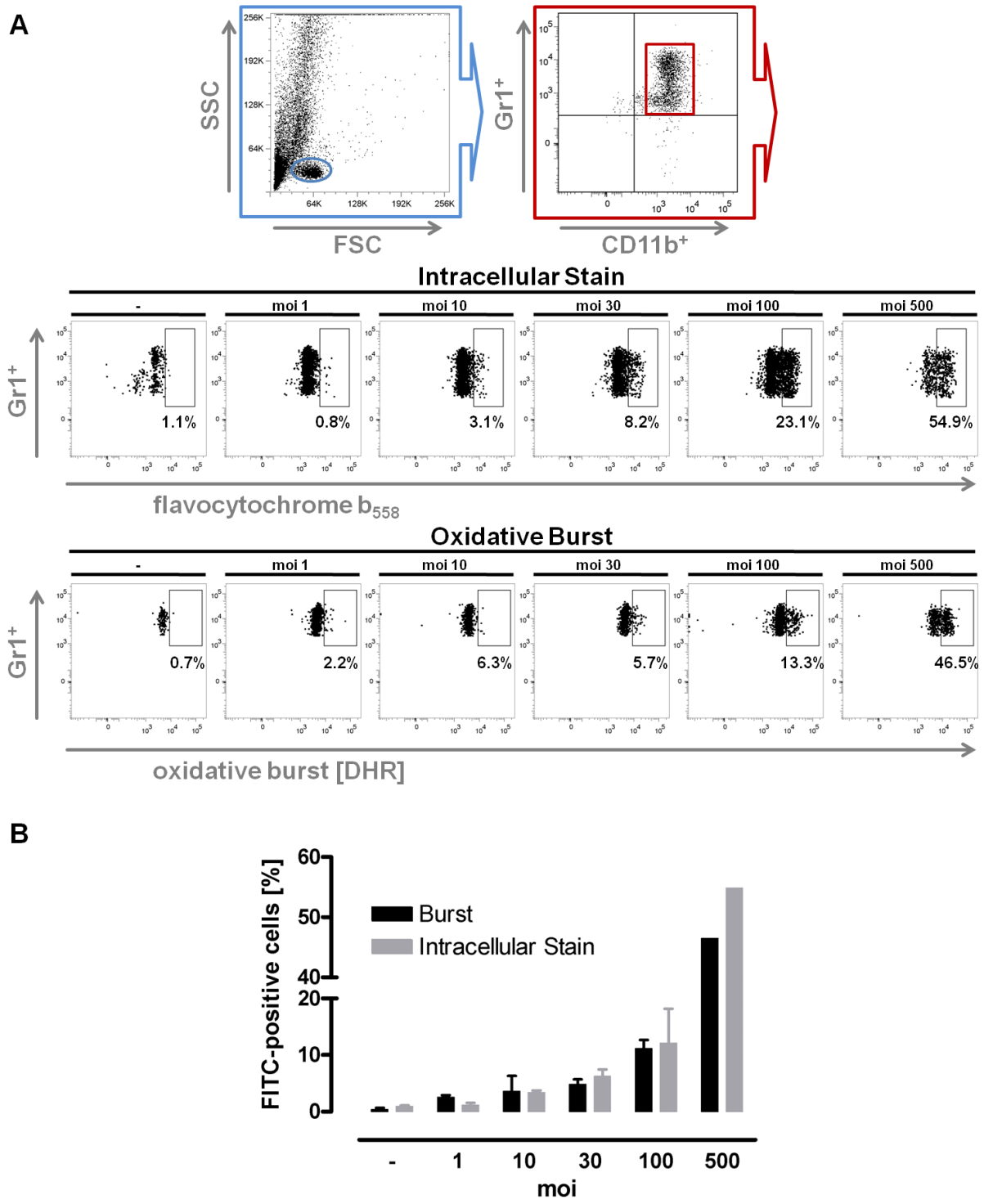

Figure 34: Gene correction of *gp91^{phox}*-deficient murine monocytes. Murine monocytes of *gp91^{phox}*-knockout mice were corrected using HIV-1-SgpSw-derived lentiviral vectors. The gene transfer efficiency (flavocytochrome b_{558} expression) was correlated to the oxidative burst-activity. **(A)** The FACS-analysis of one exemplary experiment. **(B)** Mean results for gene transfer detected by flavocytochrome b_{558} expression and the corresponding transgene function determined by ROS production.

The measured phagoburst activity during this experiment was in accordance with the data derived from the previous experiment. In contrast, the observed transduction efficiencys for eGFP-transferring vectors, analyzed by eGFP-expression, were much higher than those observed for *gp91^{phox}*-transfering vectors, analyzed by an intracellular stain against flavocytochrome b_{558}. The transduction efficiencies calculated from the intracellular stain of flavocytochrome b_{558} were in a similar range of the percentage of monocytes able to induce ROS production. The highest transduction efficiency analyzed from the intracellular stain against flavocytochrome b_{558} was achieved at the moi of 500. Due to titer limitations, the transduction at this moi could only be performed once. It resulted in 62.9% gene-corrected cells. Within the same cell population 50.9% of the monocytes produced a phagoburst.

In summary, HIV-1 vectors were used to transfer the *gp91^{phox}* gene into monocytes from *gp91^{phox}*-deficient mice and a successful restoration of the oxidative burst ability was achieved in the cells.

5 Discussion

Lentiviral vectors derived from SIVsmmPBj are able to overcome a still unknown block in primary human monocytes and transduce these quiescent cells with high efficiency. The transduction is dependent on the viral Vpx-protein. The ability to efficiently transduce monocytes opens up the possibility to use these primary cells as a putative gene therapy target. For this purpose, the generation of enhanced transfer vectors of SIVsmmPBj and HIV-2 origin is described in this thesis. For future vector designs, a fast and efficient new cloning strategy was successfully innovated. With this tool for safe monocyte transduction, a new therapeutic application for chronic granulomatous disease was conceived and the foundation to test the use of *gp91^{phox}* gene-corrected monocytes as a therapeutic for xCGD was set.

5.1 Vpx of the HIV-2/SIVsmm/SIVmac lentivirus lineage facilitates monocyte transduction

All viruses from the HIV-2/SIVsmm/SIVmac lineage encode for the accessory protein Vpx. Hence, it was suspected that not only the Vpx of SIVsmmPBj (VpxPBj), but also the protein homologues of other family members, like the Vpx of HIV-2 (VpxHIV-2) and SIVmac (VpxMAC), might also facilitate monocyte transduction. This conjecture was supported by results showing that Vpx is inevitable for virus wild-type replication of PBj, SIVmac, and HIV-2 in human and macaque macrophages (Fletcher et al., 1996; Kawamura et al., 1994; Sleigh et al., 1998; Yu et al., 1991). Accordingly, an HIV-2 two-plasmid-system (HIV-2-RodA) was investigated (Reuter et al., 2005). The structure of the vector was different to the PBj-derived two-plasmid-system, PBj-ΔEeGFP. To enable eGFP expression, the *gfp* gene was set in frame with the *nef* gene in the case of HIV-2-RodA and not expressed by an internal CMV-promoter sequence as in the case of PBj-ΔEeGFP. Both vector systems encode for all accessory genes, including *vpx*. The different ways to express eGFP on the grounds of the different vector design should only have an effect on the strength of transgene expression but not on the vector's ability to transduce primary monocytes. This transduction ability could be confirmed for HIV-2-RodA and PBj-ΔEeGFP, but not for an HIV-1 lentiviral vector system (HIV-1-NL4-3) (Figure 9). Interestingly, using the HIV-1-NL4-3 vectors at an moi of ten caused most of the monocytes to die. They stayed healthy after transduction at the same moi with PBj-ΔEeGFP and HIV-2-RodA. As all vectors were generated and titrated the same way, using the envelope expression plasmid (pMD.G2), the reason for the toxicity of the HIV-1

vector cannot be linked to particle production, but instead must be associated with the HIV-1 particle or the incorporated viral proteins themselves.

The observation that HIV-2-derived vectors are able to transduce primary human monocytes prompted the cloning of different Vpx-expression plasmids for functional analysis. Next to the existing VpxPBj plasmid (Wolfrum, 2005), expression constructs for the *vpx*-genes of HIV-2-RodA and SIVmac were generated using PCR. The expression in 293T cells was weak for VpxPBj and VpxHIV-2 but not detectable for VpxMAC. This is due to the αVpxHIV-2 monoclonal antibody which has been described to be crossreactive with VpxPBj but not with VpxMAC. To enhance the weak VpxPBj- and VpxHIV-2-expression, codonoptimized plasmids (VpxPBjsyn and VpxHIV-2syn) were obtained. Western blot analysis of these revealed a well detectable expression level.

All of the available Vpx expression plasmids, except for of the unmodified VpxHIV-2, were able to facilitate monocyte transduction of the PBj-4xKOeGFP vector. It was not further investigated whether the nonfunctional transduction with VpxHIV-2 is due to non-detectable protein levels in the vector particles, caused by insufficient incorporation because of the non-homologous PBj background, or to a non-functional protein. VpxPBj and VpxMAC, who successfully mediated monocyte transduction of PBj-4xKOeGFP, were also not detectable in the vector particles. Whereas the antibody available did not detect VpxMAC, it clearly detected VpxPBj, as the codonoptimized protein could easily be visualized. Thus, it can be concluded that minimal Vpx amounts are sufficient to drive monocyte transduction.

Altogether, the experiments prove that Vpx proteins other than VpxPBj of the HIV-2/SIVsmm/SIVmac lentivirus lineage also possess the ability to facilitate monocyte transduction. Hence, the experiments disprove the assumed uniqueness of the PBj vectors.

5.2 Generation of PBj- and HIV-2-derived lentiviral vectors

The observation that lentiviral vectors from the HIV-2/SIVsmm/SIVmac lineage other than those of the SIVsmmPBj origin enabled monocyte transduction led to the generation of two three-plasmid vector systems. One of these is based on human origin (HIV-2) and the other is based on non-human origin (SIVsmmPBj). With regard to clinical applications it could be advantageous to have a non-human vector, since in the case of an HIV infection it is unlikely to recombine with the resident HIV. On the other hand, there might be higher regulatory restrictions for the use of non-human vector systems due to their theoretical zoonotic potential. Hence, it was decided to generate an HIV-2- and an SIVsmmPBj-derived three-plasmid system. The generation of SIV-based lentiviral three-plasmid vector systems has been described by different authors for SIVmac (Dupuy et al., 2005; Mangeot et al., 2000;

Negre et al., 2000). The construction of HIV-2 derived three plasmid vectors is also described in the literature (D'Costa et al., 2001; Morris et al., 2004). The latter are basic non-SIN HIV-2 vectors and therefore not applicable for clinical purposes.

5.2.1 Gradual enhancement of a PBj-derived transfer vector

A basic PBj three-plasmid system was available in the lab. It consisted of the packaging vector pPBj-pack, the envelope plasmid pMD.G2, and the transfer vector pPBj-trans (Wolfrum, 2005). However, this system resulted in poor titers. A deletion between the splice donor and start-ATG within the pPBj-pack abrogates an incorporation of the RNA into the particles. This prevents viral replication, as has been shown for the similar HIV-2 virus (Poeschla et al., 1998). The packaging construct pPBj-pack itself had the ability to generate high amounts of vectorlike particles (data not shown), indicating that the reason for the poor titer lay in the transfer vector pPBj-trans. Therefore, only the pPBj-trans vector was the focus of a gradual enhancement. Separate enhancements of PBj-trans-SIN, such as the integration of an SFFV-*eGFP*-WPRE expression cassette (leading to pPBj-SEW-SIN) and the inclusion of the central termination sequence (CTS) downstream of the central polypurine tract (leading to pPBj-trans-cSIN) increased the vector titers as expected.

SIN-configuration

The first modification was the deletion of the second exons of Tat and Rev and of the promoter and enhancer elements within the U3 region of the 3'LTR. This step resulted in PBj-trans-SIN and led to a decrease in titer of about 2-fold. Such a negative influence on titer through the generation of SIN-vectors was also found for SIVmac generated vectors (Mangeot et al., 2000). In order to increase the mRNA expression and titer, the size of the vector mRNA was decreased by the deletion of the unnecessary second exons of *tat* and *rev*. However, it can only be speculated whether the decrease in vector size had a positive impact on the vector titer as it was compensated by the generation of the SIN-configuration.

cPPT/CTS

The reintroduction of the correct *cis*-acting cPPT/CTS element and the deletion of a large fraction of the *pol* sequence resulted in an increase in unconcentrated vector titers of approx. 2-fold, as expected. To achieve the highest possible effect, special attention was paid to integrate the cPPT/CTS element in sense orientation at a 5' vector location, as described for HIV-1 (De Rijck and Debyser, 2006; Van Maele et al., 2003). The cPPT/CTS sequence is apparently involved in the nuclear import process (Sirven et al., 2000) and inclusion of the element into HIV-1 vectors enhances transduction efficiency 2–10-fold (Zennou et al., 2000). Recent data indicate that the DNA flap formed by the interplay of cPPT and CTS during

reverse transcription is not absolutely required for vector transduction (Zufferey et al., 1997) or even wild-type HIV-1 replication (Dvorin et al., 2002; Limon et al., 2002). It can be deleted or replaced in order to reduce the risk of RCL formation and to gain space for therapeutic sequences (Schambach and Baum, 2008). These results were verified by showing, that cPPT/CTS-deficient PBj vectors derived from PBj-trans were still able to transduce human monocytes (Figure 14). Nevertheless, the cPPT/CTS-element is described to be indispensable for the transduction of neuronal cells (Liehl et al., 2007). Although the literature argues that the enhancement of titer for the PBj-trans-cSIN construct resulted from the integration of the correct cPPT/CTS-element, it is nevertheless possible that the large *pol* sequence deletion, resulting in a shorter mRNA transcript, led to a more stable mRNA expression which further enhanced the generated vector titer.

WPRE

The integration of the SFFV-*eGFP*-WPRE cassette introduced the internal SFFV-promoter, which is a strong ubiquitous promoter (Baum et al., 1997), and the woodchuck hepatitis virus posttranscriptional regulatory element (WPRE). Although the internal promoter has a great influence on the expression level of a transgene it has no effect on the titer and transduction efficiency of the vector system. In contrast, the WPRE stabilizes the vector RNA and enhances protein expression in the packaging cell line and in the target cell. This leads to an increased infectious particle formation (titer) and transgene expression (Hlavaty et al., 2005; Zufferey et al., 1999). In the case of the generated PBj-SEW-SIN vectors, this resulted in a titer increase of approximately 3-fold in comparison to PBj-trans-SIN.

cPPT/CTS and WPRE

The combination of both modifications - the corrected cPPT/CTS sequence and the insertion of a SFFV-*eGFP*-WPRE expression cassette - resulted in the construct pPBj-SEW-cSIN and a cumulative increase of the titer. Unconcentrated vector particles produced with the pPBj-SEW-cSIN transfer vector had a 10-fold increased titer compared to the origin PBj-trans vector.

SV40/RSV-element

Finally, the promoter elements of the U3-region within the 5´LTR were substituted with a chimeric SV40-enhancer/RSV-promoter element to gain a strong, Tat-independent vector RNA expression in the packaging cells. The Tat-independency of the so called pPBj-SR-SEW-cSIN transfer vector within the packaging cells was not tested, as the Tat-expressing packaging construct pPBj-pack had been used for vector production. Nevertheless, the particle production was further increased 5-fold resulting in unconcentrated titers of $5x10^5$ TU/ml, an overall 50-fold increase in comparison to the origin PBj-trans vectors. For

concentrated vectors, the increase achieved by the described enhancement steps from PBj-trans to pPBj-SR-SEW-cSIN was 10-fold and titers up to $1{,}12x10^7$ TU/ml were reached.

5.2.2 Generation of lentiviral transfer vectors by Fusion-PCR

The conventional construction of lentiviral derived transfer vectors by gradual enhancing cloning steps is a time-consuming process. A general transfer vector encompasses normally more than 7000 bp with repetitive sequences, i.e. LTR. The more cloning steps are conducted, the more mutations are likely to be included and unwanted DNA sequences in between necessary vector elements remain due to unfitting restriction sites. These sequences enlarge the homology to the wild-type virus sequences and increase the size of the transfer vector needlessly. This leads to a hampered vector production. In order to construct a lentiviral transfer vector quickly by simultaneously minimizing the non-functional DNA sequences, a novel strategy to design transfer vectors from a lentiviral origin was conceived, i.e. the generation of transfer vectors directly by Fusion-PCR.

The viral wild-type sequences of either SIVsmmPBj or HIV-2 were used as template for three different PCR reactions to yield specific segments of the transfer vector that function as the scaffold. These fragments were fused in different Fusion-PCR reactions and cloned into a vector backbone originated from the pBluescript-plasmid (Figure 7). The vectors resulting from these few cloning steps, pPBj-MCS or pHIV-2-MCS, respectively, are an ideal starting point for the integration of different vector elements, their choice depending on the transfer vector's intended purpose. In order to prove that indeed a functional transfer vector had been generated, the internal SFFV-*eGFP*-WPRE expression cassette was integrated into the MCS, resulting in PBj-SEW and HIV-2-SEW. In the absence of Vpx, the generated vector titers were lower for PBj-SEW than they were for HIV-2-SEW. These titer differences may be due to the respective packaging construct used. Another explanation for titer variations are the virus origins themselves. It cannot be expected that vectors derived from different viruses produce the same vector titers. The promoter strength of the viral LTRs, the packaging capacity mediated by the Ψ sequence, or the mRNA export by the Rev protein are possible reasons for titer variations between differently originated vectors. Nevertheless, both novel generated vectors outperformed the enhanced PBj vector PBj-SEW-cSIN generated by gradual enhancement. However, they did not reach the titers of an HIV-1-SEW-derived vector system with titers above $5x10^8$ TU/ml after concentration. This could be caused by reasons similar to those described before or by the different SD/SA profiles. In addition to the SD, the used HIV-1-SEW transfer vector contained an SA-site downstream of the RRE. In contrast, for PBj-SEW and HIV-2-SEW the SA sequence downstream of the RRE was

deleted. Only the SD was kept in the 5'UTR of the vectors for efficient vector RNA packaging. As only the SD is present in the viral construct, no splicing will occur and hence a Rev-mediated export of the transfer RNA is necessary. An efficient Rev-mediated export is dependent on a part of the splicing machinery. It should still be possible due to the present SD (Chang and Sharp, 1989), but maybe was less efficient than that for HIV-1-derived vectors.

In contrast to the vector design of PBj-trans, where the gag start-ATG was mutated to an ACG (Wolfrum, 2005), a stop codon was introduced downstream of the *gag* gene start-ATG of PBj-SEW and HIV-2-SEW to prevent Gag expression. This was performed since the beginning of the *gag* sequence could be involved in proper RNA-packaging (L. Naldini, ESGCT 2007, personal communication). Here, minimal changes can reduce the ability for particle incorporation (Ooms et al., 2004). However, the decision to abrogate gag translation downstream of the start-ATG was merely a precaution as the extension of the packaging signal into Gag is only described for the HIV-1 virus (Yu et al., 2008). The Ψ-site mapping is controversially reported for the HIV-2/SIVsmm/SIVmac lineage. Here, different sequences up- and downstream of the SD are described to be important with the accordance of 10 well-conserved nucleotides (SIVmac, ACACAAAAAA; HIV-2, ACACCAAAAA), located immediately after the SD site junction most likely critical for HIV-2 and SIVmac genomic RNA packaging (Patel et al., 2003). As the region between the LTR and the *gag* sequence was not changed during the vector design, the 'ACACCAAAAA' in the HIV-2 vectors remained unchanged. For PBj the 'CAACAAAAA' sequence found downstream the SD was most similar to the conserved HIV-2 and SIVmac sequences and therefore probably important for mRNA packaging. It was also not affected in the transfer vectors.

In conclusion, the generation of lentiviral transfer vectors by Fusion-PCR is fast, efficient and opens up multiple possibilities to easily integrate further restriction sites between various elements by including them into the primer overhangs. An example is the introduction of the multiple-cloning site intended to integrate an expression cassette as performed here. Other restriction sites could be inserted e.g. upstream of the R-region within the 5'LTR for possible insertions of miRNA target sequences, shRNAs, or insulator sequences.

5.2.3 Monocyte transduction of novel generated PBj- and HIV-2-derived lentivectors

Efficient primary human monocyte transduction by lentiviral vectors is only feasible if Vpx is incorporated into the vector particles. Although in early experiments, the detection of native

Vpx incorporation into vector particles was beneath the detection limit, a monocyte transduction was enabled (Figure 14B). The expression of the Vpx proteins was successfully improved by codonoptimization and, subsequently, the correlation between the Vpx incorporation and the ability of vector particles to transduce monocytes was shown. This incorporation of Vpx into vector particles was achieved through αVpxHIV-2 monoclonal antibodies in a Western blot. In such a blot, VpxHIV-2syn showed two bands (Figure 20). The lower one corresponds to the VpxHIV-2syn size of 17 kDa. The upper band of approximately twice this size may point to a dimer formation, due to insufficient denaturation. A cross-reactivity against proteins of the vector particles can be excluded, as the band is not visible for HIV-2 vector particles generated in the absence of VpxHIV-2syn. The dimer formation was also previously described for the related Vpr of HIV-1 (Fritz et al., 2008) and identified for Vpx (A. Berger, personal communication).

The highest monocyte transduction was achieved using HIV-2-derived lentiviral vectors. Vector particles generated in the presence of VpxHIV-2syn with the transfer vector HIV-2-SR-g'-SEW were able to transduce 64% or 50% of the monocytes at an moi of ten or one, respectively. In general, HIV-2-derived vectors were superior to PBj-derived vectors in their ability to transduce human monocytes. The reason for this is difficult to explain based on the particle design. The vectors were produced and titrated using the same protocol and the same amount of infectious particles was used for monocyte transduction. A possible explanation is a different potential of VpxHIV-2syn or VpxPBjsyn to facilitate monocyte transduction. Here the transduction experiments indicate that VpxHIV-2syn is superior to VpxPBjsyn. This conclusion is supported by the experiment in which both Vpx proteins facilitate monocyte transduction of the same 4xKOeGFP vectors. In that experiment, VpxHIV-2syn was also superior to VpxPBjsyn (Figure 11).

5.3 Clinical applications for PBj- and HIV-2-derived lentivectors

Now that PBj- and HIV-2-derived three-plasmid vector systems were available with their enhanced transduction ability of primary human monocytes, the question arose whether such vector systems are superior to HIV-1-derived vectors for possible applications in human gene therapy.

It had been confirmed for the PBj- and HIV-2-derived vectors that they do not enable an enhanced transduction of unstimulated B cells. The same is described for the transduction of unstimulated stem-cells with basic PBj-vectors in comparison to HIV-1 vectors (Kaiser,

2008). In contrast, the transduction of monocyte-derived macrophages and dendritic cells was significantly higher. Currently, the vectors are being tested for their suitability for immunotherapy applications (Kaiser, 2008).
Furthermore, the vectors are compared to HIV-1-derived vectors on different murine cell types *in vitro* and *in vivo*. A cooperation was started with the Max-Planck-Institute for Brain Research in Frankfurt (Main) to investigate the ability of the vectors to transduce murine retina. First experiments are promising, and tend to show a different target cell preference for PBj-SEW-, HIV-2-SEW-, and HIV-1-SEW-generated vectors, respectively. This transduction seems not to be influenced by the Vpx-protein.
The general *in vitro* transduction ability of murine neurons was demonstrated for HIV-2 and PBj vectors in this thesis. In cooperation with the Institute of Virology at the University of Vienna, the HIV-2 and PBj vectors are currently being compared to HIV-1 vectors in their ability to transduce differentiated brain neurons *in vivo* in presence and absence of Vpx. Efficient transduction of neuronal cells *in vivo* could be useful for clinical applications of Parkinson's disease or Alzheimer's disease. The general value of SIV-derived vectors for treatment of neurodegenerative diseases has been shown previously (Liehl et al., 2007).

The high monocyte transduction ability of the HIV-2- and PBj-derived vectors could also be beneficial for clinical applications regarding gene defects in the monocytes themselves. An example for a disease based on a gene defect in monocytes/macrophages is Gaucher's disease. In this thesis the suitability of the vector systems for treatment of another inherited disease, xCGD, was tested.

5.3.1 A novel concept of xCGD treatment

The X-linked form of the chronic granulomatous disease is based on a gene defect in the *CYBB* gene located on the x-chromosome, leading to a non-functional $gp91^{phox}$ subunit of the NADPH oxidase. The defect is prominent on phagocytes such as neutrophils and monocytes and results in an insufficient killing of bacteria and fungi. Therefore patients suffer from recurring and severe infections.
If a potential donor is present the curative treatment option of choice is the hematopoietic stem cell transplantation. Although stem cell transplantation works very well, it is problematic when ongoing infections are present at the time of transplantation (Seger, 2008). One possibility to decrease severe infections is the allogenic granulocyte transfusion, but the risk of alloimmunization to HLA antigens may complicate a later allogenic stem cell transplantation (Stroncek et al., 1996). If no donor is available for a HSCT, the gene correction of $CD34^{+}$-stem cells is a possible way to cure the disease in the future. Two trials

in Frankfurt and Zurich showed first promising results (Ott et al., 2006). Although a gene correction was possible in both patients in Frankfurt, the patients showed adverse events due to insertional mutagenesis (Grez, 2008).

In this thesis a new treatment model was conceived. It is proposed that an autologous monocyte cell transfusion after *ex vivo* $gp91^{phox}$ gene correction will help to transiently overcome severe infections. Depending on the potency of monocytes to kill pathogens, the monocytes would be able to eliminate persistent infections or even granulomas. The method could therefore prepare patients for possible stem cell transplantation.

Although the killing of monocytes is described to be less efficient than that of neutrophils (Emmendorffer et al., 1994), monocytes and their progeny cells - like inflammatory macrophages and TipDCs - are described to kill microbes (Auffray et al., 2009). The possibility of a synergistic activation, as described for the killing of *Aspergillus hyphae* by neutrophils, could increase the killing potency (Rex et al., 1990). The application of the gene-corrected monocytes is believed to be safe. As the cells used for injection would be autologous, no immune reactions like graft vs. host are anticipated. The risks resulting from insertional mutagenesis are minimal, as monocytes differentiate to macrophages and DCs, but usually no cell division occurs.

To investigate the potential of monocytes for the proposed treatment model, human and murine monocytes were investigated for their oxidative burst, phagocytosis, and *S. aureus* killing potential. Murine $gp91^{phox}$-deficient monocytes were corrected and functionally analyzed for their ability to burst.

5.3.2 Setting up the system

Isolation of monocytes

Two different monocyte subsets can be distinguished, the inflammatory and resident monocytes. To investigate the potential of monocytes for a possible clinical application of bacterial clearance after $gp91^{phox}$ gene correction, it was decided to use the inflammatory monocytes ($CD14^+$ (human), $Gr1^+$ (mouse)). In contrast to the resident monocytes ($CD16^+$ (human), $CX3CR1^+$ (mouse)), they are described to be involved in bacterial killing (Auffray et al., 2009). Human monocytes were isolated from donor blood by negative depletion (3.3.4). During this, the cell suspension was also depleted of $CD16^+$-monocytes. Therefore, the isolated monocytes were exclusively inflammatory monocytes. In order to isolate inflammatory murine monocytes, it was decided to use the bone marrow rather than blood. In the blood both monocyte subsets are present to equal quantities. The resident monocytes develop from the inflammatory monocytes upon release from the bone marrow into the blood

(Sunderkötter et al., 2004). Therefore, it was assumed that the isolation of murine bone-marrow monocytes results predominantly in $Gr1^+$-monocytes.

As the isolation of murine bone-marrow cells had not been established in the lab, it was decided to adapt the negative isolation protocol of F. Swirski and coworkers (Swirski et al., 2006) although this protocol was established for the isolation of blood monocytes. In contrast to the original procedure, the cells were not stained with antibodies directly conjugated to MicroBeads. Instead, the cells were first stained with FITC conjugated antibodies against T cells, B cells, NK cells, and erythrocytes and subsequently with MicroBeads conjugated αFITC antibodies. Isolated monocytes were analyzed using a combination of PE- or APC-labeled antibodies directed against specific cell markers of T cells (PE-CD90.2), B cells (PE-CD45R (B220)), NK cells (PE-CD49b (DX5), PE-NK1.1), and the leukocyte markers PE-Ly-6G and APC-CD11b. The Ly6G marker is negative for blood monocytes but transiently expressed on monocytes in the bone marrow. This was confirmed by FACS measurements. After the isolation protocol was established, the $Gr1^+$-monocytes were solely characterized by $Gr1^+/CD11b^+$-expression (Figure 27).

5.3.3 Functional analysis of murine monocytes for *gp91^{phox}* gene therapy

Phagocytosis, Phagoburst and *S. aureus* killing

While high phagocytosis and burst capacities were demonstrated for human and murine wt monocytes, the killing capacity was only moderate. One reason could be the lack of further stimuli necessary for monocytes activation like complement components in the *in vitro* assay (Leijh et al., 1982). The set-up for the killing of *S. aureus* bacteria by monocytes was shown to be generally effective but could be improved in the future. As the monocytes showed only a weak oxidative burst by *S. aureus* bacteria activation (data not shown), the cells were activated using PMA. PMA was added at the time of mixing the bacteria with the monocytes. A higher killing efficiency might be possible if the monocytes were PMA-stimulated at a later time, after the phagocytosis of the bacteria by the monocytes was advanced.

Another reason for the moderate killing activity could be the production of leukocidin by the bacteria. *S. aureus* is one of the major leukocidin producers. Leukocidin is a pore forming cytotoxin that kills leukocytes. M. Dinauer and colleagues described that substantially higher numbers of neutrophils are needed to fully restore host defense in experimental infection with *Staphylococcus aureus* or *Burkholderia cepacia* compared with *Aspergillus fumigatus* (Dinauer et al., 2001). Therefore, the sensitivity of the assay to test the killing potential of *gp91^{phox}* gene-corrected monocytes may be enhanced using the less resistant fungus *Aspergillus fumigates* as challenge pathogen.

Biodistribution

The biodistribution data generated for murine eGFP-monocytes in Rag-2/γc$^{-/-}$ mice indicate that the transplanted cells are found in the spleen, the bone marrow, and in the blood. Whereas the cell number in the spleen and the blood decreased four days after transplantation, the number of cells in the bone marrow seemed stable over this time. In some tissue samples, e.g. lung and liver, only a few eGFP-positive cells were found. They presumably originate from blood contaminations.

Monocytes are described to circulate in the blood stream. Therefore, the detection of eGFP positive cells in the blood was expected. As one of the functions of the spleen is to filter the blood, it was not surprising to detect high amounts of eGFP-positive cells in the spleen one day after transplantation, which are absent four days after transduction.

The constant amount of eGFP-positive cells in the bone marrow, however, was unexpected. Although Gr1^{+}-monocytes are described to home to the bone marrow in the absence of inflammation (Geissmann et al., 2003; Varol et al., 2007), the amount of cells suggests that, in addition to Gr1^{+}-monocytes also monocyte precursors were isolated. As bone-marrow cells they are presumably retargeting the bone marrow.

Monocyte half-life

Diverse specifications about the *in vivo* half-life of murine monocytes are found in the literature. They range from 43.5 +/- 7.9 h (Swirski et al., 2006) to 3 days (Mazzarella et al., 1998). In all cases the half-life has been derived for blood-monocytes. To investigate the half-life of murine bone-marrow derived Gr1^{+}-monocytes in the bloodstream, CD45.2 monocytes were isolated and transplanted into CD45.1 mice. The retention of the CD45.2 monocytes in the CD45.1 mice was traced by FACS-staining over a period of five days. The calculated half-life was 55.2 +/- 5.1 h.

The discrepancy between the described half-lives for monocytes could be due to any of three reasons: First, the difference of the monocytes' origin (bone-marrow compared to blood monocytes) could account for differences in half-life measurements. Blood-derived monocytes might have already been in the bloodstream several days before harvest. They would therefore tend to leave the bloodstream soon after transplantation. Second, the different monocyte subtypes differ in their half-life due to their function. Third, the experimental set-up used to analyze the half-life could in itself account for variations. An indirect measurement, i.e. radioactive labeling, seems more error prone than a direct measurement of CD-markers as performed in this thesis.

The half-life measured by F. Swirsky and co-workers relies on an indirect radioactivity measurement of [^{111}In]oxine-labeled CXCR2^{+}-blood-monocytes (Swirski et al., 2006) and therefore differs from the calculation of bone-marrow derived Gr1^{+}-monocytes by FACS-

analysis. The half-life of 55.2 +/- 5.1 h will most likely be long enough for the intended gene therapy application. As patients receiving *gp91^{phox}*-corrected monocytes would probably have systemic infections at the time of infusion, the monocytes would not circulate the blood, but rather respond according to the type of infection by migrating to the specific tissues (Egan et al., 2008).

Gp91^{phox} gene correction of murine xCGD-monocytes

The ability of monocytes to kill bacteria and fungi is mediated through ROS produced by the NADPH oxidase. The oxidative burst is therefore a requirement for the monocyte killing ability. Where *gp91^{phox}*-deficient monocytes are not able to produce ROS, wild-type monocytes give a strong oxidative burst *in vitro* after PMA stimulation (Figure 23). For the lentiviral *gp91^{phox}* gene transfer into murine monocytes, HIV-1-derived vectors were used. The transduction efficiency for the *gp91^{phox}* gene transfer using HIV-1-SgW-derived vectors was not as high as expected on grounds of eGFP-transferring HIV-1-SEW vector transduction. Using identical moi the murine monocyte transduction of eGFP-transferring HIV-1-SEW vectors was much higher than that of *gp91^{phox}*-transferring HIV-1-SgW vectors.

By using the *gp91^{phox}*-transferring HIV-1 vectors a phagoburst activity could be restored in *gp91^{phox}*-deficient monocytes. This result showed a positive correlation between the presence of gene-corrected monocytes and the ability to produce ROS. A correction of more than 54% of the *gp91^{phox}*-deficient monocytes was achieved. Of these, 85% showed an oxidative burst activity (Figure 34). In general, the number of *gp91^{phox}*-expressing cells within one transduction experiment was only slightly higher than the number of oxidative burst positive monocytes. It can be concluded from the experiments resulting in a low gene correction (<20%) that a single integration of the transgene seems to be sufficient to restore the phagoburst ability in monocytes. The number of copies integrated into the host genomes was not analyzed. The risk of insertional mutagenesis for the non-proliferating monocytes is marginal and therefore the number of integrations is irrelevant.

The results confirm that a gene correction of *gp91^{phox}*-deficient monocytes is possible and that the ROS production, the prerequisite for an efficient pathogen killing, was successfully restored.

5.4 Outlook

The novel PBj- and HIV-2 vectors generated in this thesis meet the current requirements for use in clinical applications. Therefore, they could be used for the *gp91^{phox}* gene correction of monocytes from xCGD patients. To test the gene correction in a human setting was not possible in this thesis as no human material was available. This test will have to be conducted in future experiments. A *gp91^{phox}* gene correction was achieved in murine monocytes. This and the confirmed ability of phagocytosis, oxidative burst, and *S. aureus* killing indicates that monocytes will be suitable to eliminate infections *in vivo*. The potency of monocytes to kill microbes and thereby eliminate persistent infections *in vivo* can be addressed in a future murine challenge experiment. With regard to the moderate *S. aureus* killing by monocytes *in vitro*, it is advised to evaluate different pathogens in an *in vitro* killing assay prior to the challenge experiments.

6 Summary (german)

Retrovirale Vektoren werden für den Gentransfer verwendet, weil sie ihr Genom stabil in das der Wirtszelle integrieren und so eine langanhaltende Expression des Transgens ermöglichen können. Während von γ-Retroviren (wie z.B. dem häufig verwendeten murinen Leukämievirus) abgeleitete Vektoren nur sich teilende Zellen transduzieren können, sind von Lentiviren abgeleitete Vektoren auch zum Gentransfer in nicht-mitotische Zellen in der Lage. Allerdings können auch mit ihnen nicht alle Typen von ruhenden Zellen transduziert werden; insbesondere sind nicht-stimulierte primäre Zellen des hämatopoetischen Systems gegen die Transduktion relativ resistent.

Um lentivirale Vektorsysteme für klinische Applikationen einsetzen zu können, muss ein sicherer Gentransfer gewährleistet werden. Deshalb verwendet man keine replizierenden Viren, sondern Vektoren, die zwar das Transgen in die Zielzelle übertragen können, aber nicht mehr replikationskompetent sind. Dies wird dadurch erreicht, dass die verschiedenen viralen Funktionen auf unterschiedliche Plasmide verteilt sind. Diese Plasmide werden in eine sogenannte Verpackungszelle eingebracht, in der alle viralen Proteine exprimiert und zu Vektorpartikeln assembliert werden. Diese verpacken aber nur das für das Transgen kodierende Genomsegment, so dass die für die Virusproteine kodierenden Gene nicht in die Zielzelle eingebracht werden. Um zu vermeiden, dass in der Verpackungszelle durch homologe Rekombination der eingebrachten Plasmide wieder komplette Virusgenome entstehen, ist die Minimierung viraler Sequenzen notwendig. Optimal wäre es jegliche Sequenzüberlappung zwischen den verschiedenen Bestandteilen des Vektorsystems zu vermeiden.

Ein klassisches lentivirales Vektorsystem besteht aus dem Verpackungskonstrukt, dem Hüllplasmidkonstrukt und dem Transfervektor. Die Vektorpartikel selbst werden dabei durch die *gag/pol*-Gene auf dem Verpackungskonstrukt kodiert. Das Hüllprotein wird von dem Hüllplasmidkonstrukt kodiert und bestimmt den Tropismus der lentiviralen Vektoren. Üblicherweise wird nicht das native, sondern ein heterologes Hüllprotein verwendet (Pseudotypisierung). Meistens wird für die Pseudotypisierung das Glykoprotein des Vesikulären Stomatitisvirus (VSV-G) verwendet, da es eine ubiquitäre Transduktion erlaubt. Das VSV-G ist zudem sehr stabil und ermöglicht eine Anreicherung der Vektoren durch Ultrazentrifugation. Der Transfervektor kodiert für die genomische Information, die in die Vektorpartikel verpackt wird und übertragen werden soll. Ein solches Transgen kann z.B. ein Markergen oder ein therapeutisch wirksames Gen sein. Die Verpackung der RNA des Transfervektors wird durch das Verpackungssignal (Ψ-Sequenz), das auf die 5'LTR-Region

folgt, gewährleistet. Nach der Transduktion wird die genetische Information des Transfergens in die genomische DNA der Zielzelle integriert. Bei der zufälligen Integration der Vektor-DNA kann es zur Insertionsmutagenese kommen. Sowohl die Integrationsstelle selbst als auch Einflüsse zwischen Promotor und Enhancer-Elementen zwischen Vektor- und genomischer-DNA können zu einer veränderten Genexpression der betroffenen Gene in der Zielzelle führen. Aus diesem Grund ist es der Transfervektor, der eine entscheidende Rolle für die Sicherheit der Vektorsysteme spielt.

Im Gegensatz zu herkömmlichen, meist von HIV-1 abgeleiteten lentiviralen Vektoren können vom simianen Immundefizienzvirus (SIV) smmPBj abgeleitete Vektoren auch primäre humane Monozyten transduzieren. Diese Fähigkeit von SIVsmmPBj-abgeleiteten Vektoren ist von dem viralen Protein Vpx (VpxPBj) abhängig, welches bei einer Produktion der Vektoren von einem weiteren Expressionsplasmid *in trans* kodiert wird. HIV-1 kodiert nicht für ein Vpx-Protein. Deshalb wurde im Rahmen dieser Arbeit zunächst untersucht, ob auch Vektorensysteme anderer Lentiviren, die ebenfalls ein *vpx*-Gen tragen, zur Transduktion von Monozyten in der Lage sind. Es stellte sich heraus, dass auch von HIV-2 abgeleitete Vektoren die gleiche Transduktionsfähigkeit wie SIVsmmPBj besitzen. Um den Einfluss der Vpx-Proteine zu untersuchen, wurden Expressionsplasmide für VpxHIV-2 und für das vom Rhesusaffenvirus SIVmac exprimierte VpxMAC generiert und nachgewiesen, dass sie wie VpxPBj eine Transduktion von Monozyten durch PBj-abgeleitete Vektoren ermöglichen. Aufgrund einer schwachen Expression wurden im weiteren Verlauf die nativen *vpxPBj*- und *vpxHIV-2*-Gene durch funktionale, kodonoptimierte Gene ersetzt.

Da Monozyten ein attraktives Ziel für die Gentherapie darstellen, sollten sichere und effiziente, von SIVsmmPBj- und HIV-2-abgeleitete Vektorsysteme konstruiert werden. Für das PBj-System waren bereits ein Verpackungsvektor sowie ein einfacher Transfervektor vorhanden. Da sowohl die Sicherheit als auch die Transduktionseffizienz der Vektoren maßgeblich durch die Transfervektoren bestimmt werden, wurde der vorhandene Transfervektor optimiert. Dies wurde konventionell durch aufeinanderfolgende Klonierungsschritte erreicht. Dabei wurden sowohl Verbesserungen vorgenommen, die wichtig für die Sicherheit des Systems sind (self-inactivating (SIN)-Konfiguration, Minimierung der viralen Sequenzen), als auch Elemente integriert, die die Vektorproduktion und damit die Effizienz des Gentransfers verbessern (*central polypurine tract* / *central termination sequence* (cPPT/CTS), *woodchuck hepatitis virus posttranscriptional regulatory element* (WPRE)). Mit den graduellen Verbesserungen der PBj-abgeleiteten Transfervektoren war es möglich den Titer im Vergleich zum Ausgangskonstrukt von $9{,}1 \times 10^5$ TU/ml auf $1{,}1 \times 10^7$ TU/ml nach Konzentration zu steigern. Hierbei wurde das

Markergen *eGFP* übertragen. Die Fähigkeit der Vektoren, Monozyten in Abhängigkeit von Vpx effizient zu transduzieren, wurde erhalten.

Generell ist eine sukzessive Verbesserung von Transfervektoren aufgrund der vielen notwendigen Klonierungsschritte und oft fehlender Restriktionsschnittstellen langwierig und kompliziert. Durch die eingeschränkten Klonierungsmöglichkeiten können überflüssige virale Sequenzen oft nicht einfach entfernt werden. Diese Probleme konnten in dieser Arbeit durch die Entwicklung einer Klonierungsstrategie, die die Neuklonierung von lentiviralen Transfervektoren stark vereinfacht, gelöst werden. Hierbei werden drei verschiedene notwendige Segmente (5'-LTR, RRE, ΔU3-3'-LTR) des Transfervektors, ausgehend von der viralen Wildtypsequenz, mittels PCR amplifiziert. Alle weiteren notwendigen Elemente, wie das cPPT/CTS oder PPT, werden über die Fortsätze der verwendeten PCR-Primer integriert. Die Primer enthalten zudem komplementäre Sequenzen, durch welche die drei Segmente anschließend durch die Methode der Fusions-PCR verknüpft werden können. Das entstandene PCR-Fragment bildet, integriert in ein bakterielles Plasmid, nunmehr das Grundgerüst des Transfervektors. Die zusätzliche Integration einer je nach Lentivirus-Hintergrund entworfenen *multiple cloning site* (MCS) in die verwendeten Primer erlaubt eine spätere Integration verschiedener Expressionskassetten.
Die Besonderheit der Generierung von Transfervektoren mittels dieser Fusions-PCR-Methode ist die Flexibilität, mit der man verschiedene Transfervektoren unterschiedlicher Lentiviren ausgehend vom Virusgenom entwickeln kann. Durch die Auswahl der Primer ist man in der Lage Schnittstellen zur Integration gewünschter Vektorelemente, wie z.B. von miRNAs, shRNAs oder Insulatoren zu integrieren. Durch eine einfache, schnelle Klonierung im Anschluss an die Fusions-PCR kann das entstandene Konstrukt zudem in ein Plasmid-Rückgrat nach Wahl eingefügt werden.

Mit dieser neuen Methode der Generation von Transfervektoren wurden von HIV-2 und SIVsmmPBj-abgeleitete Transfervektoren generiert. Hierzu wurde zunächst, wie eben beschrieben, das Grundgerüst der Vektoren, die eine individuelle MCS tragen (HIV-2-MCS und PBj-MCS), generiert. Um die Funktionalität der Transfervektoren nachzuweisen, wurde eine Expressionskassette in die MCS integriert, die das Markergen *eGFP* durch den Promotor des *spleen focus-forming virus* (SFFV) exprimiert. Zusätzlich enthält die Expressionskassette ein WPRE. Dieses stabilisiert durch RNA-Sekundärstrukturen die mRNA und erhöht somit die Expression des Transgens. Lentivirale Vektoren, die mit den neu generierten Transfervektoren (HIV-2-SEW und PBj-SEW) hergestellt wurden, erzielten nach Konzentration auf HT1080-Zellen Titer bis zu $5{,}4 \times 10^8$ TU/ml für HIV-2-SEW und $4{,}0 \times 10^8$ TU/ml für PBj-SEW.

Die neu generierten Vektoren wurden zusätzlich durch zwei weitere Modifikationen für einen sichereren Einsatz in der Gentherapie verbessert. Zum Einen wurde durch eine Punktmutation ein Stop-Codon mehrere Tripletts nach dem *gag*-Start-ATG generiert. Das Start-ATG selbst wurde nicht verändert, um einen möglichen Einfluss der Sequenz innerhalb des Ψ-Verpackungssignals nicht zu verhindern. Durch dieses Stop-Codon wird der Bildung eines potentiellen Translationsprodukts vorgebeugt. Zum Anderen wurde die U3-Sequenz der 5'LTR, welche die Promotor-Elemente enthält, durch ein externes SV40-Enhancer/RSV-Promotor-Element ausgetauscht. Dies ermöglicht eine zukünftige Tat-unabhängige Transkription des Transfervektortranskripts.

Vektorpartikel, die mit den neu generierten HIV-2 und PBj-abgeleiteten Transfervektoren hergestellt wurden, waren nach Supplementierung mit homologem, kodonoptimiertem Vpx in der Lage Monozyten effizient zu transduzieren. Die neu entwickelten HIV-2- und PBj-Vektoren stellen somit nicht nur eine Alternative zu den prominenten HIV-1-abgeleiteten Vektoren dar, sondern können darüber hinaus zusätzlich für einen Gentransfer in humane Monozyten verwendet werden. Momentan wird die Fähigkeit der neu generierten PBj- und HIV-2-abgeleiteten lentiviralen Vektoren im Vergleich zu HIV-1-abgeleiteten Vektoren zur Transduktion verschiedener anderer Zielzellen, wie z.B. von murinen Hirn-Neuronen nach *in vivo* Injektion, untersucht.

Da aufgrund der neu generierten HIV-2- und PBj-abgeleiteten lentiviralen Vektoren ein hoher Grad an Sicherheit und Effizienz für den Gentransfer in Monozyten gegeben ist, wurde im Rahmen dieser Doktorarbeit eine neue potentielle Anwendungsmöglichkeit für sie entwickelt. Diese beruht auf der Korrektur von Monozyten, die aufgrund eines Gendefekts nicht in der Lage sind $gp91^{phox}$, eine Untereinheit der NADPH-Oxidase, zu exprimieren. Die Folge ist, dass betroffene Phagozyten keine reaktiven Sauerstoffspezies bilden können, die sie für die Zerstörung von Pathogenen benötigen. Patienten, die einen solchen Gendefekt tragen, leiden unter chronischen Bakterien- und Pilzinfektionen. Die Krankheit, genannt Septische Granulomatose (engl.: *chronic granulomatous disease*), ist zu 60% auf die nicht funktionale $gp91^{phox}$-Untereinheit zurückzuführen. Diese wird über das Gen *CYBB* auf dem X-Chromosom kodiert, weshalb man die Krankheit, die auf diesem Gendefekt beruht, auch *X-linked chronic granulomatous disease* (xCGD) nennt. Obwohl hauptsächlich neutrophile Granulozyten für die Zerstörung von Pathogenen verantwortlich sind, zeigen auch Monozyten die Fähigkeit Pathogene durch den Oxidativen Burst zu eliminieren. Aus diesem Grund wurde in Kooperation mit Manuel Grez (Georg-Speyer-Haus) die Hypothese aufgestellt, dass eine Reinfusion von autologen, $gp91^{phox}$-korrigierten Monozyten einen

antibakteriellen und antimykotischen Effekt im Patienten zeigen könnte. Eine solche Behandlungsmethode wäre möglicherweise in der Lage akute Infektionsphasen einzuschränken oder vorhandene Granulome aufzulösen. Die Transduktion der ausdifferenzierten Monozyten würde jedoch, im Gegensatz zu der Transduktion von $CD34^+$-Stammzellen, keine Heilung der Krankheit bedeuten. Für eine Heilung der Krankheit bleibt die bevorzugte Therapie die Hämatopoetische Stammzelltransplantation. Sie hat, sofern ein geeigneter Spender vorhanden ist, eine sehr hohe Erfolgsrate, vorausgesetzt, es liegen keine Infektionen zu dem Zeitpunkt der Therapie vor. Eine Reinfusion von autologen, *gp91^{phox}*-korrigierten Monozyten vor der eigentlichen Transplantation wäre daher eine weitere potentielle Einsatzmöglichkeit. Sie könnte akute Infektionen abschwächen und die Patienten schonend, ohne zusätzliche Immunsupressiva, auf die Hämatopoetische Stammzelltherapie vorbereiten.

Aus diesem Grund beschäftigt sich der letzte Teil der Doktorarbeit mit der Frage, ob der lentivirale Transfer des korrekten *gp91^{phox}*-Gens in Monozyten bei der Therapie der Erkrankung hilfreich sein könnte. Für Monozyten ist die Fähigkeit zur Phagozytose, zur Bildung von reaktiven Sauerstoffspezies (Oxidativem Burst) und zur Zerstörung von Bakterien wie *Staphylococcus aureus* beschrieben. In einem ersten Schritt wurden diese Eigenschaften bei humanen Monozyten gesunder Spender nachgewiesen. Während Standard-Assays zur Untersuchung der Phagozytose und des Oxidativen Bursts von Monozyten verfügbar waren, musste ein Assay für das „Killing“ von *S. aureus* neu etabliert werden. Die Monozyten waren in der Lage, *in vitro* Phagozytose, Oxidativen Burst sowie moderates *S. aureus* „Killing“ zu bewirken.

Da in diesem frühen Stadium der Entwicklung noch kein Material von xCGD-Patienten zur Verfügung stand, wurden weitere Untersuchungen zur Korrektur von *gp91^{phox}*-defizienten Monozyten im Maus-Modell durchgeführt. Zunächst wurden die Eigenschaften von Monozyten gesunder Mäuse untersucht. Es wurden Monozyten aus dem Knochenmark aufgereinigt und Protokolle etabliert, um die erwünschten Gr1-positiven Monozyten zu identifizieren. Schließlich wurde deren Fähigkeit zur Phagozytose, zum Oxidativen-Burst und zur Abtötung von *S. aureus* Bakterien *in vitro* nachgewiesen. In Transplantationsversuchen von Monozyten aus eGFP-Mäusen in Rag-2/$\gamma c^{-/-}$-Mäuse bzw. von Monozyten aus C57BL/6-CD45.2-Mäusen in C57BL/6-CD45.1-Mäuse wurde die Biodistribution bzw. die Halbwertszeit von Maus-Monozyten bestimmt. Die Verteilung der Monozyten in verschiedenen Geweben entsprach den Erwartungen: Sie konnten nach vier Tagen nur im Blut und im Knochenmark wiedergefunden werden. Es ergab sich eine Halbwertszeit der Monozyten im peripheren Blut von 55.2 +/- 5.1 h. Insgesamt lässt sich aus den gewonnenen Daten zur Funktion,

Halbwertszeit und Verteilung der Maus-Monozyten schließen, dass mit Hilfe der etablierten Methoden ein Mausmodell zur Erprobung einer Gentherapie von xCGD sinnvoll ist.
Daraufhin wurde das *gp91^{phox}*-Gen in Monozyten von g*p91^{phox}*-Knock-out-Mäusen *ex vivo* transferiert. Hierfür mussten HIV-1-Vektoren eingesetzt werden, da sich die in dieser Arbeit konstruierten HIV-2- oder SIVsmmPBj-Vektoren als ineffizient zur Transduktion von Maus-Monozyten erwiesen haben. Für eine zukünftige Anwendung am Menschen kämen umgekehrt nur die neuen Vektoren in Frage. Mit den HIV-1-Vektoren konnte das korrekte *gp91^{phox}*-Gen in über 50% der aus Knock-out-Mäusen isolierten Monozyten eingebracht werden. In über 85% dieser Zellen wurde die Fähigkeit zum „Oxidativen-Burst“ wiederhergestellt.

Zusammenfassend kann man sagen, dass jetzt sichere und effiziente lentivirale Vektoren für den Gentransfer in primäre Monozyten zur Verfügung stehen. Die Analyse humaner und muriner Monozyten und Experimente zur Übertragung des *gp91^{phox}*-Gens lassen erwarten, dass die Korrektur von *gp91^{phox}*-defizienten Monozyten hilfreich für die Therapie der Septischen Granulomatose sein könnte, und dass das *gp91^{phox}*-Knock-out-Mausmodell zur Erprobung dieses Ansatzes geeignet ist. Als nächste Schritte zur Weiterentwicklung böten sich *in-vivo*-Belastungsexperimente von *gp91^{phox}*-Knock-out-Mäusen nach *ex-vivo* Transfer von *gp91^{phox}* sowie die Korrektur von humanen xCGD-Patienten-Monozyten *in vitro* an.

7 References

Aiken, C. (1997). Pseudotyping human immunodeficiency virus type 1 (HIV-1) by the glycoprotein of vesicular stomatitis virus targets HIV-1 entry to an endocytic pathway and suppresses both the requirement for Nef and the sensitivity to cyclosporin A. J Virol 71(8), 5871-7.

Aiuti, A., Cattaneo, F., Galimberti, S., Benninghoff, U., Cassani, B., Callegaro, L., Scaramuzza, S., Andolfi, G., Mirolo, M., Brigida, I., Tabucchi, A., Carlucci, F., Eibl, M., Aker, M., Slavin, S., Al-Mousa, H., Al Ghonaium, A., Ferster, A., Duppenthaler, A., Notarangelo, L., Wintergerst, U., Buckley, R. H., Bregni, M., Marktel, S., Valsecchi, M. G., Rossi, P., Ciceri, F., Miniero, R., Bordignon, C., and Roncarolo, M. G. (2009). Gene therapy for immunodeficiency due to adenosine deaminase deficiency. N Engl J Med 360(5), 447-58.

Alexander, B. L., Ali, R. R., Alton, E. W., Bainbridge, J. W., Braun, S., Cheng, S. H., Flotte, T. R., Gaspar, H. B., Grez, M., Griesenbach, U., Kaplitt, M. G., Ott, M. G., Seger, R., Simons, M., Thrasher, A. J., Thrasher, A. Z., and Yla-Herttuala, S. (2007). Progress and prospects: gene therapy clinical trials (part 1). Gene Ther 14(20), 1439-47.

Antoniou, M., Harland, L., Mustoe, T., Williams, S., Holdstock, J., Yague, E., Mulcahy, T., Griffiths, M., Edwards, S., Ioannou, P. A., Mountain, A., and Crombie, R. (2003). Transgenes encompassing dual-promoter CpG islands from the human TBP and HNRPA2B1 loci are resistant to heterochromatin-mediated silencing. Genomics 82(3), 269-79.

Auffray, C., Fogg, D., Garfa, M., Elain, G., Join-Lambert, O., Kayal, S., Sarnacki, S., Cumano, A., Lauvau, G., and Geissmann, F. (2007). Monitoring of blood vessels and tissues by a population of monocytes with patrolling behavior. Science 317(5838), 666-70.

Auffray, C., Sieweke, M. H., and Geissmann, F. (2009). Blood Monocytes: Development, Heterogeneity, and Relationship with Dendritic Cells. Annu Rev Immunol.

Banchereau, J., and Steinman, R. M. (1998). Dendritic cells and the control of immunity. Nature 392(6673), 245-52.

Baum, C., Itoh, K., Meyer, J., Laker, C., Ito, Y., and Ostertag, W. (1997). The potent enhancer activity of the polycythemic strain of spleen focus-forming virus in hematopoietic cells is governed by a binding site for Sp1 in the upstream control region and by a unique enhancer core motif, creating an exclusive target for PEBP/CBF. J Virol 71(9), 6323-31.

Belshan, M., and Ratner, L. (2003). Identification of the nuclear localization signal of human immunodeficiency virus type 2 Vpx. Virology 311(1), 7-15.

Bjorgvinsdottir, H., Ding, C., Pech, N., Gifford, M. A., Li, L. L., and Dinauer, M. C. (1997). Retroviral-mediated gene transfer of gp91phox into bone marrow cells rescues defect in host defense against Aspergillus fumigatus in murine X-linked chronic granulomatous disease. Blood 89(1), 41-8.

Bylund, J., Goldblatt, D., and Speert, D. P. (2005). Chronic granulomatous disease: from genetic defect to clinical presentation. Adv Exp Med Biol 568, 67-87.

Cartier, N., Hacein-Bey, S., Veres, G., Vidaud, M., Dal-Cortivo, L., Caccavelli, L., Malhaoui, N., Kiermer, V., Mittelstaedt, D., Simmons, A., Bellesme, C., Audat, F., Blanche, S., Chanaud, P., Audit, M., B., L. h., Zhao-Emmonet, J.-C., Fichelson, S., Pflumino, F., Dubart-Kupperschmitt, A., Salzman, R., Salzman, A., Bougneres, P., Fischer, A., Cavazzana-Calvo, M., and Aubourg, P. (2007). Preliminary Data from the First Hematopoietic Stem Cell Gene Therapy Trial with Lentiviral Vector Demonstrate Expression of the Therapeutic Protein in High Percentage of Lymphocytes and Monocytes in Two Patients with X-Linked Adrenoleukodystophy. ESGT 2007, Oral Presentation.

Cattoglio, C., Facchini, G., Sartori, D., Antonelli, A., Miccio, A., Cassani, B., Schmidt, M., von Kalle, C., Howe, S., Thrasher, A. J., Aiuti, A., Ferrari, G., Recchia, A., and Mavilio, F. (2007). Hot spots of retroviral integration in human CD34+ hematopoietic cells. Blood 110(6)**,** 1770-8.

Cavazzana-Calvo, M., Hacein-Bey, S., de Saint Basile, G., Gross, F., Yvon, E., Nusbaum, P., Selz, F., Hue, C., Certain, S., Casanova, J. L., Bousso, P., Deist, F. L., and Fischer, A. (2000). Gene therapy of human severe combined immunodeficiency (SCID)-X1 disease. Science 288(5466)**,** 669-72.

Chang, D. D., and Sharp, P. A. (1989). Regulation by HIV Rev depends upon recognition of splice sites. Cell 59(5)**,** 789-95.

Check, E. (2005). Gene therapy put on hold as third child develops cancer. Nature 433(7026)**,** 561.

D'Costa, J., Brown, H., Kundra, P., Davis-Warren, A., and Arya, S. (2001). Human immunodeficiency virus type 2 lentiviral vectors: packaging signal and splice donor in expression and encapsidation. J Gen Virol 82(Pt 2)**,** 425-34.

De Rijck, J., and Debyser, Z. (2006). The central DNA flap of the human immunodeficiency virus type 1 is important for viral replication. Biochem Biophys Res Commun 349(3)**,** 1100-10.

Dinauer, M. C., Gifford, M. A., Pech, N., Li, L. L., and Emshwiller, P. (2001). Variable correction of host defense following gene transfer and bone marrow transplantation in murine X-linked chronic granulomatous disease. Blood 97(12)**,** 3738-45.

Dropulic, B., and June, C. H. (2006). Gene-based immunotherapy for human immunodeficiency virus infection and acquired immunodeficiency syndrome. Hum Gene Ther 17(6)**,** 577-88.

Dull, T., Zufferey, R., Kelly, M., Mandel, R. J., Nguyen, M., Trono, D., and Naldini, L. (1998). A third-generation lentivirus vector with a conditional packaging system. J Virol 72(11)**,** 8463-71.

Dupuy, F. P., Mouly, E., Mesel-Lemoine, M., Morel, C., Abriol, J., Cherai, M., Baillou, C., Negre, D., Cosset, F. L., Klatzmann, D., and Lemoine, F. M. (2005). Lentiviral transduction of human hematopoietic cells by HIV-1- and SIV-based vectors containing a bicistronic cassette driven by various internal promoters. J Gene Med 7(9)**,** 1158-71.

Dvorin, J. D., Bell, P., Maul, G. G., Yamashita, M., Emerman, M., and Malim, M. H. (2002). Reassessment of the roles of integrase and the central DNA flap in human immunodeficiency virus type 1 nuclear import. J Virol 76(23)**,** 12087-96.

Egan, C. E., Sukhumavasi, W., Bierly, A. L., and Denkers, E. Y. (2008). Understanding the multiple functions of Gr-1(+) cell subpopulations during microbial infection. Immunol Res 40(1), 35-48.

Emerman, M., Guyader, M., Montagnier, L., Baltimore, D., and Muesing, M. A. (1987). The specificity of the human immunodeficiency virus type 2 transactivator is different from that of human immunodeficiency virus type 1. Embo J 6(12), 3755-60.

Emmendorffer, A., Nakamura, M., Rothe, G., Spiekermann, K., Lohmann-Matthes, M. L., and Roesler, J. (1994). Evaluation of flow cytometric methods for diagnosis of chronic granulomatous disease variants under routine laboratory conditions. Cytometry 18(3), 147-55.

Felber, B. K., Hadzopoulou-Cladaras, M., Cladaras, C., Copeland, T., and Pavlakis, G. N. (1989). rev protein of human immunodeficiency virus type 1 affects the stability and transport of the viral mRNA. Proc Natl Acad Sci U S A 86(5), 1495-9.

Fleming, T. J., Fleming, M. L., and Malek, T. R. (1993). Selective expression of Ly-6G on myeloid lineage cells in mouse bone marrow. RB6-8C5 mAb to granulocyte-differentiation antigen (Gr-1) detects members of the Ly-6 family. J Immunol 151(5), 2399-408.

Fletcher, T. M., 3rd, Brichacek, B., Sharova, N., Newman, M. A., Stivahtis, G., Sharp, P. M., Emerman, M., Hahn, B. H., and Stevenson, M. (1996). Nuclear import and cell cycle arrest functions of the HIV-1 Vpr protein are encoded by two separate genes in HIV-2/SIV(SM). Embo J 15(22), 6155-65.

Fogg, D. K., Sibon, C., Miled, C., Jung, S., Aucouturier, P., Littman, D. R., Cumano, A., and Geissmann, F. (2006). A clonogenic bone marrow progenitor specific for macrophages and dendritic cells. Science 311(5757), 83-7.

Freed, E. O., and Martin, M. A. (2007). HIVs and Their Replication. In Fields´ Virology, D.M.Knipe and P.M.Howley, eds. (Philadelphia: Lippincott Williams & Wilkins), 2107-2186.

Fritz, J. V., Didier, P., Clamme, J. P., Schaub, E., Muriaux, D., Cabanne, C., Morellet, N., Bouaziz, S., Darlix, J. L., Mely, Y., and de Rocquigny, H. (2008). Direct Vpr-Vpr interaction in cells monitored by two photon fluorescence correlation spectroscopy and fluorescence lifetime imaging. Retrovirology 5, 87.

Fuchs, T. A., Abed, U., Goosmann, C., Hurwitz, R., Schulze, I., Wahn, V., Weinrauch, Y., Brinkmann, V., and Zychlinsky, A. (2007). Novel cell death program leads to neutrophil extracellular traps. J Cell Biol 176(2), 231-41.

Fultz, P. N. (1991). Replication of an acutely lethal simian immunodeficiency virus activates and induces proliferation of lymphocytes. J Virol 65(9), 4902-9.

Fultz, P. N., McClure, H. M., Anderson, D. C., and Switzer, W. M. (1989). Identification and biologic characterization of an acutely lethal variant of simian immunodeficiency virus from sooty mangabeys (SIV/SMM). AIDS Res Hum Retroviruses 5(4), 397-409.

Funke, S., Schneider, I. C., Glaser, S., Muhlebach, M. D., Moritz, T., Cattaneo, R., Cichutek, K., and Buchholz, C. J. (2009). Pseudotyping lentiviral vectors with the wild-type measles virus glycoproteins improves titer and selectivity. Gene Ther.

Garriga, J., and Grana, X. (2004). Cellular control of gene expression by T-type cyclin/CDK9 complexes. Gene 337**,** 15-23.

Geissmann, F., Jung, S., and Littman, D. R. (2003). Blood monocytes consist of two principal subsets with distinct migratory properties. Immunity 19(1)**,** 71-82.

Grez, M. (2008). Gene Theraypy of Chronic Granulomatous Disease: Ups and Downs after 4 Years Follow-Up. ASGT 11th Annual Meeting, Oral Presentation.

Hacein-Bey-Abina, S., Le Deist, F., Carlier, F., Bouneaud, C., Hue, C., De Villartay, J. P., Thrasher, A. J., Wulffraat, N., Sorensen, R., Dupuis-Girod, S., Fischer, A., Davies, E. G., Kuis, W., Leiva, L., and Cavazzana-Calvo, M. (2002). Sustained correction of X-linked severe combined immunodeficiency by ex vivo gene therapy. N Engl J Med 346(16)**,** 1185-93.

Hacein-Bey-Abina, S., von Kalle, C., Schmidt, M., Le Deist, F., Wulffraat, N., McIntyre, E., Radford, I., Villeval, J. L., Fraser, C. C., Cavazzana-Calvo, M., and Fischer, A. (2003). A serious adverse event after successful gene therapy for X-linked severe combined immunodeficiency. N Engl J Med 348(3)**,** 255-6.

Henderson, L. E., Sowder, R. C., Copeland, T. D., Benveniste, R. E., and Oroszlan, S. (1988). Isolation and characterization of a novel protein (X-ORF product) from SIV and HIV-2. Science 241(4862)**,** 199-201.

Hirsch, V. M., Sharkey, M. E., Brown, C. R., Brichacek, B., Goldstein, S., Wakefield, J., Byrum, R., Elkins, W. R., Hahn, B. H., Lifson, J. D., and Stevenson, M. (1998). Vpx is required for dissemination and pathogenesis of SIV(SM) PBj: evidence of macrophage-dependent viral amplification. Nat Med 4(12)**,** 1401-8.

Hlavaty, J., Schittmayer, M., Stracke, A., Jandl, G., Knapp, E., Felber, B. K., Salmons, B., Gunzburg, W. H., and Renner, M. (2005). Effect of posttranscriptional regulatory elements on transgene expression and virus production in the context of retrovirus vectors. Virology 341(1)**,** 1-11.

Högner, K. (2007). Herstellung und Erprobung von lentiviralen Vektoren zur Übertragung des gp91phox-Gens in primäre humane Monozyten. Diplomarbeit am Paul-Ehrlich-Institut, Abteilung: Medizinische Biotechnologie.

Jarraya, B., Ralph, S., Boulet, S., Shin, M., Bonvento, G., Jan, C., Delzescaux, T., Drouot, X., Herard, A.-S., Brouillet, E., Conde, F., Day, D., Stratful, E., Miskin, J., McDonald, M., Kingsman, S. M., Hantraye, P., Mitrophanous, K., and Palfi, S. (2008). Preclinical and Clinical Development of ProSavin, an EIAV-Based Gene Therapy for Parkinson's Disease. ASGT 11th Annual Meeting, Oral Presentation.

Johnston, R. B., Jr. (2001). Clinical aspects of chronic granulomatous disease. Curr Opin Hematol 8(1)**,** 17-22.

Kaiser, J. K. (2008). Eignung von SIVsmmPBj-abgeleiteten lentiviralen Vektoren für die Transduktion primärer Zellen und für immuntherapeutische Anwendungen. Dissertation am Paul-Ehrlich-Institut, Abteilung: Medizinische Biotechnologie.

Kappes, J. C., Wu, X., and Wakefield, J. K. (2003). Production of trans-lentiviral vector with predictable safety. Methods Mol Med 76**,** 449-65.

Karlsson Hedestam, G. B., Fouchier, R. A., Phogat, S., Burton, D. R., Sodroski, J., and Wyatt, R. T. (2008). The challenges of eliciting neutralizing antibodies to HIV-1 and to influenza virus. Nat Rev Microbiol 6(2), 143-55.

Kawamura, M., Sakai, H., and Adachi, A. (1994). Human immunodeficiency virus Vpx is required for the early phase of replication in peripheral blood mononuclear cells. Microbiol Immunol 38(11), 871-8.

Kikuta, A., Ito, M., Mochizuki, K., Akaihata, M., Nemoto, K., Sano, H., and Ohto, H. (2006). Nonmyeloablative stem cell transplantation for nonmalignant diseases in children with severe organ dysfunction. Bone Marrow Transplant 38(10), 665-9.

Kimura, H., Sawada, T., Oshima, S., Kozawa, K., Ishioka, T., and Kato, M. (2005). Toxicity and roles of reactive oxygen species. Curr Drug Targets Inflamm Allergy 4(4), 489-95.

Kingsman, S. M., Mitrophanous, K., and Olsen, J. C. (2005). Potential oncogene activity of the woodchuck hepatitis post-transcriptional regulatory element (WPRE). Gene Ther 12(1), 3-4.

Kotsopoulou, E., Kim, V. N., Kingsman, A. J., Kingsman, S. M., and Mitrophanous, K. A. (2000). A Rev-independent human immunodeficiency virus type 1 (HIV-1)-based vector that exploits a codon-optimized HIV-1 gag-pol gene. J Virol 74(10), 4839-52.

Leijh, P. C., van den Barselaar, M. T., Daha, M. R., and van Furth, R. (1982). Stimulation of the intracellular killing of Staphylococcus aureus by monocytes: regulation by immunoglobulin G and complement components C3/C3b and B/Bb. J Immunol 129(1), 332-7.

Levine, B. L., Humeau, L. M., Boyer, J., MacGregor, R. R., Rebello, T., Lu, X., Binder, G. K., Slepushkin, V., Lemiale, F., Mascola, J. R., Bushman, F. D., Dropulic, B., and June, C. H. (2006). Gene transfer in humans using a conditionally replicating lentiviral vector. Proc Natl Acad Sci U S A 103(46), 17372-7.

Lewinski, M. K., Yamashita, M., Emerman, M., Ciuffi, A., Marshall, H., Crawford, G., Collins, F., Shinn, P., Leipzig, J., Hannenhalli, S., Berry, C. C., Ecker, J. R., and Bushman, F. D. (2006). Retroviral DNA integration: viral and cellular determinants of target-site selection. PLoS Pathog 2(6), e60.

Liehl, B., Hlavaty, J., Moldzio, R., Tonar, Z., Unger, H., Salmons, B., Gunzburg, W. H., and Renner, M. (2007). Simian immunodeficiency virus vector pseudotypes differ in transduction efficiency and target cell specificity in brain. Gene Ther 14(18), 1330-43.

Limon, A., Nakajima, N., Lu, R., Ghory, H. Z., and Engelman, A. (2002). Wild-type levels of nuclear localization and human immunodeficiency virus type 1 replication in the absence of the central DNA flap. J Virol 76(23), 12078-86.

Mangeot, P. E., Negre, D., Dubois, B., Winter, A. J., Leissner, P., Mehtali, M., Kaiserlian, D., Cosset, F. L., and Darlix, J. L. (2000). Development of minimal lentivirus vectors derived from simian immunodeficiency virus (SIVmac251) and their use for gene transfer into human dendritic cells. J Virol 74(18), 8307-15.

Mazzarella, G., Petillo, O., Margarucci, S., Calabrese, C., and Peluso, G. (1998). Role of monocyte/macrophage population in immune response. Monaldi Arch Chest Dis 53(1), 92-6.

Mills, E. L., Rholl, K. S., and Quie, P. G. (1980). X-linked inheritance in females with chronic granulomatous disease. J Clin Invest 66(2), 332-40.

Miyoshi, H., Blomer, U., Takahashi, M., Gage, F. H., and Verma, I. M. (1998). Development of a self-inactivating lentivirus vector. J Virol 72(10), 8150-7.

Montini, E., Cesana, D., Schmidt, M., Sanvito, F., Ponzoni, M., Bartholomae, C., Sergi Sergi, L., Benedicenti, F., Ambrosi, A., Di Serio, C., Doglioni, C., von Kalle, C., and Naldini, L. (2006). Hematopoietic stem cell gene transfer in a tumor-prone mouse model uncovers low genotoxicity of lentiviral vector integration. Nat Biotechnol 24(6), 687-96.

Morris, K. V., Gilbert, J., Wong-Staal, F., Gasmi, M., and Looney, D. J. (2004). Transduction of cell lines and primary cells by FIV-packaged HIV vectors. Mol Ther 10(1), 181-90.

Mouy, R., Fischer, A., Vilmer, E., Seger, R., and Griscelli, C. (1989). Incidence, severity, and prevention of infections in chronic granulomatous disease. J Pediatr 114(4 Pt 1), 555-60.

Mühlebach, M. D., Wolfrum, N., Schule, S., Tschulena, U., Sanzenbacher, R., Flory, E., Cichutek, K., and Schweizer, M. (2005). Stable Transduction of Primary Human Monocytes by Simian Lentiviral Vector PBj. Mol Ther.

Naik, S. H., Metcalf, D., van Nieuwenhuijze, A., Wicks, I., Wu, L., O'Keeffe, M., and Shortman, K. (2006). Intrasplenic steady-state dendritic cell precursors that are distinct from monocytes. Nat Immunol 7(6), 663-71.

Naldini, L., Blomer, U., Gage, F. H., Trono, D., and Verma, I. M. (1996a). Efficient transfer, integration, and sustained long-term expression of the transgene in adult rat brains injected with a lentiviral vector. Proc Natl Acad Sci U S A 93(21), 11382-8.

Naldini, L., Blomer, U., Gallay, P., Ory, D., Mulligan, R., Gage, F. H., Verma, I. M., and Trono, D. (1996b). In vivo gene delivery and stable transduction of nondividing cells by a lentiviral vector. Science 272(5259), 263-7.

Negre, D., Mangeot, P. E., Duisit, G., Blanchard, S., Vidalain, P. O., Leissner, P., Winter, A. J., Rabourdin-Combe, C., Mehtali, M., Moullier, P., Darlix, J. L., and Cosset, F. L. (2000). Characterization of novel safe lentiviral vectors derived from simian immunodeficiency virus (SIVmac251) that efficiently transduce mature human dendritic cells. Gene Ther 7(19), 1613-23.

Okabe, M., Ikawa, M., Kominami, K., Nakanishi, T., and Nishimune, Y. (1997). 'Green mice' as a source of ubiquitous green cells. FEBS Lett 407(3), 313-9.

Ooms, M., Huthoff, H., Russell, R., Liang, C., and Berkhout, B. (2004). A riboswitch regulates RNA dimerization and packaging in human immunodeficiency virus type 1 virions. J Virol 78(19), 10814-9.

Ott, M. G., Schmidt, M., Schwarzwaelder, K., Stein, S., Siler, U., Koehl, U., Glimm, H., Kuhlcke, K., Schilz, A., Kunkel, H., Naundorf, S., Brinkmann, A., Deichmann, A., Fischer, M., Ball, C., Pilz, I., Dunbar, C., Du, Y., Jenkins, N. A., Copeland, N. G., Luthi, U., Hassan, M., Thrasher, A. J., Hoelzer, D., von Kalle, C., Seger, R., and Grez, M. (2006). Correction of X-linked chronic granulomatous disease by gene therapy, augmented by insertional activation of MDS1-EVI1, PRDM16 or SETBP1. Nat Med 12(4), 401-9.

Pancio, H. A., and Ratner, L. (1998). Human immunodeficiency virus type 2 Vpx-Gag interaction. J Virol 72(6), 5271-5.

Patel, J., Wang, S. W., Izmailova, E., and Aldovini, A. (2003). The simian immunodeficiency virus 5' untranslated leader sequence plays a role in intracellular viral protein accumulation and in RNA packaging. J Virol 77(11), 6284-92.

Poeschla, E., Gilbert, J., Li, X., Huang, S., Ho, A., and Wong-Staal, F. (1998). Identification of a human immunodeficiency virus type 2 (HIV-2) encapsidation determinant and transduction of nondividing human cells by HIV-2-based lentivirus vectors. J Virol 72(8), 6527-36.

Pollock, J. D., Williams, D. A., Gifford, M. A., Li, L. L., Du, X., Fisherman, J., Orkin, S. H., Doerschuk, C. M., and Dinauer, M. C. (1995). Mouse model of X-linked chronic granulomatous disease, an inherited defect in phagocyte superoxide production. Nat Genet 9(2), 202-9.

Rada, B. K., Geiszt, M., Kaldi, K., Timar, C., and Ligeti, E. (2004). Dual role of phagocytic NADPH oxidase in bacterial killing. Blood 104(9), 2947-53.

Ramezani, A., Hawley, T. S., and Hawley, R. G. (2003). Performance- and safety-enhanced lentiviral vectors containing the human interferon-beta scaffold attachment region and the chicken beta-globin insulator. Blood 101(12), 4717-24.

Recillas-Targa, F., Valadez-Graham, V., and Farrell, C. M. (2004). Prospects and implications of using chromatin insulators in gene therapy and transgenesis. Bioessays 26(7), 796-807.

Reeves, E. P., Lu, H., Jacobs, H. L., Messina, C. G., Bolsover, S., Gabella, G., Potma, E. O., Warley, A., Roes, J., and Segal, A. W. (2002). Killing activity of neutrophils is mediated through activation of proteases by K+ flux. Nature 416(6878), 291-7.

Reuter, S., Kaumanns, P., Buschhorn, S. B., and Dittmar, M. T. (2005). Role of HIV-2 envelope in Lv2-mediated restriction. Virology 332(1), 347-58.

Rex, J. H., Bennett, J. E., Gallin, J. I., Malech, H. L., and Melnick, D. A. (1990). Normal and deficient neutrophils can cooperate to damage Aspergillus fumigatus hyphae. J Infect Dis 162(2), 523-8.

Rogister, B., and Moonen, G. (2001). Microexplant Cultures of the Cerebellum. Protocols for Cell Culture, 3rd Ed., Ed.: S. Fedoroff and A. Richardson, Human Pess, Inc., Totowa, NJ.

Rohloff, L.-H., Wiesner, A., and Götz, P. (1994). A fluorescence assay demonstrating stimulation of phagocytosis by haemolymph molecules of Galleria mellonella. Journal of Insect Physiology 40(12), 1045-1049.

Schambach, A., and Baum, C. (2008). Clinical application of lentiviral vectors - concepts and practice. Curr Gene Ther 8(6), 474-82.

Schambach, A., Bohne, J., Baum, C., Hermann, F. G., Egerer, L., von Laer, D., and Giroglou, T. (2006a). Woodchuck hepatitis virus post-transcriptional regulatory element deleted from X protein and promoter sequences enhances retroviral vector titer and expression. Gene Ther 13(7), 641-5.

Schambach, A., Mueller, D., Galla, M., Verstegen, M. M., Wagemaker, G., Loew, R., Baum, C., and Bohne, J. (2006b). Overcoming promoter competition in packaging cells improves production of self-inactivating retroviral vectors. Gene Ther 13(21), 1524-33.

Schroder, A. R., Shinn, P., Chen, H., Berry, C., Ecker, J. R., and Bushman, F. (2002). HIV-1 integration in the human genome favors active genes and local hotspots. Cell 110(4), 521-9.

Seger, R. A. (2008). Modern management of chronic granulomatous disease. Br J Haematol 140(3), 255-66.

Seger, R. A., Gungor, T., Belohradsky, B. H., Blanche, S., Bordigoni, P., Di Bartolomeo, P., Flood, T., Landais, P., Muller, S., Ozsahin, H., Passwell, J. H., Porta, F., Slavin, S., Wulffraat, N., Zintl, F., Nagler, A., Cant, A., and Fischer, A. (2002). Treatment of chronic granulomatous disease with myeloablative conditioning and an unmodified hemopoietic allograft: a survey of the European experience, 1985-2000. Blood 100(13), 4344-50.

Sirven, A., Pflumio, F., Zennou, V., Titeux, M., Vainchenker, W., Coulombel, L., Dubart-Kupperschmitt, A., and Charneau, P. (2000). The human immunodeficiency virus type-1 central DNA flap is a crucial determinant for lentiviral vector nuclear import and gene transduction of human hematopoietic stem cells. Blood 96(13), 4103-10.

Sleigh, R., Sharkey, M., Newman, M. A., Hahn, B., and Stevenson, M. (1998). Differential association of uracil DNA glycosylase with SIVSM Vpr and Vpx proteins. Virology 245(2), 338-43.

Srivastava, S., Swanson, S. K., Manel, N., Florens, L., Washburn, M. P., and Skowronski, J. (2008). Lentiviral Vpx accessory factor targets VprBP/DCAF1 substrate adaptor for cullin 4 E3 ubiquitin ligase to enable macrophage infection. PLoS Pathog 4(5), e1000059.

Stein, S., Siler, U., Ott, M. G., Seger, R., and Grez, M. (2006). Gene therapy for chronic granulomatous disease. Curr Opin Mol Ther 8(5), 415-22.

Stroncek, D. F., Leonard, K., Eiber, G., Malech, H. L., Gallin, J. I., and Leitman, S. F. (1996). Alloimmunization after granulocyte transfusions. Transfusion 36(11-12), 1009-15.

Suggs, S. V., Wallace, R. B., Hirose, T., Kawashima, E. H., and Itakura, K. (1981). Use of synthetic oligonucleotides as hybridization probes: isolation of cloned cDNA sequences for human beta 2-microglobulin. Proc Natl Acad Sci U S A 78(11), 6613-7.

Sunderkötter, C., Nikolic, T., Dillon, M. J., Van Rooijen, N., Stehling, M., Drevets, D. A., and Leenen, P. J. (2004). Subpopulations of mouse blood monocytes differ in maturation stage and inflammatory response. J Immunol 172(7), 4410-7.

Suzuki, Y., and Craigie, R. (2007). The road to chromatin - nuclear entry of retroviruses. Nat Rev Microbiol 5(3), 187-96.

Swirski, F. K., Pittet, M. J., Kircher, M. F., Aikawa, E., Jaffer, F. A., Libby, P., and Weissleder, R. (2006). Monocyte accumulation in mouse atherogenesis is progressive and proportional to extent of disease. Proc Natl Acad Sci U S A 103(27), 10340-5.

Towbin, H., Staehelin, T., and Gordon, J. (1979). Electrophoretic transfer of proteins from polyacrylamide gels to nitrocellulose sheets: procedure and some applications. Proc Natl Acad Sci U S A 76(9), 4350-4.

Van Maele, B., De Rijck, J., De Clercq, E., and Debyser, Z. (2003). Impact of the central polypurine tract on the kinetics of human immunodeficiency virus type 1 vector transduction. J Virol 77(8), 4685-94.

Varol, C., Landsman, L., Fogg, D. K., Greenshtein, L., Gildor, B., Margalit, R., Kalchenko, V., Geissmann, F., and Jung, S. (2007). Monocytes give rise to mucosal, but not splenic, conventional dendritic cells. J Exp Med 204(1), 171-80.

von Planta, M., Ozsahin, H., Schroten, H., Stauffer, U. G., and Seger, R. A. (1997). Greater omentum flaps and granulocyte transfusions as combined therapy of liver abscess in chronic granulomatous disease. Eur J Pediatr Surg 7(4), 234-6.

Winkelstein, J. A., Marino, M. C., Johnston, R. B., Jr., Boyle, J., Curnutte, J., Gallin, J. I., Malech, H. L., Holland, S. M., Ochs, H., Quie, P., Buckley, R. H., Foster, C. B., Chanock, S. J., and Dickler, H. (2000). Chronic granulomatous disease. Report on a national registry of 368 patients. Medicine (Baltimore) 79(3), 155-69.

Wolach, B., Gavrieli, R., de Boer, M., Gottesman, G., Ben-Ari, J., Rottem, M., Schlesinger, Y., Grisaru-Soen, G., Etzioni, A., and Roos, D. (2008). Chronic granulomatous disease in Israel: clinical, functional and molecular studies of 38 patients. Clin Immunol 129(1), 103-14.

Wolfrum, N. (2005). Untersuchung der besonderen Transduktionseigenschaften eines SIVsmmPBj Vektors und Etablierung eines davon abgeleiteten Dreiplasmid-Vektorsystems. Dissertation am Paul-Ehrlich-Institut, Abteilung: Medizinische Biotechnologie.

Wolfrum, N., Muhlebach, M. D., Schule, S., Kaiser, J. K., Kloke, B. P., Cichutek, K., and Schweizer, M. (2007). Impact of viral accessory proteins of SIVsmmPBj on early steps of infection of quiescent cells. Virology.

Wu, X., Conway, J. A., Kim, J., and Kappes, J. C. (1994). Localization of the Vpx packaging signal within the C terminus of the human immunodeficiency virus type 2 Gag precursor protein. J Virol 68(10), 6161-9.

Wu, X., Li, Y., Crise, B., and Burgess, S. M. (2003). Transcription start regions in the human genome are favored targets for MLV integration. Science 300(5626), 1749-51.

Wu, X., Wakefield, J. K., Liu, H., Xiao, H., Kralovics, R., Prchal, J. T., and Kappes, J. C. (2000). Development of a novel trans-lentiviral vector that affords predictable safety. Mol Ther 2(1), 47-55.

Yu, E. T., Hawkins, A., Eaton, J., and Fabris, D. (2008). MS3D structural elucidation of the HIV-1 packaging signal. Proc Natl Acad Sci U S A 105(34), 12248-53.

Yu, X. F., Yu, Q. C., Essex, M., and Lee, T. H. (1991). The vpx gene of simian immunodeficiency virus facilitates efficient viral replication in fresh lymphocytes and macrophage. J Virol 65(9), 5088-91.

Zennou, V., Petit, C., Guetard, D., Nerhbass, U., Montagnier, L., and Charneau, P. (2000). HIV-1 genome nuclear import is mediated by a central DNA flap. Cell 101(2), 173-85.

Zhang, F., Thornhill, S. I., Howe, S. J., Ulaganathan, M., Schambach, A., Sinclair, J., Kinnon, C., Gaspar, H. B., Antoniou, M., and Thrasher, A. J. (2007). Lentiviral vectors containing an enhancer-less ubiquitously acting chromatin opening element (UCOE) provide highly reproducible and stable transgene expression in hematopoietic cells. Blood 110(5)**,** 1448-57.

Zhen, L., King, A. A., Xiao, Y., Chanock, S. J., Orkin, S. H., and Dinauer, M. C. (1993). Gene targeting of X chromosome-linked chronic granulomatous disease locus in a human myeloid leukemia cell line and rescue by expression of recombinant gp91phox. Proc Natl Acad Sci U S A 90(21)**,** 9832-6.

Zufferey, R., Donello, J. E., Trono, D., and Hope, T. J. (1999). Woodchuck hepatitis virus posttranscriptional regulatory element enhances expression of transgenes delivered by retroviral vectors. J Virol 73(4)**,** 2886-92.

Zufferey, R., Dull, T., Mandel, R. J., Bukovsky, A., Quiroz, D., Naldini, L., and Trono, D. (1998). Self-inactivating lentivirus vector for safe and efficient in vivo gene delivery. J Virol 72(12)**,** 9873-80.

Zufferey, R., Nagy, D., Mandel, R. J., Naldini, L., and Trono, D. (1997). Multiply attenuated lentiviral vector achieves efficient gene delivery in vivo. Nat Biotechnol 15(9)**,** 871-5.

8 Abbreviations

A	amper
ADA-SCID	adenosine deaminase-deficient severe combined immunodeficiency
AIDS	Acquired Immune Deficiency Syndrome
ALD	adrenoleukodystrophy
Amp	ampicillin
APC	allophycocyanin
approx.	approximately
ATCC	American Type Culture Collection
BAF	barrier-to-autointegration factor
bp	base pairs
BSA	bovine serum albumin
°C	degree Celsius
CCR5	chemokine (C-C motif) receptor 5
CD	cluster of differentiation
cDC	splenic dendritic cell
CGD	chronic granulomatous disease
CMV	cyto-megalo-virus
cPPT	central polypurine tract
CTS	central termination sequence
CXCR4	chemokine (C-X-C motif) receptor 4
DAPI	4',6-diamidino-2-phenylindole
DC	dendritic cell
DHR	dihydrorhodamine
DMEM	Dulbecco`s modified Eagle medium
DNA	deoxyribonucleic acid
E. coli	Escherichia coli
ECL	enhanced chemiluminescence
EDTA	ethylene-diamine-tetra-acetate
eGFP	enhanced green fluorescent protein
EIAV	equine infectious anemia virus
Env	envelope protein
et al.	and others
FACS	fluorescence activated cell sorting
FCS	fetal calf serum
FITC	fluorescence isothiocyanate
flavo. b_{558}	flavocytochrome b_{558}
FSC	forward scatter
g	gram or gravitational acceleration
Gag	group-specific-antigen
gp	glycoprotein
h	hour
HIV-1	Human immunodeficiency virus-1
HIV-2	Human immunodeficiency virus-2
HLA	human leukocyte antigens
HRP	horseradish peroxidase
HSC	hematopoietic stem cells

HSCT	hematopoietic stem cell transplantation
i.e.	*id est*, that is
i.v.	intravenous
IFN	interferon
IL	interleukin
IN	integrase
iNOS	inducible nitric oxide synthase
kb	kilobase pair
kDa	kilodalton
l	liter
LB	Luria-Bertani
LTR	long terminal repeat
m	meter
M	molar
m-	milli
MA	matrix
mAb	monoclonal antibody
MDP	macrophage and dendritic cell precursor
MLV	murine leukaemia virus
moi	multiplicity of infection
MOPS	morpholinepropanesulfonate
mRNA	messenger RNA
n	number
n-	nano
NADPH	nicotinamide adenine dinucleotide phosphate
NC	nucleocapsid
NEAA	non essential amino acids
NEB	New England Biolabs
Nef	negative factor
NK cell	natural killer cell
NPC	nuclear pore complex
N-terminal	aminoterminal
PBj	see SIVsmmPBj
PBS	primer binding site or phosphate buffered saline
PCR	polymerase chain reaction
pDC	plasmacytoid dendritic cell
PE	R-Phycoerythrin
phox	phagocytic oxidase
PIC	pre-integration complex
PMA	phorbol 12-myristate 13-acetate
Pol	polymerase
PPT	polypurine tract
RCL	replication competent lentivirus
Rev	regulator of virion expression
RNA	ribonucleic acid
RNase	ribonuclease
ROS	reactive oxygen species
rpm	revolutions per minute

RPMI	culture medium developed in the “Roswell Park Memorial Institute”
RRE	Rev-responsive element
RSV	Rous-Sarkom-Virus
RT	room temperature or reverse transcriptase
RTC	reverse transcription complex
S. aureus	Staphylococcus aureus
SA	splice acceptor
SCID-X1	X-linked severe combined immunodeficiency
SD	slice donor
sec	second
SFFV	spleen focus-forming virus
SIN	self-inactivating
SIVdrl	Simian immunodeficiency virus of drill monkeys
SIVmac	Simian immunodeficiency virus of rhesus macaques
SIVmnd-2	Simian immunodeficiency virus of mandrills
SIVrcm	Simian immunodeficiency virus of red-capped mangabey
SIVsmm	Simian immunodeficiency virus of sooty mangabey monkeys
SSC	side scatter
SV40	Simian virus 40
TAE	Tris-acetate-EDTA
TAR	trans activation response
Tat	transactivator of transcription
Tip-DC	TNF-α/iNOS-producing dendritic cell
TNF-α	Tumor Necrosis Factor α
tRNA	transfer RNA
TU	transducing units
UCOE	ubiquitously acting chromatin opening elements
UTR	Untranlational region
UV	Ultraviolet
V	volt
Vif	virion infectivity factor
Vpr	viral protein r
Vpu	viral protein u
Vpx	viral protein x
VSV-G	glycoprotein of vesicular stomatitis virus
w/v	weight/volume
WPRE	woodchuck hepatitis virus posttranscriptional regulatory element
xCGD	X-linked chronic granulomatous disease
α	anti-
µ	micro-
Ψ	psi-packaging signal of retroviral genomic RNA

9 Appendix

9.1 Plasmid map of pVpxPBjsyn

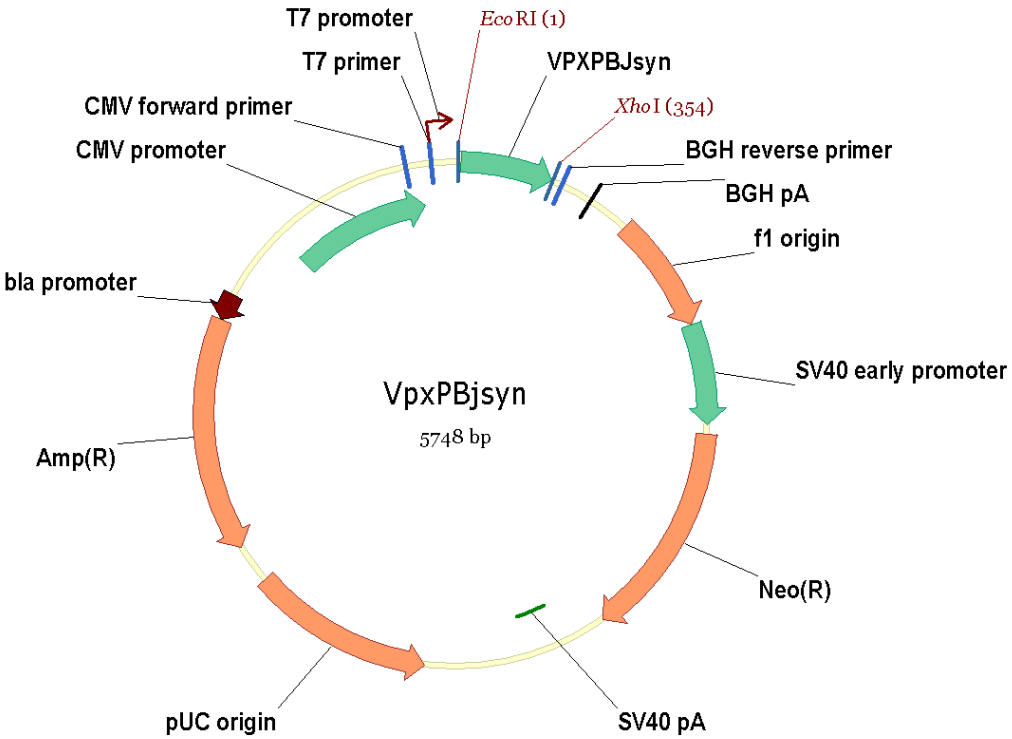

9.2 Plasmid map of pMD.G2

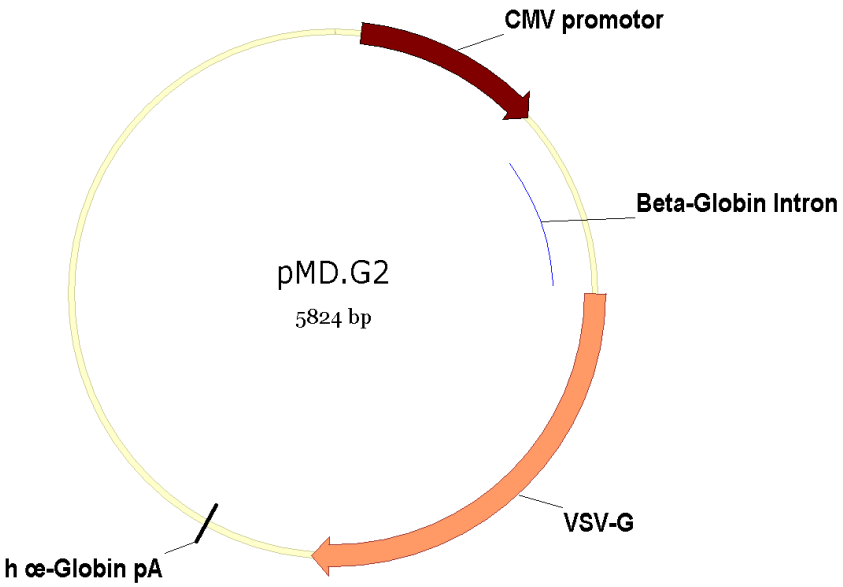

9.3 Plasmid map of pCMVΔR8.9

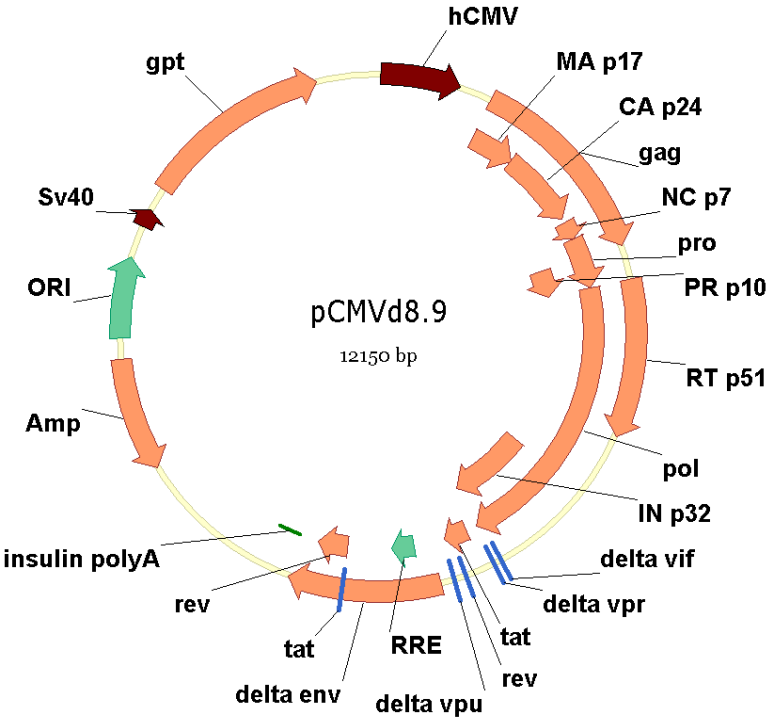

9.4 Plasmid map of pPBj-pack

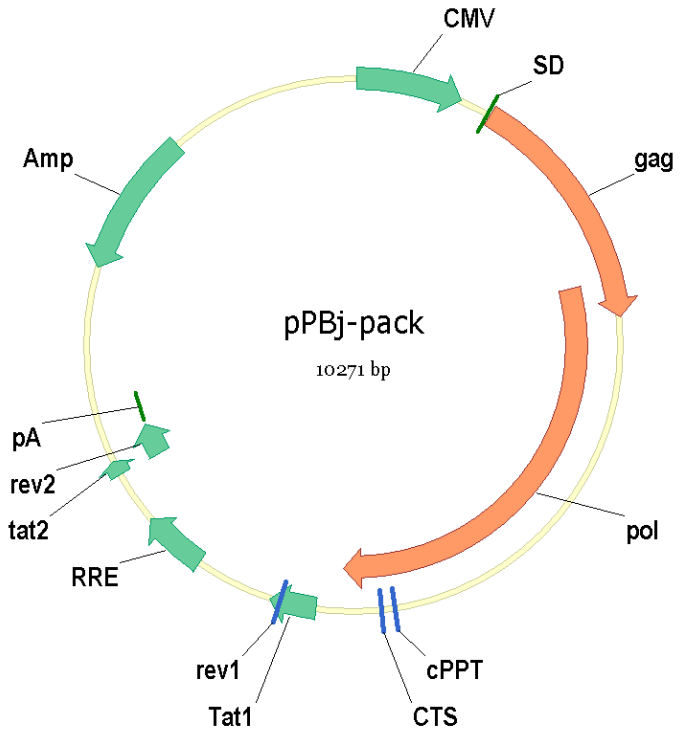

9.5 Plasmid map of pHIV-2d4

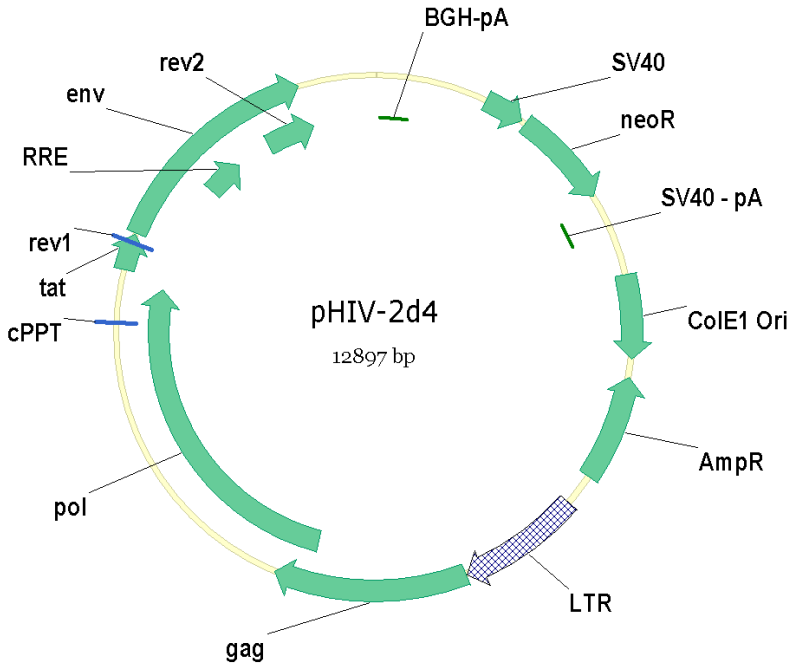

9.6 Plasmid map of pPBj-SR-SEW-cSIN

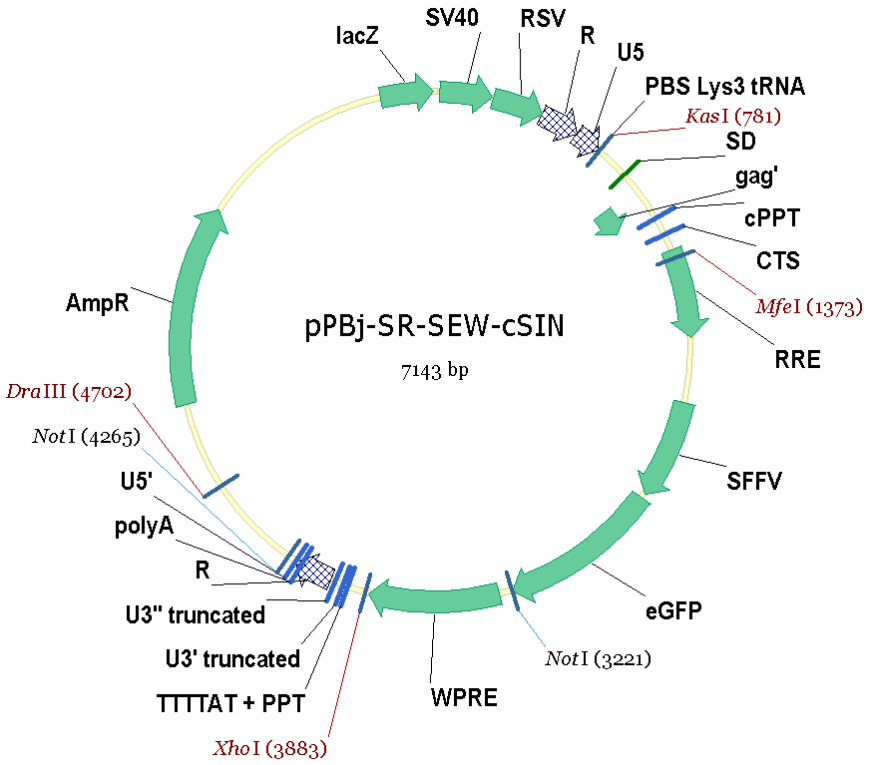

9.7 Plasmid map of pPBj-MCS

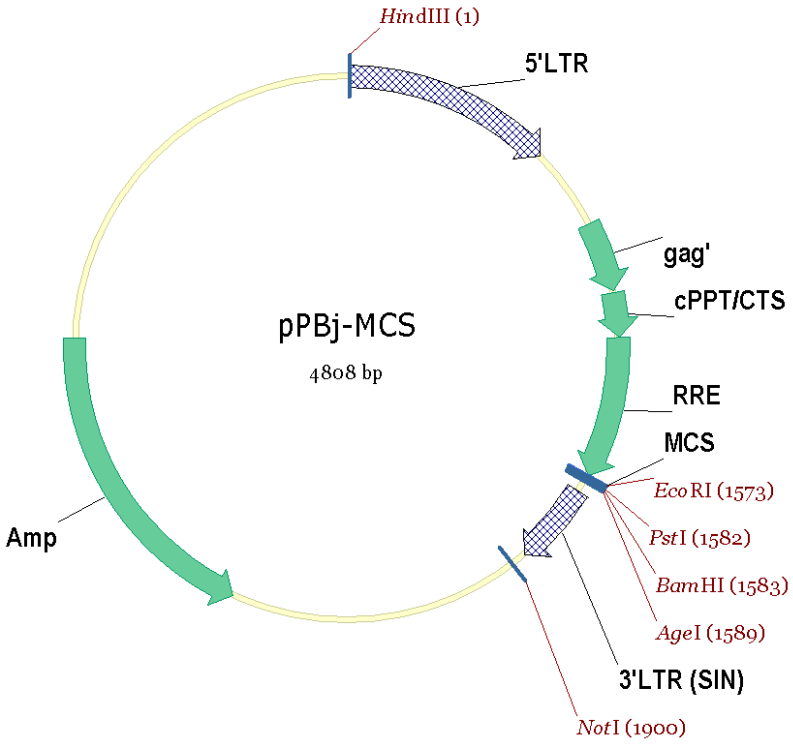

9.8 Plasmid map of pPBj-SR-g'-SEW

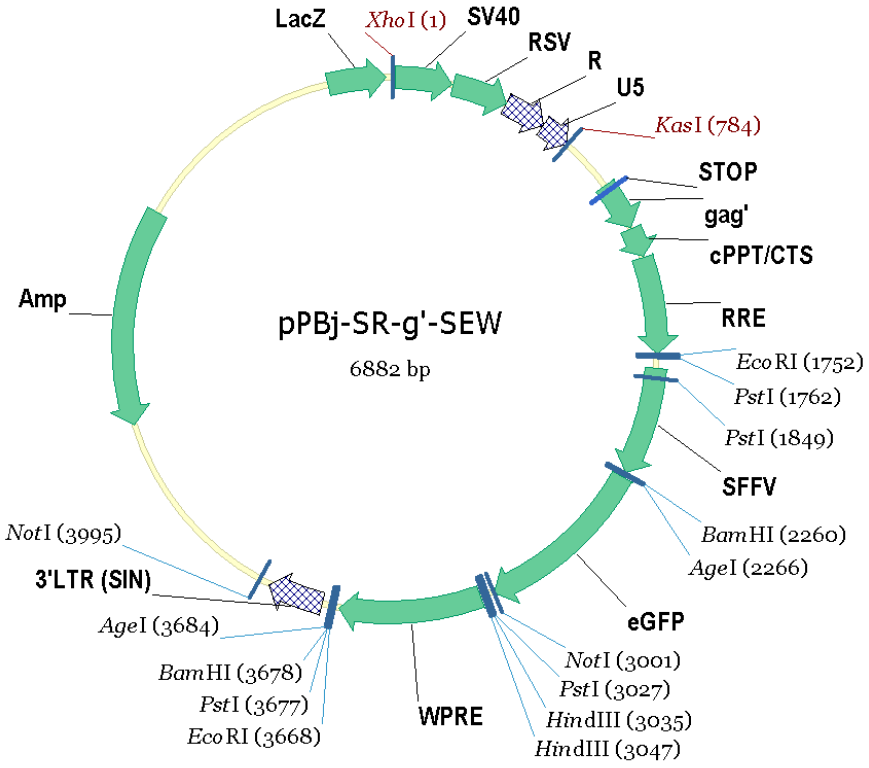

9.9 Plasmid map of pHIV-2-MCS

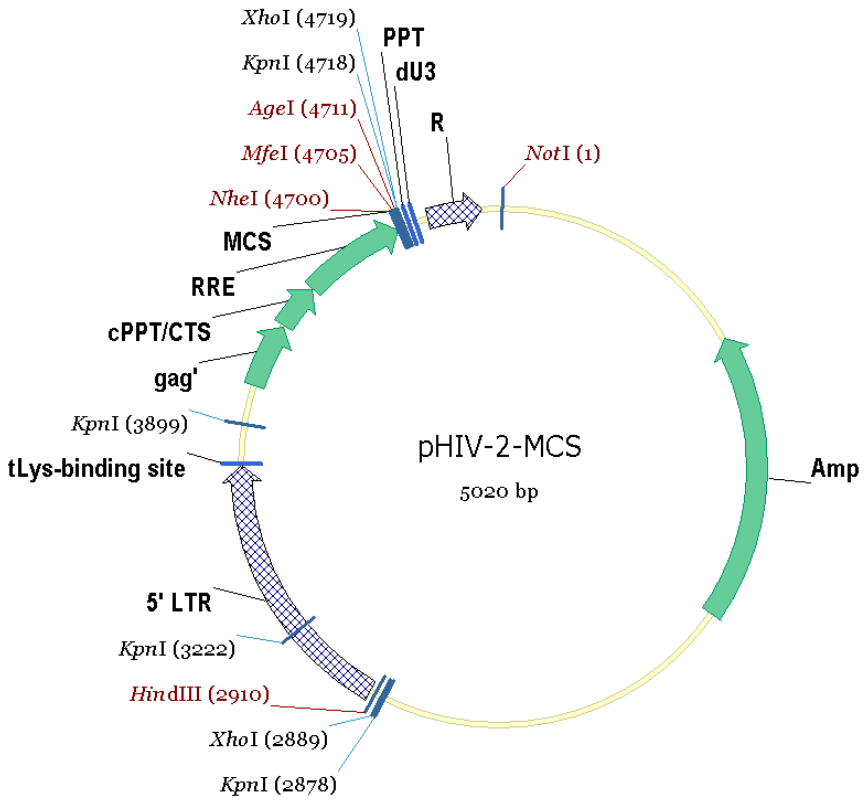

9.10 Plasmid map of pHIV-2-SR-g'-SEW

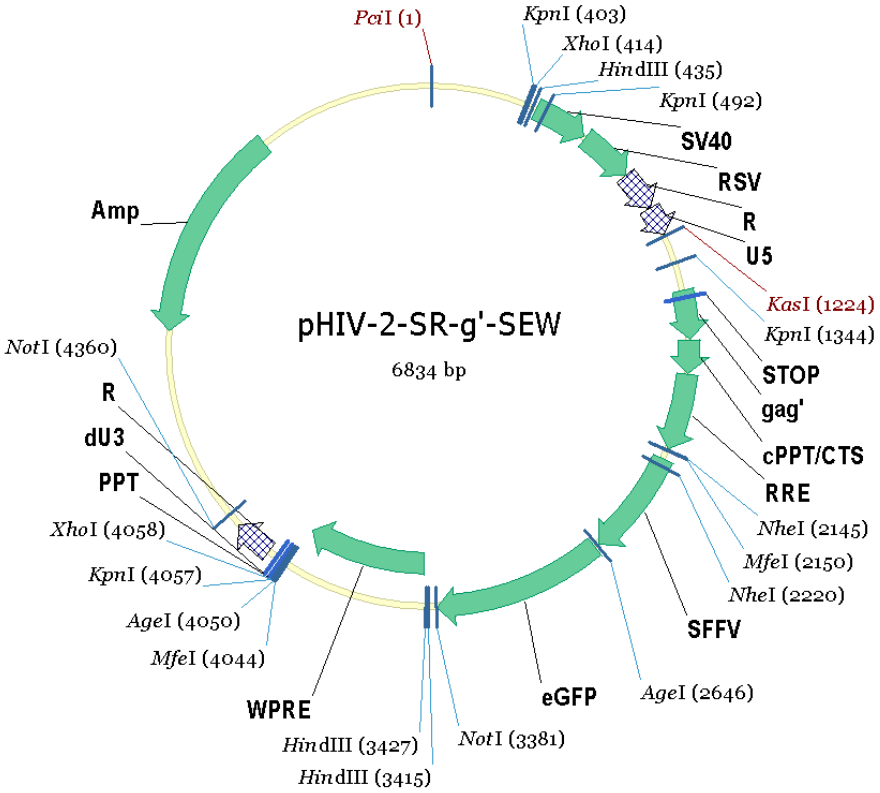

9.11 Plasmid map of pHIV-2-SgW

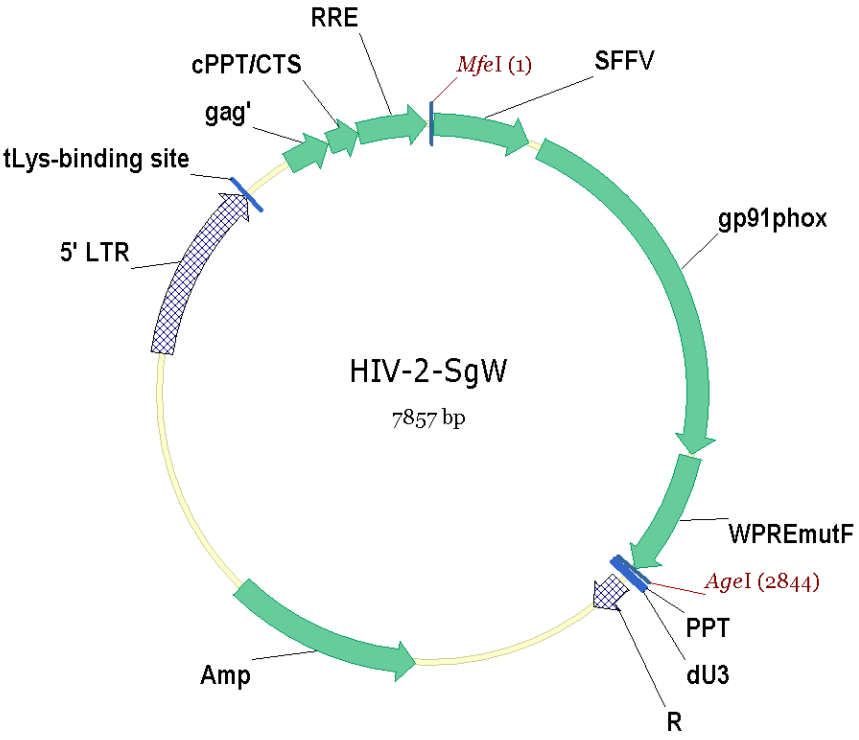

9.12 Plasmid map of pHIV-1-SgpSw

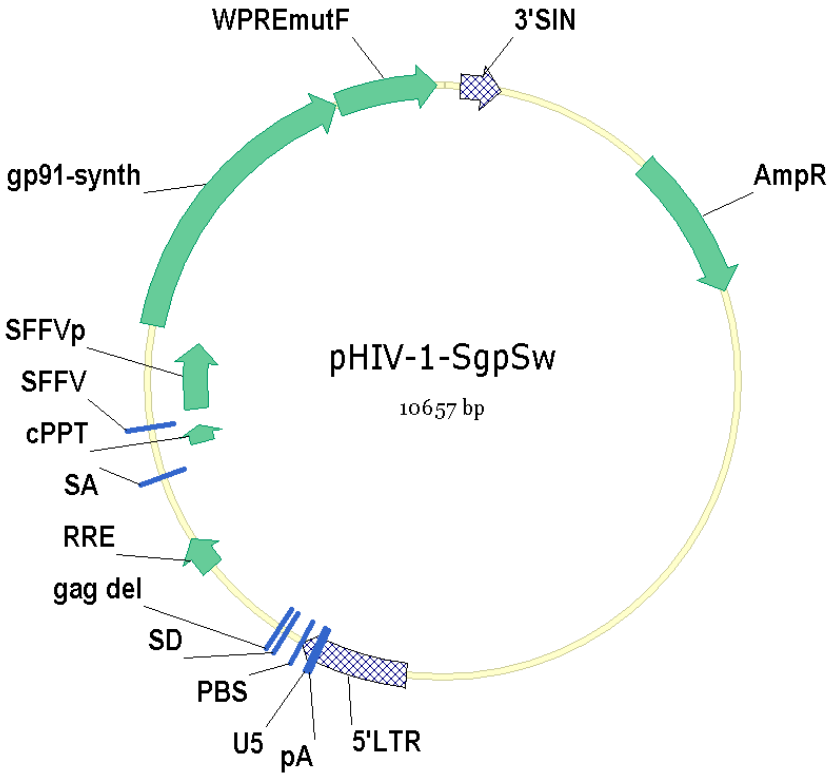

9.13 Plasmid map of pHIV-1-SEW

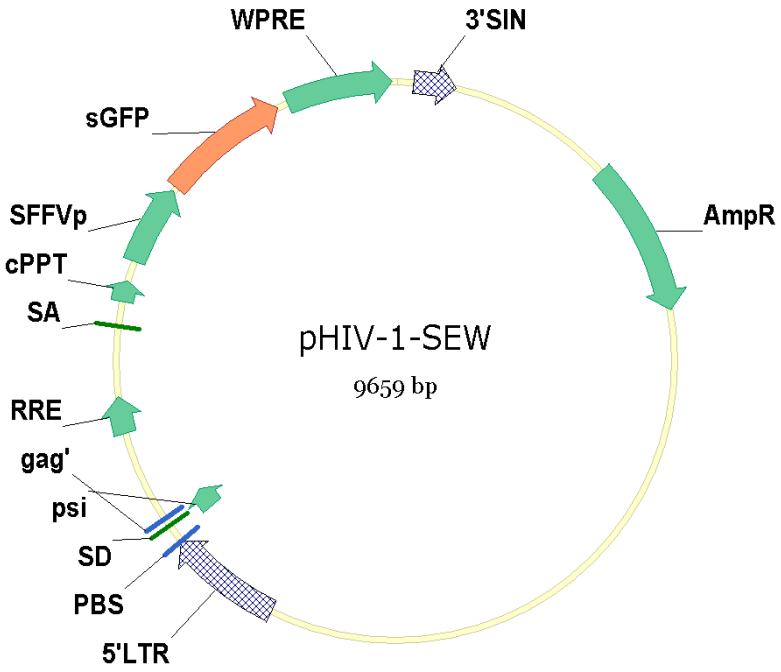

10 Danksagung

Zum Abschluss meiner Doktorarbeit möchte ich mich bei allen Personen bedanken, die am Gelingen dieser Arbeit beteiligt waren und die mich während der letzten Jahre unterstützt haben.

Herrn Prof. Dr. Klaus Cichutek danke ich dafür, unter herausragenden Bedingungen am Paul-Ehrlich-Institut zu promovieren und für seine offene und zielgerichtete Diskussionsbereitschaft.

Herrn Prof. Dr. Matthias Schweizer danke ich dafür, dass er mir das Graduierten-Kolleg-Stipendium angeboten hat und nicht nur dadurch ein erstklassiges Umfeld zum Erstellen der Arbeit bereitgestellt hat.

Herrn Prof. Dr. Volker Dötsch danke ich, dass er freundlicherweise die Betreuung von Seiten der Johann Wolfgang Goethe-Universität übernommen hat.

Ein besonderer Dank gebührt Dr. Silke Schüle, die für alles ein offenes Ohr hatte und mir mit Rat und Tat zur Seite stand. Ohne ihr Organisationstalent, ihre Motivationskünste und die so wichtigen Schulterklopfer wäre vieles schwerer geworden.

Frau Prof. Dr. Ulrike Köhl und Herrn Dr. Manuel Grez danke ich für die hilfreiche Betreuung von Seiten des Graduiertenkollegs 1172 „Biologicals“.

Christian Brendel danke ich sehr für seine Unterstützung und Hilfsbereitschaft bei Fragen und Experimenten, die mit dem Thema der xCGD im Zusammenhang stehen.

Ich danke…

- …Julia Brachert für das Bereitstellen von *S. aureus*
- …Julia Brynza and Dr. Brigitte Anliker für die Hilfe bei der Transduktion muriner Neurone
- …Katrin Högner für ihre Hilfe als meine Praktikantin und Diplomandin
- …Theresa Frenz und Linda Sender für ihre Hilfe beim LSRII-FACS
- …Janine Kimpel für die Hilfe beim Transplantieren von Mäusen und der Analyse derer Gewebe
- …Dorothea Kreuz für die Unterstützung bei Mausexperimenten
- …Dr. Axel Schambach für das Überlassen des SV40/RSV-Elements
- …Dr. Anja Schmidt und Dr. Jan-Müller Berghaus für die vielen Blutentnahmen
- …Sibylle Wehner für die Hilfe bei der Durchführung der murinen Knochenmarks-ausstriche
- …meiner Tante Dr. Liane Platt-Rohloff für das Korrekturlesen der Arbeit

Ein besonderes Dankeschön geht an meine guten Freunde Ferdinand „Babbsack“ Kopietz und Mario Perkovic. Ich danke Euch für die ständig gute Laune, eure Ehrlichkeit und dass man mit Euch durch „dick und dünn“ gehen kann.

Sabrina Funke, Ute Burkhardt und Stephan Schultze-Strasser danke ich für die gute Zeit, die wir zusammen bei diversen Vorlesungen und den Summer-Schools des GKs hatten.

Allen Mitarbeitern der Abteilung Medizinische Biotechnologie möchte ich für die gemeinsame Zeit, die gegenseitige Hilfe und Unterstützung danken. Besonders erwähnen möchte ich Marion Battenberg, André Berger, Elea Conrad, Dr. Egbert Flory, Henning Hofmann, Sabrina Janssen, Julia Kaiser, Tanja „Maxi“ Kearns, Daniela Marino, Dr. Michael Mühlebach,

Senthil Mungan Thyagarajan, Prof. Dr. Carsten Münk, Sylvia Panitz, Dr. Ralf Sanzenbacher, Fr. Schmidt, Benjamin Rengstl, Fr. Varga und Jörg Zielonka.

Meinen Eltern und besonders meiner Frau danke ich, dass sie mir zu jeder Zeit den Rücken gestärkt haben und immer für mich da sind.

11 Curriculum Vitae

Persönliche Daten

Name:	Björn-Philipp Kloke
Geburtsdatum:	20. Juli 1979
Geburtsort:	Berlin-Steglitz
Staatsangehörigkeit:	deutsche
Familienstand:	verheiratet

Promotion

09.2005 - 03.2009	Doktorarbeit am Paul-Ehrlich-Institut in Langen, Abteilung Medizinische Biotechnologie, Fachgebiet Virale Gentransfer-Arzneimittel unter der Leitung von Herrn Prof. Dr. K. Cichutek in der Arbeitsgruppe von Herrn Prof. Dr. M. Schweizer Thema: „Development of SIVsmmPBj- and HIV-2-derived lentiviral vector systems to correct *gp91^{phox}* gene defects in monocytes“

Stipendium

09.2005 - 09.2008	Doktoranden-Stipendium innerhalb des DFG-Graduiertenkollegs 1172 „Biologicals“ der Johann Wolfgang Goethe-Universität in Frankfurt a. M.

Studium

08.2003 - 05.2005	Hauptstudium der Biochemie an der Johann Wolfgang Goethe-Universität in Frankfurt. mit dem Abschluss „**Diplom-Biochemiker**“ (Note: sehr gut) Diplomarbeit unter Prof. Dr. C. Münk “Charakterisierung der spezifischen Interaktion von APOBEC3 mit dem viralen Protein Vif”
09.2002 - 07.2003	Student der molekularen Mikrobiologie der University of Aberdeen mit dem Abschluss des “**Bachelor of Science**”
10.2000 - 09.2002	Grundstudium der Biochemie an der Johann Wolfgang Goethe-Universität in Frankfurt

Zivildienst

07.1999 - 06.2000	Waldhaus-Klinik, Abt. für Psychiatrie, in Berlin-Nikolassee

Schulausbildung

Brüssel, Mai 1999	**Abitur**
01.1997 - 05.1999	Deutsche Schule Brüssel
08.1996 - 01.1997	Milwaukie High School, OR/USA
08.1994 - 07.1996	Deutsche Schule Brüssel
08.1992 - 07.1994	Droste-Hülshoff-Gymnasium, Berlin
08.1986 - 07.1992	Schweizerhof-Grundschule, Berlin

12 Publikationen

Originalartikel

Björn-Philipp Kloke, Silke Schüle, Michael D. Mühlebach, Nina Wolfrum, Klaus Cichutek, Matthias Schweizer (2009) Generation of SIVsmmPBj- and HIV-2- derived lentiviral vectors for transduction of primary human monocytes. *in Vorbereitung*

Björn-Philipp Kloke, Saskia Reddies, Marion Battenberg, Klaus Cichutek, Carsten Münk (2009) The Vif Interaction Domain in APOBEC3C Switched in HIV-2 During Host-Adaptation to Humans. *in Vorbereitung*

Silke Schüle, Björn-Philipp Kloke, Julia Kaiser, Sabine Heidmeier, Sylvia Panitz, Nina Wolfrum, Klaus Cichutek, Matthias Schweizer (2009) Restriction of HIV-1 replication in monocytes is abolished by Vpx of SIVsmmPBj. Eingereicht bei *Virus Research*

Mario Perković, Stanislaw Schmidt, Rebecca A. Russell, Benjamin Stauch, Henning Hofmann, Ferdinand Kopietz, Björn-Philipp Kloke, Jörg Zielonka, Heike Ströver, Johannes Hermle, Dirk Lindemann, Vinay K. Pathak, Gisbert Schneider, Martin Löchelt, Klaus Cichutek, Carsten Münk (2009) Species-specific Inhibition of APOBEC3C by the Prototype Foamy Virus Protein Bet. *J Biol Chem*. 284(9), 5819-26.

Nina Wolfrum, Michael Mühlebach, Silke Schüle, Julia Kaiser, Björn-Philipp Kloke, Klaus Cichutek, Matthias Schweizer (2007) Impact of viral accessory proteins of SIVsmmPBj on early steps of infection of quiescent cells. *Virology*. 364(2), 330-41.

Carsten Münk, Jörg Zielonka, Hanne Constabel, Björn-Philipp Kloke, Benjamin Rengstl, Marion Battenberg, Francesca Bonci, Mauro Pistello, Martin Löchelt, Klaus Cichutek (2007). Multiple Restrictions of Human Immunodeficiency Virus Type 1 in Feline Cells. *J Virol*. 81(13)**,** 7048-60.

Patentanmeldung

Europäische Patentanmeldung am 16.11.2006 (06124262.4; Veröffentlichungsnr.1923468) und PCT-Anmeldung am 16.11.2007 (PCT/EP2007/009934;Veröffentlichungsnr. WO/2008/058752) mit dem Titel „Lentiviral vectors for gene transfer in quiescent (G0) cells" Erfinder: Klaus Cichutek, Matthias Schweizer, Björn-Philipp Kloke, Silke Schüle

Vorträge

Björn-Philipp Kloke, Silke Schüle, Katrin Högner, Nina Wolfrum, Klaus Cichutek, Matthias Schweizer
Development of an SIV_{smm}PBj- and a HIV-2-derived three-plasmid vector system,
Third European Congress of Virology, Nürnberg 2007

Björn-Philipp Kloke, Klaus Cichutek, Carsten Münk
Characterization of the Vif Interaction domain in APOBEC3C
Third European Congress of Virology, Nürnberg 2007

Björn-Philipp Kloke, Silke Schüle, Katrin Högner, Nina Wolfrum, Klaus Cichutek, Matthias Schweizer
Development of an SIVsmmPBj- and a HIV-2-derived three-plasmid vector system
Clinigene, Barcelona 2007

Carsten Münk, Hanne Constabel, Jörg Zielonka, Björn-Philipp Kloke, Sarah Chareza, Marion Battenberg, Martin Löchelt, Klaus Cichutek
Multiple Restrictions of HIV-1 in Feline Cells
GFV, München 2006

Carsten Münk, Mario Perkovic, Johannes Hermle, Björn-Philipp Kloke, Sarah Chareza, Martin Löchelt, Klaus Cichutek
The PFV Bet protein protects HIV and SIV against APOBEC3-induced deamination by a novel pachway not involving the proteasome.
Cold Spring Harbor, Retroviruses 2006

Posterpräsentationen

Björn-Philipp Kloke, Silke Schüle, Christian Brendel, Manuel Grez, Matthias Schweizer and Klaus Cichutek
Gene transfer of *gp91^{phox}* by an SIVsmmPBj-derived lentivector into monocytes from chronic granulomatous disease patients
GFV, Leipzig 2009 and ASGT, San-Diego 2009

Björn-Philipp Kloke, Silke Schüle, Katrin Högner, Christian Brendel, Manuel Grez, Matthias Schweizer und Klaus Cichutek
Gene transfer of *gp91^{phox}* by an SIVsmmPBj-derived lentivector into monocytes from chronic granulomatous disease patients
ASGT, Boston 2008

Silke Schüle, Björn-Philipp Kloke, Julia Kaiser, Sabine Heidmeier, Klaus Cichutek und Matthias Schweizer
Primary Human Monocytes Using HIV-1-Derived Vector Particles Is Enhanced by the Viral Protein Vpx Provided by SIVsmPBj-Derived Virus-Like Particles.
ASGT, Boston 2008

Björn-Philipp Kloke, Silke Schüle, Nina Wolfrum, Klaus Cichutek and Matthias Schweizer
Generation of an SIVsmmPBj-derived vector system for transduction of quiescent cells
Cold Spring Harbor, Retroviruses 2008

Björn-Philipp Kloke, Silke Schüle, Katrin Högner, Christian Brendel, Nina Wolfrum, Manuel Grez, Klaus Cichutek and Matthias Schweizer
Development of an SIVsmmPBj-derived three-plasmid vector system for gene-transfer of *gp91^{phox}* into human monocytes
ESGCT, Rotterdam 2007

Silke Schüle, Sabine Heidmeier, Björn-Philipp Kloke, Julia Kaiser, Klaus Cichutek and Matthias Schweizer
Transduction of primary human monocytes/macrophages using HIV-1-derived vector particles is enhanced by the viral protein VpxPBj provided by SIVsmPBj-derived vector-like particles
Third European Congress of Virology, Nürnberg 2007

Björn-Philipp Kloke, Silke Schüle, Katrin Högner, Nina Wolfrum, Klaus Cichutek and Matthias Schweizer
Development of an SIVsmmPBj- and a HIV-2-derived three-plasmid vector system
Clinigene, Barcelona 2007 and DG-GT, Heidelberg 2007

Björn-Philipp Kloke, Nina Wolfrum, Silke Schüle, Julia Kaiser, Matthias Schweizer and Klaus Cichutek
Development of an SIV_{smm}PBj-derived three-plasmid vector system
ESGT, Athens 2006

Silke Schüle, Nina Wolfrum, Julia Kaiser, Björn-Philipp Kloke, Klaus Cichutek and Matthias Schweizer
Transduction of primary human monocytes/macrophages using HIV-1-derived vector particles is enhanced by the viral protein VpxPBj provided by SIVsmPBj derived vector-like particles
ESGT, Athens 2006

Björn-Philipp Kloke, Nina Wolfrum, Silke Schüle, Julia Kaiser, Klaus Cichutek and Matthias Schweizer
Development of an SIV_{smm}PBj-derived three-plasmid vector system
Cold Spring Harbor, Retroviruses 2006

Björn-Philipp Kloke, Martin Löchelt, Marion Battenberg, Klaus Cichutek and Carsten Münk
Characterization of Feline:Human APOBEC3 Chimeras
GFV, Hannover 2005

Eidesstattliche Versicherung

Ich erkläre hiermit an Eides Statt, dass ich die vorgelegte Dissertation mit dem Titel

„Development of SIVsmmPBj- and HIV-2-derived lentiviral vector systems to correct *gp91^{phox}* gene defects in monocytes“

selbständig und nur mit den angegebenen Quellen und Hilfsmitteln angefertigt habe.

Langen, den 08.04.09

Björn-Philipp Kloke